Ana Raquel Carvalho Sousa

Master of Science

Testing the protective effect of a candidate small molecule in a *Drosophila* model of Amyotrophic Lateral Sclerosis (ALS).

Dissertation submitted in partial fulfillment
of the requirements for the degree of

Master of Science in
Biomedical Engineering

Adviser: Dr. César Mendes, Principal Investigator,
Chronic Diseases Research Center (CEDOC)

Co-adviser: Dr. Carla Quintão, Associate Professor,
NOVA School of Science and Technology (FCT NOVA)

Examination Committee

Chairperson: Dr. Célia Maria Reis Henriques
Raporteur: Dr. Federico Herrera Garcia
Member: Dr. César Miguel Pereira Soares Mendes

FACULDADE DE
CIÊNCIAS E TECNOLOGIA
UNIVERSIDADE NOVA DE LISBOA

September, 2019

Testing the protective effect of a candidate small molecule in a *Drosophila* model of Amyotrophic Lateral Sclerosis (ALS).

This document was created using the (pdf)LaTeX processor, based in the "novathesis" template[1], developed at the Dep. Informática of FCT-NOVA [2].
[1] https://github.com/joaomlourenco/novathesis [2] http://www.di.fct.unl.pt

Acknowledgements

First and foremost, I would like to thank my supervisor, César Mendes, for granting me this opportunity and for his constant guidance, encouragement and friendship. I would also like to thank Cláudia Nunes Santos for the unwavering support, motivation and for the time spent discussing perspectives. I am grateful to Carla Quintão for trusting in my effort and accepting to be my cosupervisor. To Regina Menezes and Rita João Ramos for all the help every time I needed.

I felt glad for having so great lab colleagues who provided me with an excellent atmosphere for doing research. I thank Ana Cabrita for the shared "thesis-pressure" moments, English lessons and (of course) napkins. To Anna Hobbiss for all the support and interesting conversations. To Ricardo Custódio for all the great discussions and joyful moments. A special thanks to Alexandra Medeiros for the patience, encouragement, friendship and the great suggestions in every step of this work. She was undoubtedly one of the people who helped me the most in this project.

I would also like to thank my friends, and colleagues at university for their optimism and encouragement which made my stay at studies more enjoyable. Special thanks go to Ana Pinheiro for countless times of understanding, for sharing with me all my successes and failures and for making every silly moment even more fun. Many thanks also to Joana Martins, Beatriz Costa and Joana Inácio for their advice and inspiration. In addition, a special thanks to my roommates, Pedro Carmo, Teresa Antunes and Miguel Duarte, for encouraging me to pursue my objectives, for all the deep conversations during dinner, for always listening and giving me words of confidence and for all the fun moments spent in "4º Esquerdo".

Last but not least, I am extremely grateful to my family, especially my parents, for their love, caring and sacrifices for preparing me for my future. I would not be this stronger without you as my inspiration.

"I am just a child who has never grown up. I still keep asking these 'how' and 'why' questions. Occasionally, I find an answer."

Stephen Hawking

Abstract

Amyotrophic Lateral Sclerosis is a fatal neurodegenerative disease affecting upper and lower motor neurons. Patients display progressive paralysis with death typically resulting from diaphragmatic failure. Considerable evidence points out for a significant, but nevertheless complex genetic contribution for both ALS forms, familial and sporadic. Hence, subsequent work has identified a broad set of mutated genes associated with ALS symptoms, including Fused in Sarcoma (FUS).

Not surprisingly, current efforts to develop new treatments for ALS involve the identification of small molecules that counteract the cellular hallmarks of the pathology. Ample evidence suggests that small bioactive molecules such as polyphenols have protective effects in neurodegenerative disorders. In fact, many studies have been supporting the possibility of changing the progression of the neurodegeneration through diet.

Our study had a two-fold objective: to characterize the neuronal and kinematic decay of a *Drosophila* model of ALS; to test the protective effect of a small molecule previously identified for its capability to improve cellular growth of a yeast model overexpressing FUS. Since *Drosophila* has a relatively complex nervous system and a stereotyped set of motor outputs, it represents a step forward in the validation of this promising small molecule.

Consistent with previous transgenic models, the *Drosophila* model of ALS overexpressing human FUS alleles (wild type and R521C) exhibited locomotor deficits, impairment of the climbing ability, reduced reproduction and shortened life span, with the degree of severity of mutant FUS phenotypes more aggressive than the wild type form. Furthermore, a detailed analysis of the locomotor pattern of the flies modelling ALS, using the custom-made FlyWalker system, revealed that the motor phenotype of these flies is evident after 14 days of FUS wild type expression. In addition, FUS wild type transgenic flies exposed to 10 mM of the small molecule showed a significant increase in the survival rate. Collectively, we conclude that the *Drosophila* model captures important aspects of human FUS-based ALS, providing a useful tool to test the efficacy of bioactive molecules.

Keywords: Amyotrophic Lateral Sclerosis; Fused in Sarcoma; Neurodegeneration; Polyphenols

Resumo

A Esclerose Lateral Amiotrófica (ELA) é uma doença neurológica degenerativa fatal. Nesta patologia, os neurónios motores que conduzem a informação do cérebro aos músculos, passando pela medula espinhal, morrem prematuramente. Deste modo, os pacientes sofrem paralisia gradual e morte precoce devido à perda de capacidades essenciais, como andar, falar, engolir e até mesmo respirar. Com os avanços da genética molecular, alguns genes responsáveis por ambas as formas clínicas da doença (esporádica e familiar) foram caracterizados, incluindo o SOD1 (Superoxide Dismutase 1), o TDP-43 (Transactive Response DNA-binding protein-43) e o FUS (Fused in Sarcoma). Além disso, alguns mecanismos celulares associados à neurodegeneração incluem a agregação de proteínas, o stress do Retículo Endoplasmático, o stress oxidativo e a neuroinflamação.

Atualmente, os esforços para desenvolver novos tratamentos para a ELA involvem a identificação de moléculas que contrariem as características celulares da patologia. Amplas evidências sugerem que moléculas bioativas, tais como os polifenóis, têm efeitos protetores nas doenças neurodegenerativas. De fato, muitos estudos têm apoiado a possibilidade de alterar a progressão da neurodegeneração através da dieta.

Portanto, o nosso estudo teve dois principais objetivos: por um lado, caracterizar o decaimento neuronal e cinemático de um modelo de *Drosophila* de ELA e por outro, testar o efeito protetor de uma pequena molécula bioactiva previamente identificada pela sua capacidade de melhorar o crescimento celular de um modelo de levedura que expressa FUS. Uma vez que a *Drosophila* possui um sistema nervoso relativamente complexo e um conjunto estereótipado de neurónios motores, representa um excelente modelo animal para a validação desta molécula promissora.

Consistente com os modelos transgénicos anteriores, o modelo de *Drosophila* de ELA expressando alelos FUS humanos (tipo selvagem e R521C, uma mutação comum em pacientes com ELA) exibiu neurodegeneração, dificuldades locomotoras, capacidade de subida comprometida e reprodução e vida útil reduzida, sendo os fenótipos dos mutantes mais agressivos do que os da forma selvagem. Além disso, uma análise detalhada do padrão locomotor das moscas que modelam a ELA, usando o sistema FlyWalker, revelou que o fenótipo motor dessas moscas é evidente após 14 dias de expressão do FUS (forma selvagem). Adicionalmente, as moscas transgénicas do tipo FUS selvagem expostas a 10

mM da molécula bioactiva mostraram um aumento significativo na taxa de sobrevivência.

Deste modo, concluímos que o modelo de *Drosophila* de ELA possui aspetos importantes da doença humana, sendo uma ferramenta importante para testar a eficácia de moléculas bioactivas.

Palavras-chave: Esclerose Lateral Amiotrófica; FUS; Neurodegeneração; Polifenóis

Contents

List of Figures

List of Tables

Acronyms

ALS Amyotrophic Lateral Sclerosis.

CNS Central Nervous System.

ER Endoplasmic Reticulum.

fALS familial Amyotrophic Lateral Sclerosis.

FDA Food and Drug Administration.

FTD Frototemporal Dementia.

fTIR frustrated Total Internal Reflection.

FUS Fused in Sarcoma.

LMN Lower Motor Neurons.

MND Motor Neuron Disease.

NMJ Neuromuscular Junction.

PBP Pseudobulbar Palsy.

PCA Principal Component Analysis.

PLS Primary Lateral Sclerosis.

PMA Progressive Muscular Atrophy.

ROS Reactive Oxygen Species.

sALS sporadic Amyotrophic Lateral Sclerosis.

SOD1 Superoxide Dismutase 1.

TDP-43 Transactive Response DNA-binding protein-43.

UMN Upper Motor Neurons.

Chapter 1

Introduction

1.1 Context and Motivation

Amyotrophic Lateral Sclerosis is an adult-onset neurodegenerative disorder characterized by the loss of motor neurons in the brain or spinal cord leading to progressive paralysis and consequently death from respiratory failure within 3-5 years after diagnosis on average [2, 66].

ALS, like most of the neurodegenerative disorders, starts focally and spreads progressively: symptoms begin with weakness or muscle cramping and progress to paralysis of nearly all skeletal muscles. Due to improved care, evidence has shown that survival is increasing [24] but some mechanisms implicated in the death of the motor neurons are still unclear and there is no effective therapy for preventing the neurodegeneration. Thus, ALS disease has a fatal progressive course [66, 72, 76].

About 10% of cases of ALS are transmitted within families, frequently as dominant traits. Nevertheless, Mendelian genes were also found mutated in individuals with no family history, suggesting a complex genetic contribution to both ALS forms, sporadic and familial. Thus, advances in genetic testing techniques led to the discovery of some ALS causative genes, including Superoxide Dismutase 1 (SOD1), Transactive Response DNA-binding protein-43 (TARDBP or TDP-43) and Fused in Sarcoma (FUS)[66].

Due to the large number of gene mutations associated with this disease, a plethora of toxic mechanisms mediating the degeneration and death of motor neurons have been proposed. Several hypothesis have emerged leading to the identification of genetic and biochemical markers and providing therapeutic targets including protein aggregation, ER stress and impairment of protein degradation, mitochondrial dysfunction and neuroinflammation, among others [2, 66].

In 1995, the Food and Drug Administration (FDA) approved the first drug for ALS treatment known as riluzole, a glutamate antagonist. In May 2017, the FDA approved

edaravone, a potent free radical scavenger. However, these drugs only slow the advance of the disease meaning that the search for a cure continues. It is thus essential to unveil the mechanisms implicated in ALS pathogenesis to find early and specific diagnostic methods and develop effective therapies that allow not only to decrease disease progression but also to deal with the secondary consequences such as respiratory failure. Therefore, pharmaceutical companies and medical centers have been sponsoring clinical trials to test several drugs that are thought to be protective against ALS pathology. Furthermore, recent studies have suggested that bioactive compounds such as polyphenols are protective for several neurodegenerative disorders [16, 49, 72].

One powerful approach for studying the mechanisms underlying neurodegenerative diseases has been the use of animal models. Indeed, invertebrates such as *Drosophila melanogaster* have been proven extremely valuable as a model organism for human neurodegenerative disorders such as ALS [36]. Hence, genetic studies using *Drosophila* have provided novel insights into disease development. These models are also excellent *in vivo* systems for the testing of bioactive molecules [38, 42]. Thus, the principal objective of this study was to test the therapeutic benefits of a small bioactive molecule (Compound C) on the progressive neurodegeneration induced by ALS-related FUS alleles, using *Drosophila* as a model organism. Compound C was previously tested for its protective properties in a yeast model overexpressing FUS, one of the genetic hallmarks of the disease.

1.2 Amyotrophic Lateral Sclerosis

ALS is marked by the degeneration of motor neurons which are a group of efferent neurons, within the spinal cord and the brain, that makes synapses with muscle fibers to control muscle activity. There are two main types of motor neurons namely upper motor neurons (UMN) and lower motor neurons (LMN). Upper motor neurons originate in the brain (motor cortex) and project downward to connect with lower motor neurons. The latter localize both in the brainstem and the spinal cord and their axons connect directly with muscles at the Neuromuscular Junction (NMJ). Thus, they connect the Central Nervous System (CNS) with the target muscle to be innervated (Figure 1.1) [22, 66].

ALS was first described in 1869 by Jean-Martin Charcot. He suggested that "the name reflects both the degeneration of corticospinal motor neurons, whose descending axons in the lateral spinal cord appear scarred ("lateral sclerosis"), and the demise of spinal motor neurons, with secondary denervation and wasting of muscle ("amyotrophy")" [66]. However, the disease only became well-known when the baseball player Lou Gehrig announced his ALS diagnosis in 1939. Therefore, Amyotrophic Lateral Sclerosis is also known as Charcot disease, Lou Gehrig's disease or motor neuron disease (MND). There are four other known MNDs: Primary Lateral Sclerosis (PLS), Progressive Muscular Atrophy (PMA), Progressive Bulbar Palsy (PBP) and Pseudobulbar Palsy [76].

There are two types of ALS disease. The most common form is sporadic ALS (sALS),

accounting for 90-95% of the cases, which has no genetically inherited component. Approximately 5-10% of the cases are inherited from a family member and are classified as family-type ALS (fALS). The disease is considered familial when there are two or more family members affected. Usually, the onset is earlier in fALS, although the clinical presentation of inherited ALS and sporadic ALS is similar [1, 66, 69].

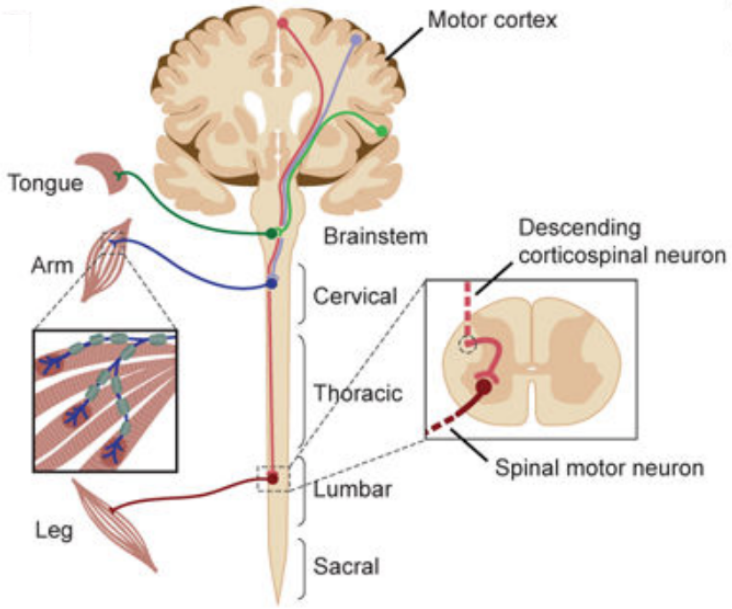

Figure 1.1: **The components of the nervous system impacted in ALS pathogenesis.** Descending corticospinal motor neurons (upper motor neurons) are the first ones affected by ALS, they project from the motor cortex to synapses in the brainstem and spinal cord. Bulbar or spinal motor neurons (lower motor neurons) projects from the brainstem or spinal cord to skeletal muscles [Adapted from [66]].

ALS is an orphan disease affecting, in general, 1-2 individuals per 100.000 each year in most countries. Since ALS has a rapid lethality, its prevalence is much lower. Although rare, ALS is the most common motor neuron disease affecting people of all races and ethnicities with a higher prevalence among Caucasians [16, 34, 65].

1.2.1 Clinical phenotypes

Usually, the first symptoms begin between 50 and 65 years old with the median age-onset of 64 years. According to statistics, only 5% of the cases correspond to an age-onset younger than 30 years old, while the beginning over 80 years old presents a high incidence (10.2/100.000 in men and 6.1/100.000 in women) which can set aging as a risk factor for the disease [6, 76].

ALS has a wide phenotypic variability and often shows clinical overlap with other neurodegenerative disorders being frontotemporal dementia (FTD) the most common.

Thus, identification of specific phenotypes is essential to develop strategies to measure disease progression and improve survival [66].

Different phenotypes can be distinguished based on the body region first affected at disease onset. When ALS symptoms begin in the arms or legs, it is termed "limb onset"ALS. In this case, individuals may have difficulties with simple tasks such as writing or walking. On the other hand, ALS that begins by affecting the muscles of speech, chewing and swallowing is referred as "bulbar[1] onset"ALS. Limb onset is found in around 80% of the cases but most patients will develop symptoms in both bulbar region and limbs as the disease progresses (Figure 1.2) [34, 53].

ALS affects both upper and lower motor neurons. However, ALS beginning usually presents symptoms associated with only upper or lower motor neuron involvement leading to a wrong diagnosis. Thus, patients can be diagnosed with primary lateral sclerosis (PLS), presenting only UMN level phenotype, or progressive muscular atrophy, which has only LMN participation (PMA). As the disease progresses, ALS exhibit a detectable involvement of both UMN and LMN, and diagnosis reclassification must be accomplished to discard previous diagnostics of PLS or PMA (Table 1.1) [34, 57, 66].

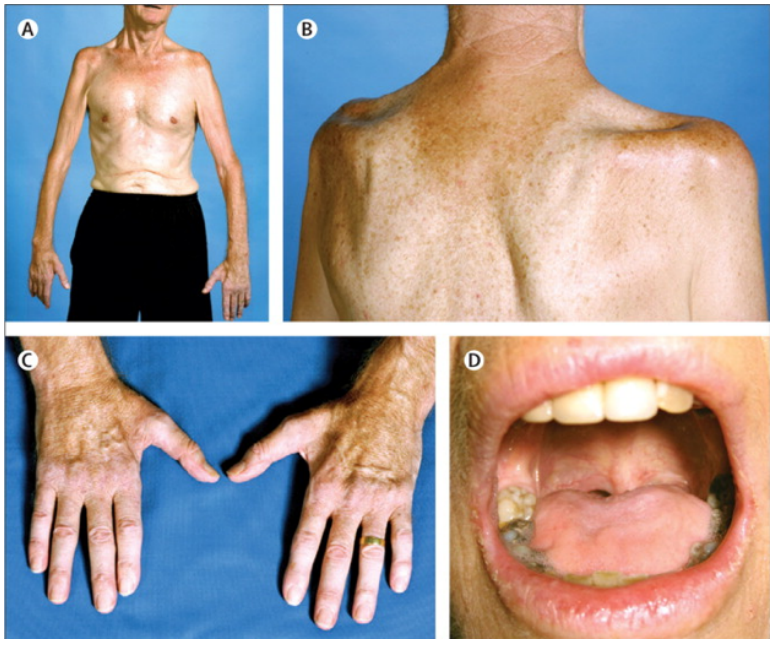

Figure 1.2: **ALS clinical phenotypes.** (A) Wasting of upper limb leading to an inability to lift arms against gravity. (B) Recessions above and bellow the scapular spine showing wasting of supraspinatus and infraspinatus muscles and partial loss of deltoid muscle. (C) Disproportionate wasting of the thenar muscles and also the first dorsal interossei comparatively with hypothenar muscles in hand – the typical "split-hand."(D) Substantial wasting of the tongue muscles in bulbar onset ALS [Adapted from [34]].

[1] Bulbar region is an area of the brain composed of the cerebellum, medulla and pons [57].

Table 1.1: **Clinical presentations in amyotrophic lateral sclerosis.** Symptoms are divided by affected motor neuron. Both UMN and LMN have to be affected for ALS diagnosis [34, 53].

Upper motor neuron sign in bulbar onset	Spasticity; Spastic dysarthria.
Lower motor neuron sign in bulbar onset	Tongue wasting; Weakness; Fasciculations; Flaccid dysarthria; Later dysphagia.
Upper motor neuron sign in limb onset	Spasticity; Weakness; Brisk deep tendon reflexes.
Lower motor neuron sign in limb onset	Fasciculations; Muscle atrophy; Weakness.

Some factors influence prognosis. Low survival is associated with bulbar-onset disease, older ages at the time of disease development and early respiratory muscle dysfunction while high survival is related with the limb-onset disease, younger age at the beginning of the disorder and delayed diagnostic [34, 73].

In final disease stages, patients need help with daily life activities and if they develop dyspnea at rest, the death becomes imminent. Usually, patients die from respiratory failure or other pulmonary complications. Sometimes they are kept alive by tracheostomy assisted ventilation developing a profound state motor paralysis known as "totally-locked-in-state" (TLS) in which all voluntary movements are lost [28, 48, 73].

1.2.2 Genetics

"There is considerable evidence of a genetic contribution to all ALS"[2].

Sporadic ALS refers to the cases that have no familial inheritance. However, technological advances in DNA sequencing revealed the presence of mutations in ALS genes in the sporadic population, confirming the genetic contribution also in this form of the disease. Thus, the cause of sALS probably involves a combination of genetic and environmental factors. Familial ALS occurs as a result of mutations in a specific genetic locus and the inheritance is primarily autosomal dominant following a Mendelian pattern [5, 11, 66, 76].

In the last years, several studies contributed to generate a list of genes whose mutations are associated with both types of ALS. Given that one of the principal objectives of this work was to test the effect of a small molecule in a *Drosophila* model overexpressing FUS, the following topic will discuss the role of this gene [66].

1.2.2.1 Fused in Sarcoma (FUS)

Fused in Sarcoma is a RNA-binding protein, ubiquitously expressed in all cells, that plays an important role in the regulation of RNA transcription, splicing and transport. The N-terminal of FUS protein has properties for transcriptional activation and the C-terminal contains domains involved in RNA-protein interactions [58, 62].

The majority of FUS mutations (accounting for 4% of fALS and less than 1% of sALS) are missense mutations in the C terminus of the protein, where the nuclear localization signal (NLS) is positioned (Figure 1.3). The most common mutations in human ALS patients are 'R521H' and 'R521C'. FUS has nuclear and cytoplasmic expression and shuttles between the cytoplasm and the nucleus. FUS mutations lead to a gain-of-toxicity mechanism that involves the redistribution of the protein from the nucleus to the cytoplasm [60]. Thus, postmortem analysis of brain and spinal cord tissues from ALS patients carrying FUS mutations demonstrated compromised FUS nuclear localization and abnormal cytoplasmic FUS inclusions in neurons and glia. Furthermore, it has been proposed that the overexpression of wild type FUS in vulnerable neurons may be one of the causes of the disease [36, 45, 56, 72].

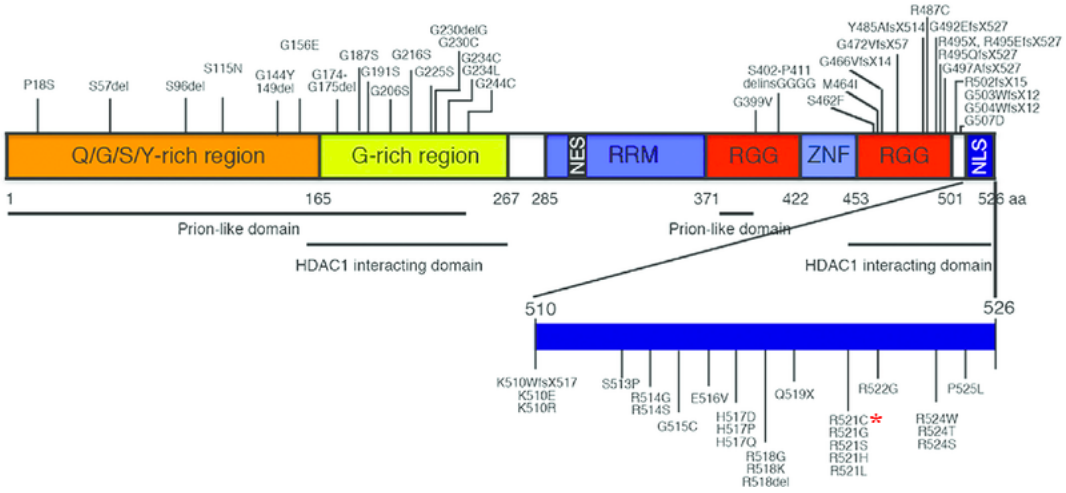

Figure 1.3: **Schematic diagrams showing functional domains in FUS proteins and FUS mutations identified in ALS.** The human FUS gene is located on chromosome 16p11.2. The full length human FUS protein contains 526 amino acids that can be further divided into distinct functional domains, such as the "prion-like" or low complexity (LC) domain that contains the Q/G/S/Y-rich region (amino acids 1-165) and the G-rich region (amino acids 165-267), the Arginine-rich motif (RRM, amino acids 285-371), two Arg-Gly-Gly (RGG)-repeat regions (amino acids 371-422 and 453-501), interrupted by a Cys2-Cys2 zinc-finger motif (ZNF)(amino acids 422-453), and a non-conventional nuclear localization signal (NLS)(amino acids 510-526). Other structural and functional domains in FUS include the prion-like domains and the HDAC1-interacting domains. R521C mutation is higlighted by the red asterisk [Adapted from [62]].

1.2.3 Pathogenic mechanisms

There are a large number of gene mutations associated with this disease. Thus, several pathogenic mechanisms by which motor neurons degenerate have been proposed and it seems likely that the combination of these mechanisms, instead of a single mechanism, contributes to the neurodegeneration. The identification of toxic mechanisms is essential for understanding disease progression and for the development of effective therapies. The following topics discuss some principal mechanisms [8].

1.2.3.1 Free radical-mediated oxidative stress

In the last years, the interest in reactive oxygen species (ROS) have been increasing. They are natural bioproducts of the normal metabolism of oxygen and can be generated in the human body through several endogenous systems, exposure to various physicochemical conditions or pathophysiological states. However, an imbalance between ROS production and cell's antioxidant defenses causes ROS accumulation and consequently oxidative damage. In other words, disturbances in the cell's ability to detoxify reactive species lead to the accumulation of free radicals that can damage cell components including lipids, proteins and DNA, causing mutagenesis. Moreover, due to the accumulation of free radical damage in cells, organisms become aged and more susceptible to several diseases including ALS [19, 49, 76].

Increased oxidative damage and accumulation of free radicals were found in cerebrospinal fluid (CSF) and urine samples of ALS patients [76].

1.2.3.2 ER stress and unfolded protein response

Endoplasmic reticulum (ER) is the cellular organelle responsible for protein synthesis, posttranslational processing, folding of newly synthesized proteins and delivering the biologically active proteins to their proper target sites. Accumulation of unfolded and misfolded proteins in the lumen of ER (excessive influx) or perturbations in the typical environment necessary for protein folding leads to ER stress. In this regard, a physiological response known as Unfold Protein Response (UPR) is triggered off in the cell to relieve ER stress by transcriptionally regulating ER chaperones and other proteins, attenuating the overall translation rate and increasing the degradation of misfolded proteins. However, if the ER functions are severely affected and it is not possible to restore the cell integrity, the cell undergoes apoptosis [31, 59, 66].

Previous studies found deposits of granular or amorphous material in the ER lumen of sporadic ALS patients, which can be associated to an accumulation of misfolded proteins, suggesting a relation between ER stress and motor neuron degeneration [31].

1.2.3.3 Protein aggregates

Protein aggregation represents one of the principal pathological hallmarks of ALS. Under normal conditions, cells can handle mutant proteins sufficiently well preventing their toxic gain of function and also their sequestration into inclusions. However, under pathophysiological circumstances, the ubiquitin proteasome system (UPS), that is activated to maintain protein quality control, could become overloaded. This leads to the engulfment of cells, which become defective in the disposal of altered macromolecules [7, 46, 50].

Recent studies have identified molecular constituents of ALS-linked cellular aggregates, including FUS. Despite strong evidence that protein aggregation is a hallmark of ALS, many questions remain about the role, formation and mechanism-of-action of these protein aggregates [7].

1.2.3.4 Neuroinflammation

The occurrence of a neuroinflammatory reaction is usually found in neurodegenerative disorders (including ALS) and consists of activated glial cells, mainly microglia and astrocytes, and T cells. Microglia are the resident macrophages [2] in the nervous system; they constantly monitor the extracellular environment, interacts with astrocytes and neurons and are the first line of defense against infection or injury to the nervous system. Astrocytes are ectodermal cells that have many complex functions in the nervous system such as regulating extracellular neurotransmitter concentrations, supporting surrounding neurons and maintain extracellular ion balance. Finally, T cells are a type of lymphocyte which infiltrates the CNS modulating the neuroinflammatory reaction differently in each stage of disease progression [52].

Several studies have shown that microglial activation is usually triggered by the infiltration of helper T cells[3] and cytotoxic T cells[4]. The presence of T cells is rare in early ALS stages, but readily infiltrate the spinal cord as the disease progresses. At the end stage of disease cytotoxic T cells predominate; thus, some hypothesis suggests that it explains why neuroprotective action ultimately fails (Figure 1.4) [52].

In the last years the interest in the contribution of microglia, astrocytes and T cells to motor neurons degeneration has been increasing and has given rise to clinical trials of drugs targeting neuroinflammatory reactions in ALS patients [52, 66].

[2] Macrophages are specialized cells involved in the detection, phagocytosis and destruction of bacteria and other harmful organisms [21].

[3] Helper T cells are a type of T cell that helps stimulate B cells (type of white blood cell of the lymphocyte subtype) to make antibodies and activates macrophages to kill ingested microorganisms [29].

[4] Cytotoxic T cells are a type of T cell that kills virally infected cells and tumours [68].

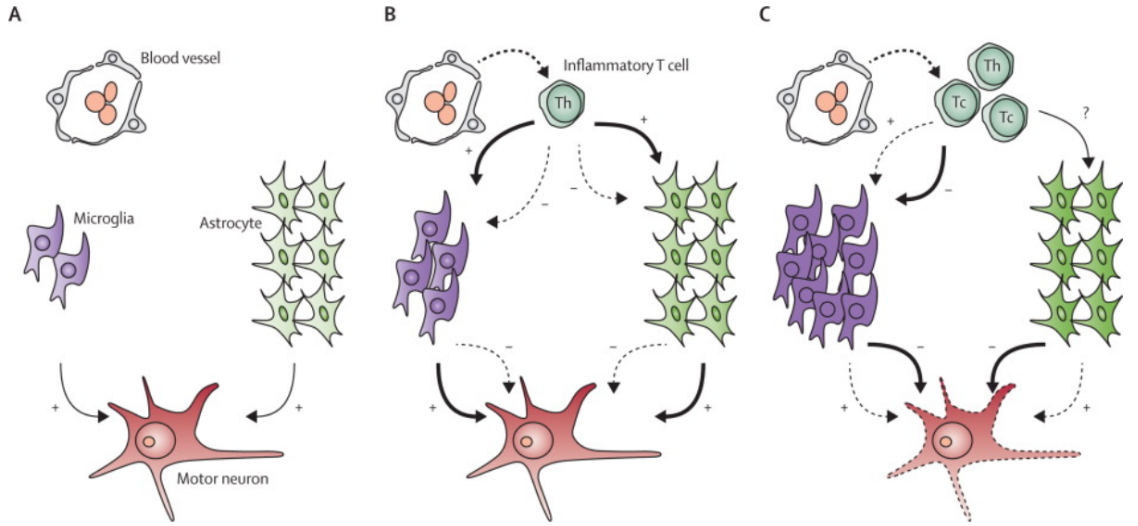

Figure 1.4: **Interaction of inflammatory T cells with microglia and astrocytes in ALS pathology.** (A) At asymptomatic stages of the disease, almost no T cells are found in the spinal cord. (B) At early stages of the disease, inflammatory T cells infiltrate the spinal cord from the blood. These T cells are mainly helper T cells which interact with surrounding microglia and astrocytes. Here, their neuroprotective action (thick arrow, +) overcome their neurotoxic effect (dashed arrow, -). (C) At later disease stages, cytotoxic T cells predominate in the spinal cord. These cells could trigger the production of a neurotoxic environment (thick arrows, -) instead of a neuroprotective environment (dashed arrows, +) surrounding motor neurons leading to their degeneration and consequently death. Th = helper T cell. Tc = cytotoxic T cell [Adapted from[52]].

1.2.3.5 Mitochondrial dysfunction

Mitochondria are rod-shaped organelles considered the "powerhouse" of cells since they convert energy into ATP which is essential for cells metabolism. They also have roles in vital processes including the production of cellular respiration, calcium homeostasis and control of apoptosis. Previous studies reported functional defects and morphological changes of mitochondria in skeletal muscle of ALS patients suggesting that mitochondrial abnormalities could be related to ALS. Moreover, a proposed mechanism suggests that mutant SOD1 is imported into mitochondria damaging this organelle and activating cell death [14, 41, 76].

1.2.3.6 Impaired axonal structure and disrupted transport

Motor neurons typically have extremely long axons (on the order of meter long) that can be vulnerable to damage. Axons conduct electrical impulses known as action potentials but also transports organelles, RNA, proteins and lipids to and from a neuron's cell body. Axonal transport is crucial for the survival of motor neurons and can be anterograde or retrograde. It is called anterograde transport when it moves away from the cell body, toward the synaptic structures at the neuromuscular junction, mediated by kinesins. On

the other hand, moving toward the cell body is called retrograde transport and it is mediated by cytoplasmic dynein [17, 76].

Dysfunction of both axonal transport, anterograde and retrograde, and axonal cytoskeletal disorganization, especially of neurofilaments, have been identified as causes of motor neuron degeneration. Defects in axonal transport can lead to an accumulation of neurofilaments, mitochondria and autophagosomes in motor neurons. In this regard, some experiments have shown that in the presence of ALS-linked SOD1 mutants, both anterograde and retrograde transport are slowed, months before degeneration. In addition, several studies have shown that mutation in dynactin, an activator of cytoplasmic dynein, has been associated with a reduction in retrograde transport leading to motor neurons degeneration [17, 66].

1.2.3.7 Glutamate-induced excitotoxicity

During glutamatergic neurotransmission, glutamate released from the presynaptic neuron activates ionotropic glutamate receptors[5] in the postsynaptic neuron. The activation of these glutamate receptors leads to the influx of Na+ and Ca2+ into the cell causing depolarization and the generation of an action potential. Afterwards, glutamate is removed from the synaptic cleft by excitatory amino acid transporters (EAATS). However, an increased release of glutamate or a failure to rapidly remove synaptic glutamate induces excitotoxity[6]. Nevertheless, it remains unclear if glutamate-induced excitotoxicity is a primary defect responsible for motor neuron degeneration or it is the result of ALS (Figure 1.5) [71].

[5] The ionotropic glutamate receptors are ligand-gated cation channels [71].

[6] Excitotoxicity describe the neuronal degenerative changes caused by over-stimulation of the glutamate receptors [63, 71].

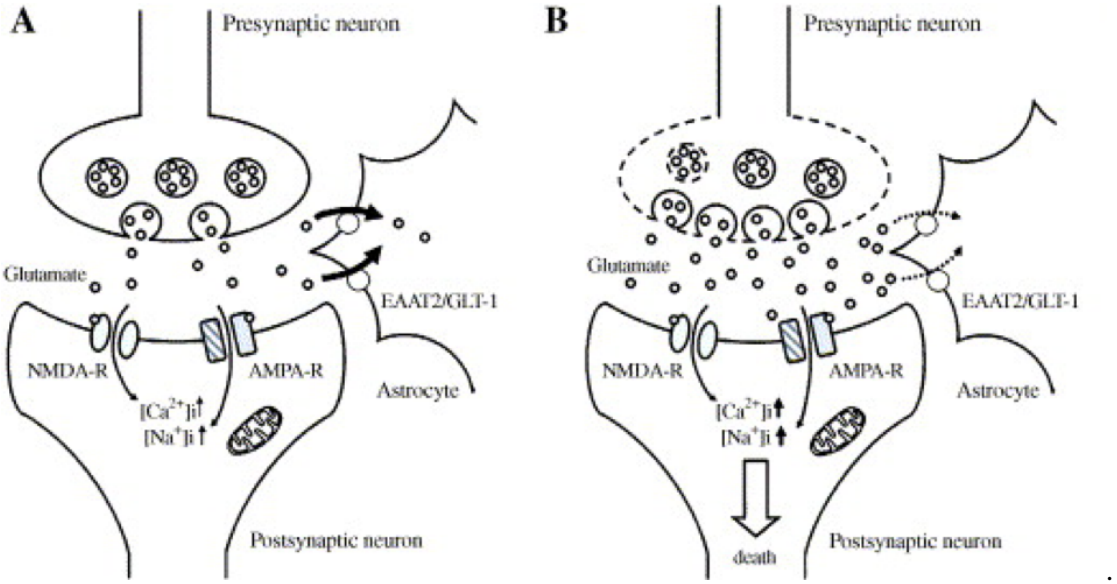

Figure 1.5: **Glutamatergic neurotransmission and excitotoxicity.** (A) Under the normal process, glutamate is released from the presynaptic neuron into the synaptic cleft activating the NMDA and AMPA ionotropic receptors in the postsynaptic neuron. This leads to the influx of Na+ and Ca+ ions into the cell causing depolarization and generation of an action potential. (B) Classical excitotoxity is induced by an increase of extracellular glutamate concentration. This can be caused by an increased release of glutamate or failure in reuptake of glutamate into the astrocytes by EAAT2/GLT-1 transporter. Thus, glutamate receptors are excessively stimulated giving rise to an excessive increase of the intracellular concentration of Na+ and Ca+ that can trigger motor neuron death. [Adapted from[71]].

Glutamate excitotoxicity has been associated with ALS due to the detection of high glutamate concentrations in the cerebrospinal fluid (CSF) of several patients with sporadic ALS. Moreover, the main argument for the role of excitotoxity in ALS is that riluzole, a clinical drug that slows the progression of the disease, has anti-excitotoxic properties [15, 71].

1.2.4 Treatment

Currently, there is no available treatment to stop or reverse the progressive degeneration of motor neurons in ALS. However, two clinical drugs can slow the progression of symptoms and prevent complications. The first drug approved by the FDA for the treatment of ALS was riluzole, a glutamate antagonist that blocks voltage-gated sodium channels leading to a decrease in the pre-synaptic release of glutamate. In May 2017, the FDA approved edaravone, an intravenous drug that counteracts the excessive oxidative stress in ALS by removing the free radicals in the nervous system. Indeed, these drugs only prolong the survival and delay the use of surrogate approaches such as mechanical ventilation. Hence, more than two decades after the acceptance of riluzole, the search for new therapeutic strategies is essential [20, 46, 47, 51].

1.3 Bioactive small molecules

Many studies have been supporting the possibility of changing the progression or the development of neurodegenerative diseases through diet. Indeed, several findings have been suggesting that bioactive molecules such as polyphenols[7], the most abundant in our diet, have protective effects in neurodegenerative disorders [23]. They are thought to be effective in the prevention or reduction of the impact of reactive oxygen species associated with oxidative stress and neurodegeneration because of their strong capability to induce intracellular signaling pathways related to gene expression and cell survival [32]. Hence, actual studies are trying to test their neuroprotective properties and also understand which of the hundreds of natural polyphenols available in our diet provide better effects [39, 49, 64].

Jimenez-Del-Rio *et al.* demonstrated that pure polyphenols such as gallic acid, ferulic acid, caffeic acid, coumaric acid, propyl gallate, epicatechin, epigallocatechin, and epigallocatechin gallate protect, rescue and, most importantly, restore the impaired movement activity induced by paraquat[8] in *Drosophila melanogaster* [32]. Similarly, Maccioni *et al.* revealed that standardized phytotherapic extracts, from medicinal plants widely used in Ayurvedic medicine, restored anomalous locomotion (i.e. impaired climbing performance with unexpected hyperactivity) and electrophysiological responses in a *Drosophila* model of ALS [39].

However, it remains unclear what concentrations are necessary to these small molecules reach the brain and what biologically active forms are need to exert beneficial effects. Therefore, more research is necessary to identify the molecular pathways and intracellular targets responsible for the protective effects of polyphenols [3].

1.3.1 Compound C

Edible berries are considered one of nature's treasure chests not only because they are an enjoyable fruit that provides energy, nutrients and dietary fiber, but also because they contain a large number of polyphenols with health-promoting properties. However, berries contain complex polyphenols mixtures making difficult to associate any interesting pharmacological activity to a single small molecule. For this reason, under the European BacHBerry project, more than twenty selected berry extracts, based on their metabolomic profile, were systematically analyzed to identify small molecules that have protective properties against neurodegenerative disorders. These extracts were tested on different *Saccharomyces cerevisiae* strains overexpressing proteins related to Alzheimer's, Parkinson's, Huntington's or ALS disease that confer toxicity in yeast. After the identification of blackberry (*Rubus genevieri*) extract as having bioactivity against ALS, it was fractionated

[7] "Polyphenols are a group of chemical substances present in plants, fruits, and vegetables, characterized by the presence of one or more than one phenol unit per molecule with several hydroxyl groups on aromatic rings" [32].

[8] Paraquat is a superoxide generator that induces oxidative stress [37].

and the obtained fractions were re-tested in the yeast model of ALS overexpressing FUS protein. All fractions were analyzed for its content by liquid chromatography coupled to mass spectrometry and some isolated small molecules from the bioactive fractions were re-tested. This screening revealed that Compound C displayed significant bioactivity in the yeast ALS model. So, Compound C was identified as a powerful protectant against pathological mechanisms associated with ALS disease in a yeast model overexpressing FUS (Figure 1.6) [30].

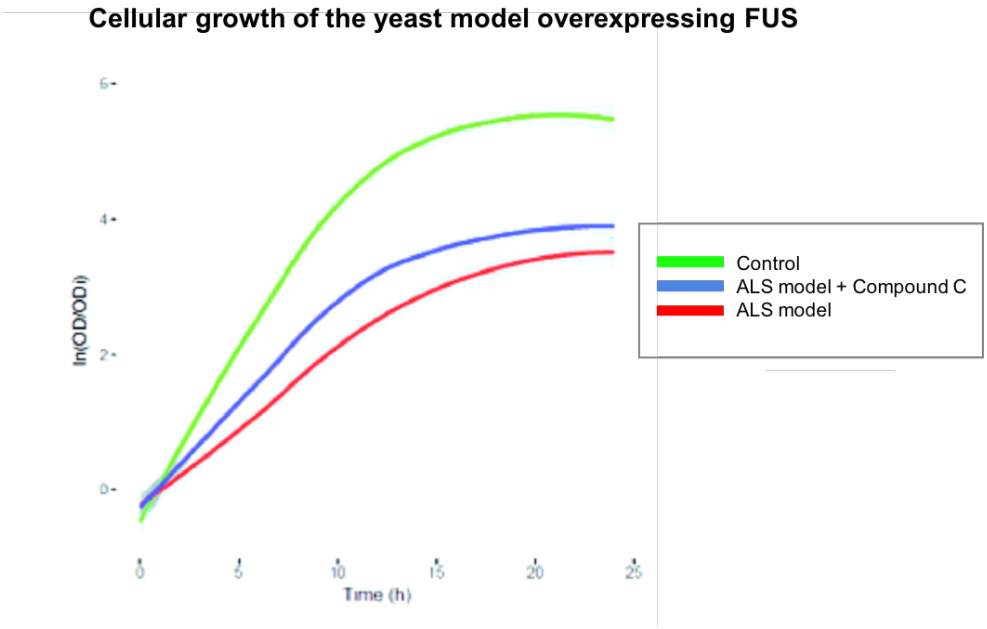

Figure 1.6: **Compound C protects the yeast model of ALS from FUS toxicity.** FUS overexpression impairs cellular growth (red) compared with the control (green) and treatment with Compound C rescues cellular growth (blue) [Unpublished results].

1.4 *Drosophila melanogaster* as a model system to study FUS-induced ALS disease

As an animal model, *Drosophila* has several advantages that make it extremely useful and important for biomedical research. Indeed, the relative simplicity, short lifespan, easy and cheap maintenance, approachable physiology and huge availability of powerful genetic tools make it a very attractive model to the study of several topics such as development, behavior and the basis of human disease [49, 67].

In particular, *Drosophila* models containing ALS-associated transgenes have been important tools for understanding disease pathogenesis. Previous studies showed that the expression of wild type or mutant human FUS alleles such as FUS[R521C] in the eye, motor neurons or the nervous system of the fly leads to eye degeneration, defects in locomotion and increase in mortality [36]. Thus, the *Drosophila* model of ALS overexpressing

human FUS alleles recapitulates the majority of ALS characteristics including progressive motor deficits, motor neuron degeneration and early lethality. However, the ALS-like phenotypes in these animal models are highly dependent on transgene expression levels and severity of phenotypes correlate with level of protein overexpression [77].

Interestingly, the homolog of human FUS gene in *Drosophila* corresponds to cabeza (caz) gene on X chromosome, that shares 53% amino acid identity to its mammalian counterpart. The *Drosophila* Caz protein has 399 amino acids and is expressed in neurons, glia and muscle cells [62].

1.5 Objectives and proposed approaches

This project had two main goals:

- Characterize the neuronal and kinematic decay of a *Drosophila* model of ALS;
- Test the effect of candidate small molecule (Compound C) in the motor decay of the *Drosophila* model of ALS.

Since FUS is one of the principal candidates in ALS development, our first step was to mimic the human disease by overexpressing human wild type FUS and human FUS with targeted mutagenesis (R521C). Once we profiled the mutant FUS induced degeneration at the kinematic level, we tested the protective effect of a small molecule (Compound C) previously tested for their capability to improve cellular growth of the yeast model overexpressing FUS.

The use of adult *Drosophila* as a model to test the efficacy of small molecules has multiple advantages. First, it allows challenging neurons in an *in vivo*, whole body context. Second, due to the fly's relatively short life span, it is possible to follow in a feasible time period the degeneration of motor activity. Finally, we can quantify with high detail a large set of locomotor features of animals undergoing degeneration, allowing detecting any relevant suppressions in the motor decay process.

To achieve the proposed goals, we performed survival, climbing and egg laying assays and we also analyzed the neurodegeneration in the fly eyes. Furthermore, a detailed analysis of the locomotor pattern of the flies modeling ALS disease using the FlyWalker was done. This approach was used to correlate cellular demise with specific kinematic consequences to the animals and most importantly, to quantitatively profile neurodegeneration that was critical to detect putative suppression of the neurodegenerative phenotype. Finally, we indirectly quantified the number of motor neurons establishing synapses with leg muscles.

Since the ultimate goal was to ameliorate the locomotor symptoms associated with ALS pathology, we fed the flies with Compound C in these experiments and tested its effect on the motor decay induced by the expression of FUS alleles.

CHAPTER 2

MATERIAL AND METHODS

2.1 Preparation of the fly food

The two concentrations of Compound C tested (7.5mM and 10mM) were obtained through successive dilutions, starting from a stock solution of Compound C dissolved in DMSO (500mM). In the cases that the flies were treated with RU486, 20µL of this compound was added to the 10 mM or 7.5 mM solutions (Figure 2.1).

Finally, 150µL of the selected solution were impregnated in the vials containing fly food overnight. With this method, the compound was not mixed in all the food, it just impregnated a few centimeters. However, given that the flies were transferred to new vials twice a week, they just ate the food at the surface.

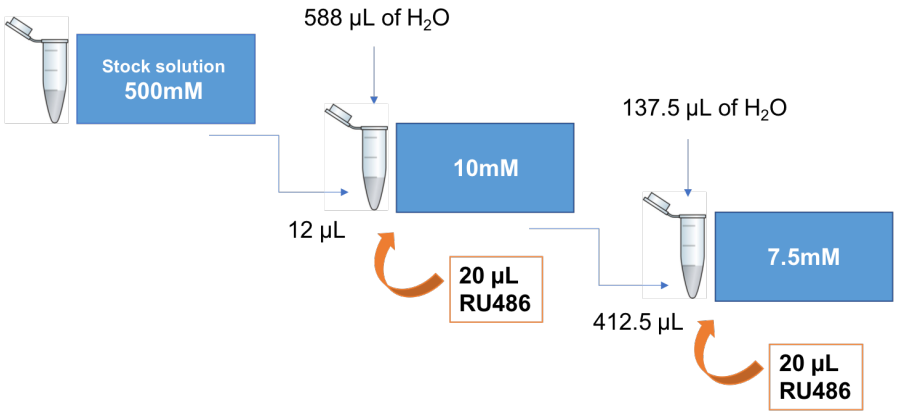

Figure 2.1: Protocol followed to obtain the different concentrations of Compound C tested.

2.2 Fly eye imaging

Eye phenotypes of one-day-old female flies were evaluated using Leica S6E and the images were acquired on Zeiss Stereo LUMAR stereoscope. The flies were placed at -80ºC for five minutes, before the imaging. For each genotype, 10 to 30 flies were evaluated. Embryos, larvae and pupae were exposed to DMSO or Compound C throughout their development and maintained at 25ºC in incubators without light.

2.3 Life span assay

Flies were crossed in the absence of DMSO, Compound C or RU486 on a standard food medium. Day 1 adult females were transferred on to new experimental vials containing fly food mixed either with DMSO or Compound C dissolved in DMSO, with (+) or without (-) RU486 (1 mM), at a density of 25 flies per vial for each genotype (n=3). Deaths were scored every two days and flies were transferred to fresh food two times a week. All the flies were maintained at 25ºC in incubators under a 12 h light/dark cycle.

2.4 Climbing assay

Motor function was assessed by a negative geotaxis response assay, commonly called climbing assay. Briefly, groups of 10 males of the same age of each genotype were placed into 18-cm-long vials, at room temperature for environmental acclimatization, and 10 min later they were tapped to the bottom of the vial. The climbing time was recorded when 50% of the population (five flies) crossed the 8-cm or the 15-cm finish line. At least 50 flies were tested in five independent groups of males per condition. Results are the average climbing time of these separate trials. The males were exposed to vehicle (DMSO) or Compound C from day one adult-stage and maintained at 25ºC in incubators under a 12 h light/dark cycle.

2.5 Egg laying assay

Reproductive outputs of the flies expressing FUS alleles were assessed by quantifying the number of laid eggs and emerged larvae. Briefly, five males and 15 virgin females, for each condition, were used for mating. After seven days of mating, males were discarded. At the selected time-points (seven, 14 and 21 days), ten female flies of each group were randomly selected and placed into apple juice agar plates during 24 hours and then the number of laid eggs was quantified using Leica S6E. Five days later, the number of emerged larvae was also registered (Figure 2.2). Adult flies, eggs and larvae were maintained at 25ºC in incubators under a 12 h light/dark cycle. Females were exposed to vehicle (DMSO) or Compound C, both mixed with RU486, from day one adult stage. This experiment was performed two times (n=2).

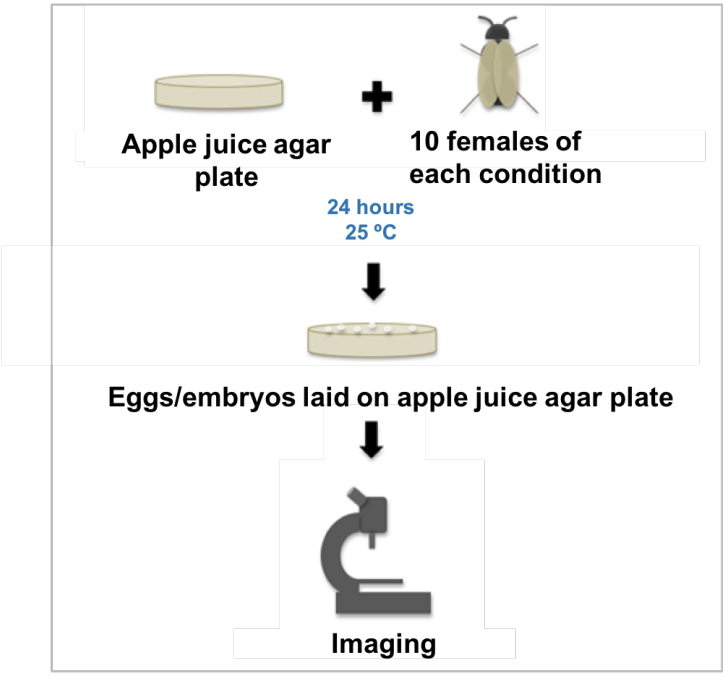

Figure 2.2: Schematic showing the procedure of the egg laying assay.

2.6 Quantification of motor neuron projection in the leg NMJ

In order to keep leg motor neuron axonal morphology intact for imaging, the legs were dissected and fixated carefully. Five flies per condition were selected and placed into empty tubes. To remove the hydrophobicity of the cuticle, the flies were washed in ethanol (not more than one minute). Afterwards, they were rinsed three times in 0.3% Triton in 1x phosphate buffered saline (PBS) (for one, five and 30 minutes in each wash) to increase penetration of the fixative inside the leg and then, the flies were dissected in this medium. Basically, the head and the abdomen of the flies were removed using forceps and then the coxa-thorax junction was gently but firmly pushed using the tip of fine forceps until the leg detached. Subsequently, the fixation was done in 4% paraformaldehyde (PFA) in PBS overnight at 4°C (approximately 20 hours total). Later, the legs were washed three times in PBT, for 20 minutes each wash at room temperature. Finally, the legs were mounted into glass slides using 70% glycerol medium. The imaging was done with a Zeiss LSM710 confocal microscope using a 40x water immersion objective.

2.7 FlyWalker basis

It is challenging to quantify walking behavior in *Drosophila* due to its small size and the lack of available tools. In order to overcome this limitation, Mendes *et al.* described an approach that can be used to examine the walking patterns of *Drosophila melanogaster*. The authors developed an optical touch sensor that is based in frustrated Total Internal Reflection (fTIR) method coupled with high-speed video imaging which detects the fly's body and leg contacts on the floor during locomotion [43].

Total Internal Reflection occurs when light travels from a medium with a high refractive index, in this case optical glass, to one with a lower refractive index such as air. If the angle of incidence is higher than the critical angle (as compared to the normal of the surface), defined by Snell's Law, the light is internally reflected rather than refracted. However, when a denser material such as the tarsus of an insect leg touches the surface of the glass, the locally 'frustrated' total internal reflection will scatter the light and that can be recorded by a high-speed video camera (Figure 2.3) [40, 43, 44].

Each movie is acquired at 250 frames per second and it can be analyzed frame-by-frame. In each frame, the fTIR effect allows to visualize the fly legs that are in contact with the glass and also the fly body due to the background light (Figure 2.3). Afterwards, the tracking of each tarsal contact and the fly body is done with the FlyWalker program (Figure 2.4). This custom-made software evaluates the fTIR signals in terms of pixel intensity in each movie and outputs several graphs and user-defined kinematic parameters that can be used to describe fly walking behavior with high temporal and spatial resolution. The parameters include step, spatial and gait parameters [43].

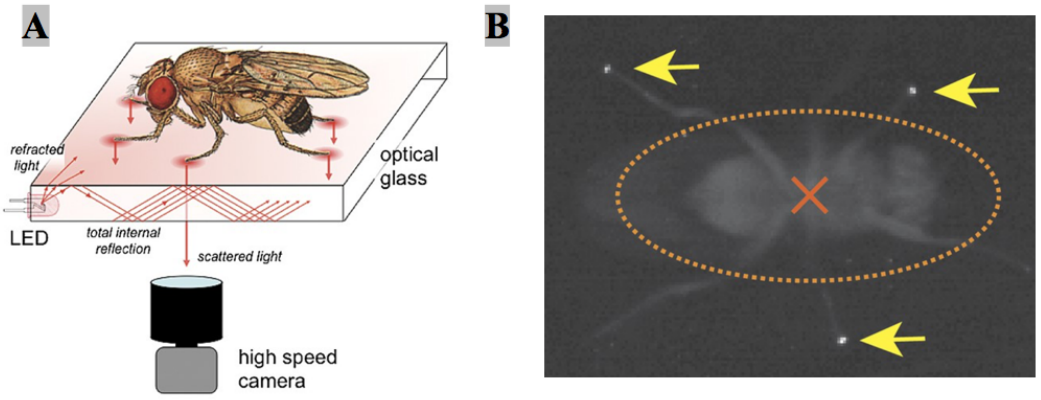

Figure 2.3: **Schematic of the fTIR optical effect.** (A) Detailed description of the fTIR apparatus. Light that comes from LED light sources located at the edges of an optical glass propagates within the glass by internal reflection. Tarsal contacts lead to light scattering which can be recorded by a high-speed video camera. (B) Single frame of a fTIR movie. The fTIR effect can be seen for three legs in stance phase (yellow arrows). The orange dashed ellipse corresponds to the body delimitation; the center of the body is indicated by an orange cross [Adapted from[43]].

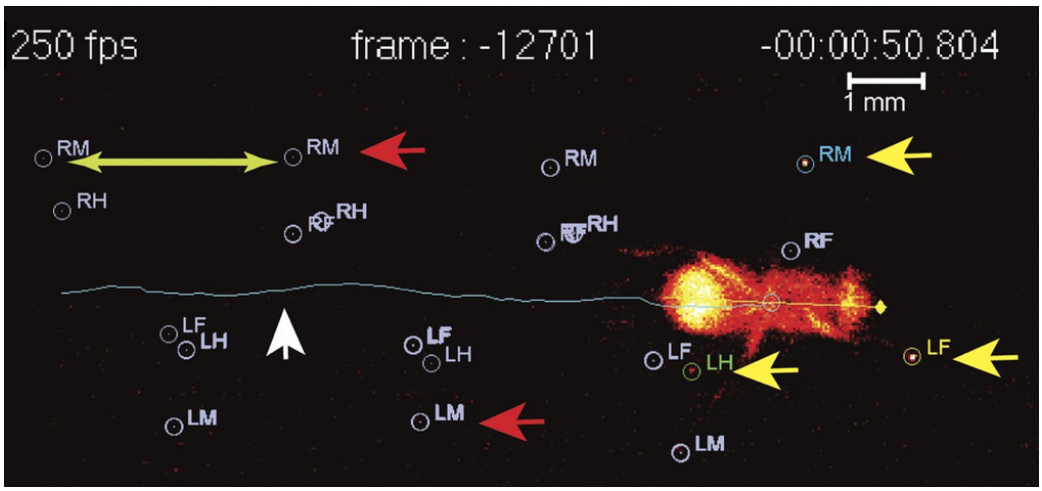

Figure 2.4: **Image generated by the FlyWalker software.** The fly's footprints and body center are tracked throughout the video. It is possible to identify the present footprints (yellow arrows), the past footprints (red arrows) and the fly body and trajectory (white arrow). Step length, which is defined as the distance between two consecutive footprints, can also be visualized (green arrows) [Adapted from[43]].

2.7.1 Step parameters

Drosophila has six legs and, in a step cycle, each leg goes through a period of stance phase, in which the leg is touching the ground, or a swing phase meaning that it is up in the air. Previous findings have shown that, in several insect species, when the speed increases, stance phase duration becomes shorter and swing phase duration remains predominantly constant; at the higher speeds, the duration of both stance and swing phases becomes equal [25, 74].

One of the parameters that it is possible to extract from FlyWalker analysis are the step parameters that are related to individual leg movement. These parameters include the duration of stance and swing phases, step frequency (number of steps per second), step period (time taken to complete one leg cycle), step length (distance between two successive footprints of the same leg), average speed and swing speed (Figure 2.5) [43].

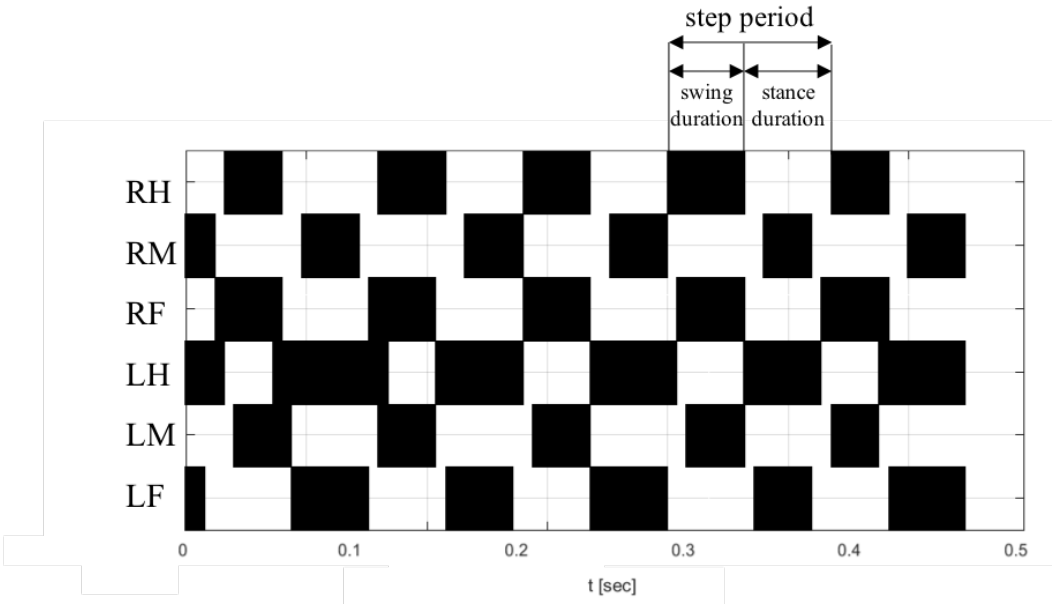

Figure 2.5: **Step pattern of a general fly walking at 40 mm/s (average) obtained with the FlyWalker software.** The swing and the stance phases are represented by the black and white regions, respectively. The step period, swing duration and stance duration are indicated by the arrows [Adapted from [43]].

2.7.2 Spatial parameters

The spatial parameters are related to the perception of the surface. They analyze the first and last moments that the leg contacts with the glass surface and how much straight are the stance traces generated between those moments. The onset of these traces, which corresponds to the position where the leg first touches the glass, is termed the Anterior Extreme Position (AEP) while the end of stance traces, before the tarsi enter swing phase, corresponds to the Posterior Extreme Position (PEP). For each stance trace, a smoothed version of the trace is generated and the average of the difference between these two lines allows to calculate the stance linearity index parameter. Thus, faster flies have straighter stance traces (lower stance linearity indexes) when compared with slower flies. Another spatial parameter is the stance straightness index that corresponds to the ratio between the displacement (AEP-PEP vector length) and the path length. Footprint clustering is also a relevant spatial parameter and it is related to the clustering of the AEP's and PEP's. This parameter corresponds to the standard deviation from the average position for all AEP's or PEP's calculated for each leg. For instance, if the footprint clustering value of the foreleg AEP is small, it means that the AEP coordinates were similar for all the foreleg steps in the video (Figure 2.6) [43].

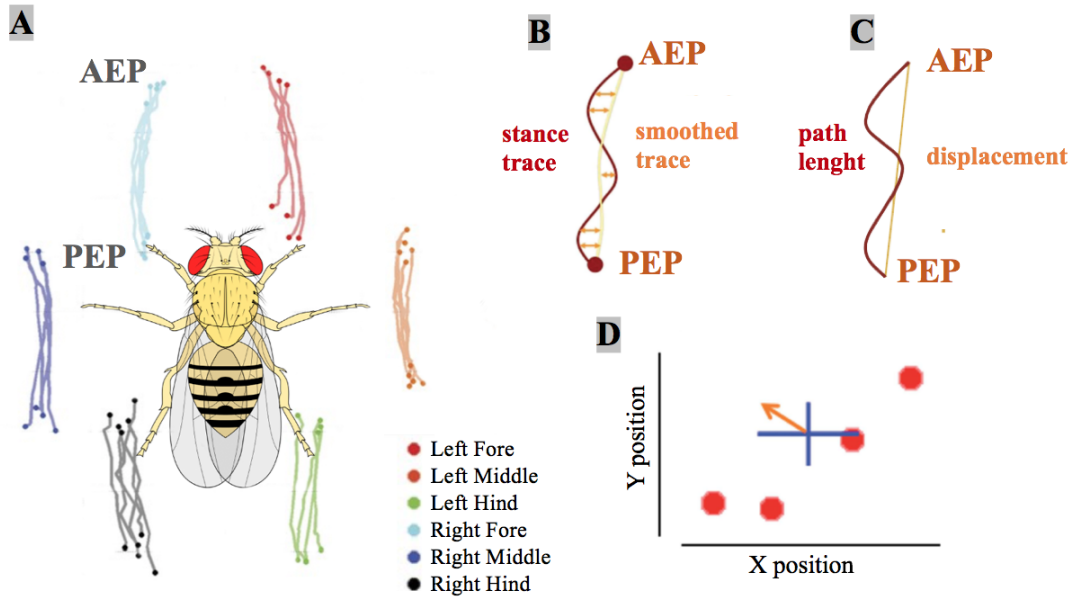

Figure 2.6: **Schematic diagram of general spatial parameters obtained with the FlyWalker software.** (A) Representation of the stance strances for each leg of a general fly. AEP and PEP positions are also identified. (B) Method to calculate the stance linearity index. It can be obtained by computing the average difference between an actual stance trace and a smoothed trace. (C) The stance straightness index indicates how much wiggly is the body center relative to each footprint and corresponds to the ratio between the displacement and the path length. (D) Method to quantify footprint clustering. An average ±STD xy point is generated (blue cross) for each set of AEP/PEP footprints (red circles). The footprint clustering value is calculated as the vector sum of the two STD values (orange arrow) [Adapted from[43]].

2.7.3 Gait parameters

Gait parameters analyze coordination between legs. Insect gaits can be either tripod or tetrapod (Figure 2.7), depending on the speed and body load. Flies usually walk using tripod gait which is characterized by three legs in stance phase and three legs in swing phase at any one time. Each group of three legs is constituted, on one side, by the fore and hind legs and, on the contralateral side, by the middle leg. In contrast, a tetrapod gait is characterized by two legs in swing phase and the remaining four legs in stance phase. The two legs in swing phase are localized on contralateral sides and are offset by one segment. It is also observed several non-canonical stance combinations that do not fit in these idealized gaits. In addition, at slow speeds flies occasionally walk with only one leg in swing phase which characterizes the so-called 'wave gait' in which individual legs swing in a wave-like pattern from front to back [43].

For each video, a step pattern can be generated (Figure 2.5) and the instantaneous speed and gait characteristics are simultaneously plotted with high temporal resolution (Figure 2.7). The instantaneous speed plot has a wave-like appearance in which the minimum speeds correspond to the transition between phases, when the stance switches

to a different group of legs. For each frame in a video, it is possible to classify if the fly is in a tripod, tetrapod or non-canonical stance (sometimes wave gait is also used). These results are plotted in a gait map that graphically shows the gaits used over time (yellow for tripod, blue for tetrapod, and grey for non-canonical). To quantify the gait maps, the tripod, tetrapod and non-canonical indexes are calculated. These gait indexes correspond to the percentage of frames in a video that displays leg combinations defined by the tripod, tetrapod and non-canonical gait, respectively [43].

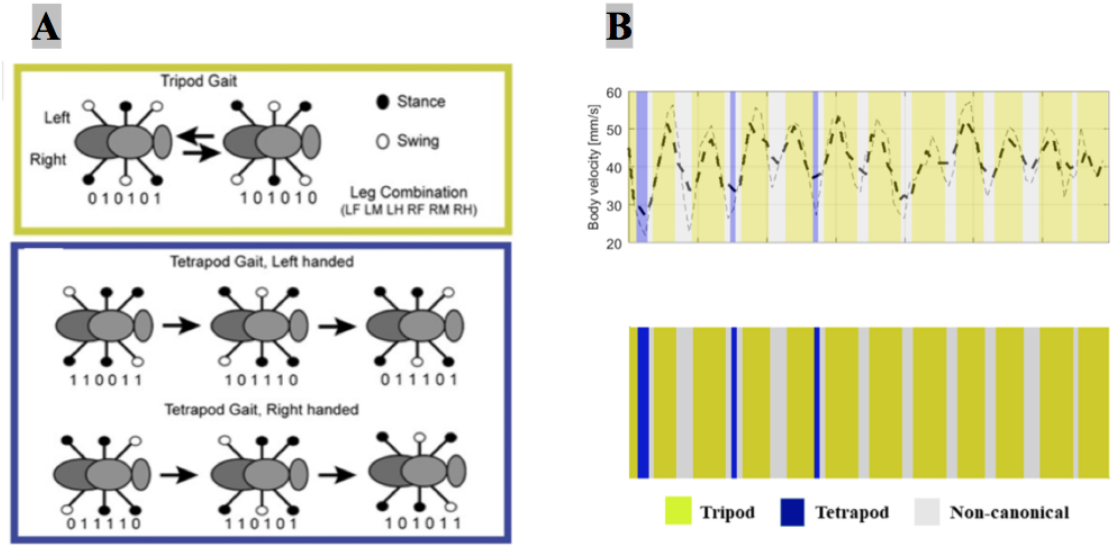

Figure 2.7: **Schematic diagram of some gait parameters obtained with the FlyWalker software.** (A) Representation of the different gaits and leg combinations used by the flies during the walk. Black circles and '1' corresponds to stance phase and white circles and '0' means swing phase. (B) Speed and gait graphs obtained with the FlyWalker software for a general fly walking at 40mm/s on average. The color code corresponds to the gaits used by the fly overtime in all the movie. It is possible to visualize that this female fly used mostly the tripod gait which corresponds to higher values of body velocity [Adapted from [43]].

2.8 FlyWalker procedure

2.8.1 Fly preparation

The flies used to perform the FlyWalker analysis were raised at the same conditions as outlined in the survival assay. Before the acquisition, each group of flies was anesthetized with ice and placed 30 minutes into empty vials to clean their legs.

2.8.2 Data acquisition

The image acquisition was done with a *Photron* (1024 x 336) or a *Point Grey* camera (2048 x 1088), both at a frame rate of 250 frames/s. It was necessary to clean up the

optical glass where the flies walk with optic cleaning fluid before the acquisitions. Each fly was inserted into the fly chamber using a mouth aspirator and the acquisition of the data started immediately after the insertion; thus, flies did not have time to adapt to the surrounding environment. Moreover, the duration of the acquisition did not last longer than one minute. For each time point, approximately seven to ten flies were evaluated.

2.8.3 Movie cropping

The temporal cropping of the movies acquired with the *Point Grey* and the *Photron* cameras was done with the *StreamPix* 6.5.0.0 and the Photron FASTCAM Viewer 3.6.9.1 (PFV3) software, respectively. The videos were temporally cropped by selecting the first and the last frames, giving rise to small sequences of .png files. The chosen sequences contained a series of five to six step cycles for each leg, where the fly walks straight and from left to right. Then, the sequences acquired with the *Point Grey* were load in Image J software to be spatially cropped in order to have a smaller image containing the sequence of interest. The movies acquired with the *Photron* camera were cropped temporally and spatially using the same software, PFV3. In total, approximately 120 movies were cropped.

2.8.4 Fly tracking using the FlyWalker software

The custom-made FlyWalker software, written in MATLAB® R2016b, was used to perform the fly tracking process. The first step was to load the sequence to be analyzed through this software. Then, the length of the fly was measured, with the option "ruler"available in the interface, and introduced in the software settings. Moreover, the threshold values for the legs and body were defined in the settings to optimize the auto-tracking process. After the auto-tracking, the detection of the legs and the center of the body were confirmed. If there were detected any defects, it was done hand correction. If not, the evaluation of the movie proceeded. The evaluation process resulted in a set of graphs (including the stance traces, the step pattern, the gait map,...) and also a Microsoft Excel file with all the kinematic parameters that describe the walking patterns of each fly.

2.8.5 Data analysis

The Excel file includes a summary line containing all the parameters and their values. To compare different conditions, these lines were all grouped in another Excel file. Then, for each motor parameter, a scatter graph containing the raw data of the different groups was generated using the Excel tools. From here, it was possible to observe and select the relevant variables for further analysis. The parameters were considered relevant when it was possible to distinguish the groups of interest in the scatter plots.

Based on this first approach, the next step was to calculate the residual values using a script written in R. Given that most of the kinematic parameters vary with speed, the

R script determined the best fit regression model for the control condition and then it computed the residual values for each experimental condition in relation to this regression model. After, the data was expressed as the difference to the residual-normalized line in PCA, heat map and box plots. To perform statistical tests, it was necessary to verify if the data was normally distributed and homoscedastic (i.e. equal variance for all predictors). The normality assumption was confirmed using the Shapiro-Wilk test and the homoscedasticity assumption was confirmed using the Levene's Test. Afterwards, if the data was considered normally distributed and homoscedastic, the test used was one-way-ANOVA. The null hypothesis of this test is that the means of all groups considered were the same. If the null hypothesis was rejected (p-value < 0.05), it was performed the Tukey's post hoc test between each group and the control. Otherwise, if data was not normal and homoscedastic, non-parametric tests were performed. In these cases, for comparisons of more than three groups, it was used Kruskal-Wallis analysis of variance. If the null hypothesis, that the median of all groups was the same, was rejected (p-value < 0.05), the Dunn's post hoc test was performed to see the significant differences between each group and the control. The graphic representations such as the heat maps and the PCA were made with scripts written in Python 3.4 software. The box plots were done with GraphPad Prism software version 7.

2.8.5.1 Residual values - Detailed explanation

To calculate the residual values, a regression analysis was performed in order to find the best fit (linear or non-linear) for each parameter of the control condition. Afterwards, the residuals were obtained by computing the distance of each value (including control values) to the regression model (Figure 2.8). There was one residual for each data point. They were positive if they were above the regression model and negative if they were below the regression line. If the point passed through the regression line, the residual at that point was zero.

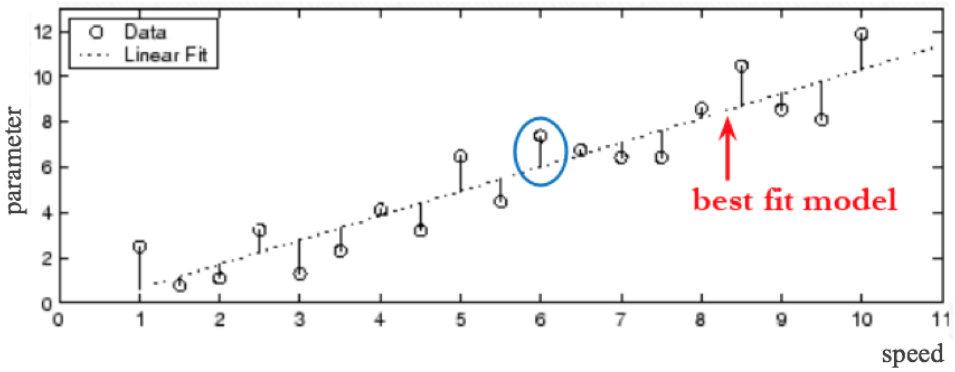

Figure 2.8: **Method to obtain residual values.** The best fit model is indicated by the red arrow. A residual is the vertical distance between a data point and the regression line (blue).

2.8.5.2 Principal Component Analysis (PCA)

Principal Component Analysis is a technique commonly used for dimensionality reduction. Briefly, it projects a complex dataset onto a lower-dimensional space that still contains most of the information in the large set. Since PCA "ignores" class labels, it can be described as an "unsupervised" algorithm. Thus, the objective of this method is to find directions (called principal components) that maximize the variance of the data. The first principal component explains the most extensive variance in the original data set. The second principal component is determined in the same way, with the condition that it is perpendicular to the first principal component and that it accounts for the next highest variance. This continues until a total of n principal components have been computed, equal to the original number of variables. For visualization, usually the first one, two or three principal components are used to plot the data in an attempt to reveal any groupings [33, 70].

2.9 Overall statistical considerations

Most of statistical analyses were done using GraphPad Prism software version 7. For the survival assays, it was performed a Log-rank (Mantel–Cox) test. For climbing and egg laying assays, it was performed a two-way ANOVA followed by a Tukey post-test. In the FlyWalker analysis, statistical tests were performed as outlined above. It was used "ns"for non-significant data. Statistic significant were considered when $*pvalue \leq 0.05, **pvalue \leq 0.01, ***pvalue \leq 0.001$.

Chapter 3

Results and Discussion

3.1 Ectopic expression of human FUS alleles leads to neurodegeneration in *Drosophila* eyes

In order to observe the effects of the expression of human ALS-related FUS alleles in the fly eyes, transgenic flies overexpressing wild type (WT) or mutant (R521C) human FUS in the eyes were generated using the GAL4/UAS system. Comparing to the control (UAS-GFP), the expression of FUS alleles using GMR-gal4, an eye driver, caused severe neurodegeneration in *Drosophila* eyes characterized by disorganized ommatidia and loss of pigmentation and mechanosensory bristles. Moreover, the FUS alleles reflected the expected strength, with the phenotype of mutant human FUS more aggressive than the wild type form. Nonetheless, the misexpression of FUS[WT] also induced neurodegeneration (Figure 3.1).

These results demonstrate that the expression of human ALS-related FUS alleles causes neurodegenerative phenotypes which is consistent with the gain-of-toxicity mechanism that has been proposed for ALS disease. Furthermore, they confirm that the FUS[R521C] allele causes stronger degeneration that the wild type version [36].

In addition, it was analyzed the expression of other FUS alleles such as FUS[R518K] and FUS[R521H] in the fly eyes. However, no differences were observed regarding the control which was probably due to problems in transgene generation (data not shown).

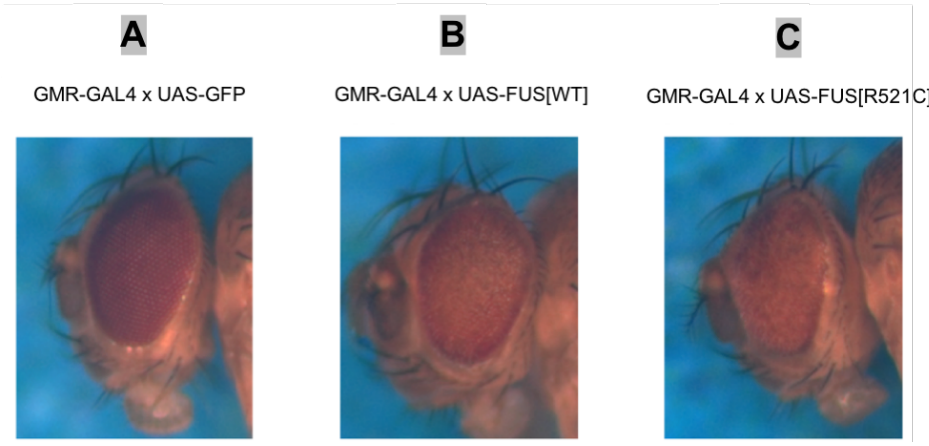

Figure 3.1: Imaging of day 1 adult fly eye expressing FUS alelles (B,C) under the control of GMR-gal4 driver (A).

3.1.1 Compound C does not ameliorate the neurodegenerative phenotype in the fly eyes

To try to suppress the neurodegenerative phenotype, flies with the same genotype as above were fed with Compound C during development. Given that Compound C was dissolved in DMSO, another batch of flies was supplied only with DMSO in order to use it as a control for further comparison. Thus, two concentrations of Compound C were tested: 7.5mM and 10mM (Figure 3.2).

After the treatment with Compound C, no visible modifications were found in the fly eyes. In addition, the eye phenotypes of the flies fed with DMSO were similar to the ones found for the standard condition (Figure 3.1).

Taken together, the results suggest that, in these concentrations, DMSO is not toxic for the flies and the exposure of the fly to a medium supplemented with Compound C does not ameliorate the neurodegenerative phenotypes caused by the expression of FUS alleles in the eyes.

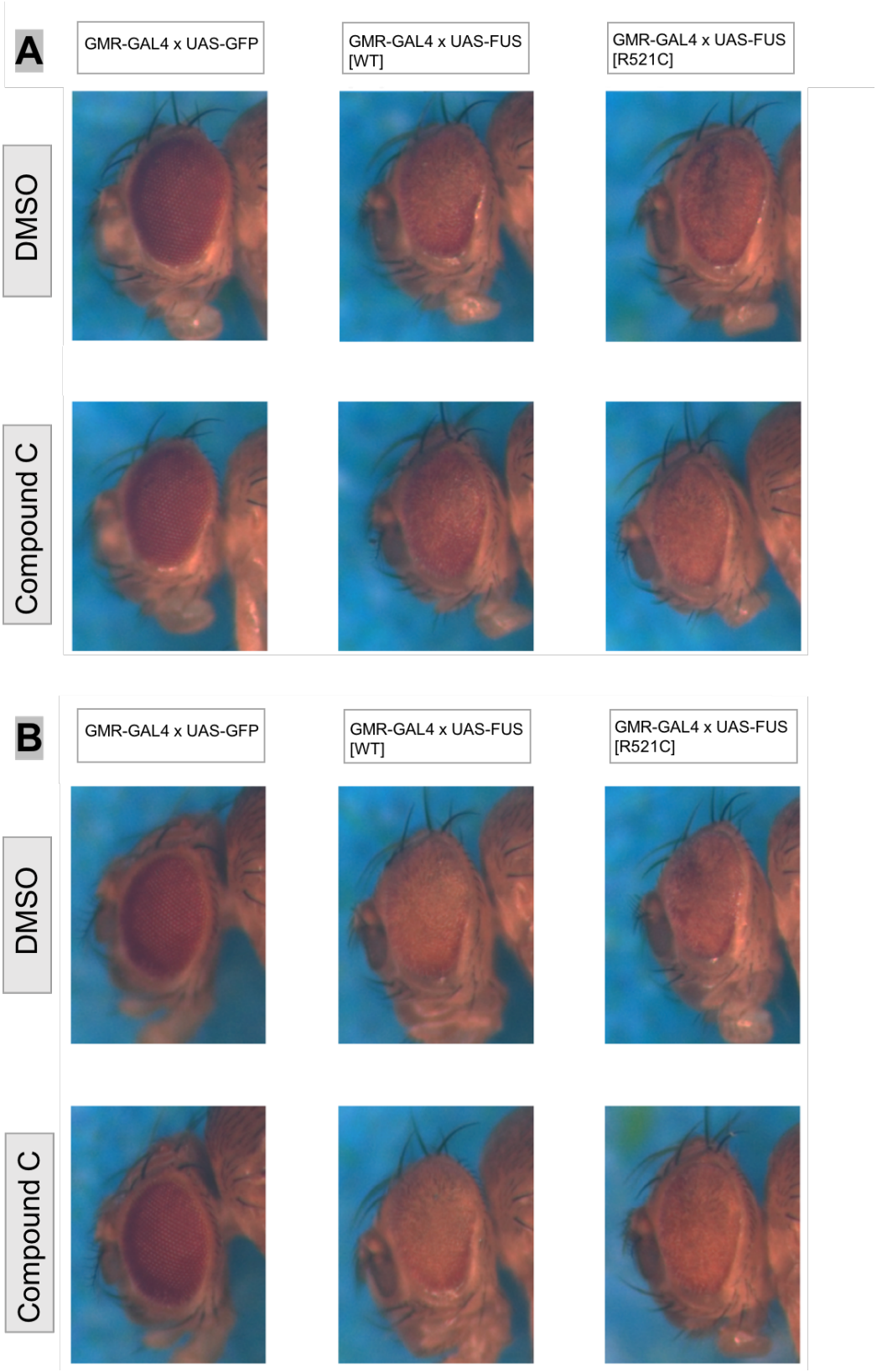

Figure 3.2: **Eye neurodegenerative phenotypes after the treatment with Compound C.** These flies were supplemented with (A) 7.5mM and (B) 10 mM of DMSO (first row) and Compound C (second row) during development.

3.2 Conditional expression of human FUS alleles in *Drosophila* neurons increases mortality

To mimic the human disease in *Drosophila*, FUS alleles were overexpressed in the neurons of the fly using the conditional expression system ElaV-GeneSwitch (ElaV-GS). Briefly, following treatment with RU486, the Gene Switch protein was transcriptionally activated and bound to UAS inducing the expression of the respective FUS protein specifically in the nervous system [36].

Then, the effects of the neuronal FUS expression on the life span of the flies were determined by monitoring their survival rate from day one adult stage on. Given that one of the objectives of this project was to test the protective effect of Compound C, it was considered two groups of females flies: one fed with standard food mixed with the vehicle and another one supplied with Compound C (10mM). In each group, three genotypes were considered: ElaV-GS;UAS-GFP (control), ElaV-GS;UAS-FUS[WT] and ElaV-GS;UAS-FUS[R521C], each one treated with or without RU486 (1mM). For each condition, 75 flies were analyzed.

In the group fed with the vehicle, there was very low mortality in the flies expressing the driver alone treated with (+) or without (-) RU486, since >90% flies were viable after 30 days of DMSO exposure in both cases. However, the induction of FUS[WT] and FUS [R521C] in adult neurons caused a decline in the survival rate when compared with the driver alone, even in RU486 untreated flies (-), which was not expected. Furthermore, the induction of FUS[R521C] drastically shortened the life span when compared with FUS[WT]. These findings revealed a mutation-dependent decline in the life span of the FUS[R521C] expressing animals. However, flies expressing FUS[WT] also exhibited a decline in life span, but the degree of severity was less than mutant FUS animals (Figure 3.3).

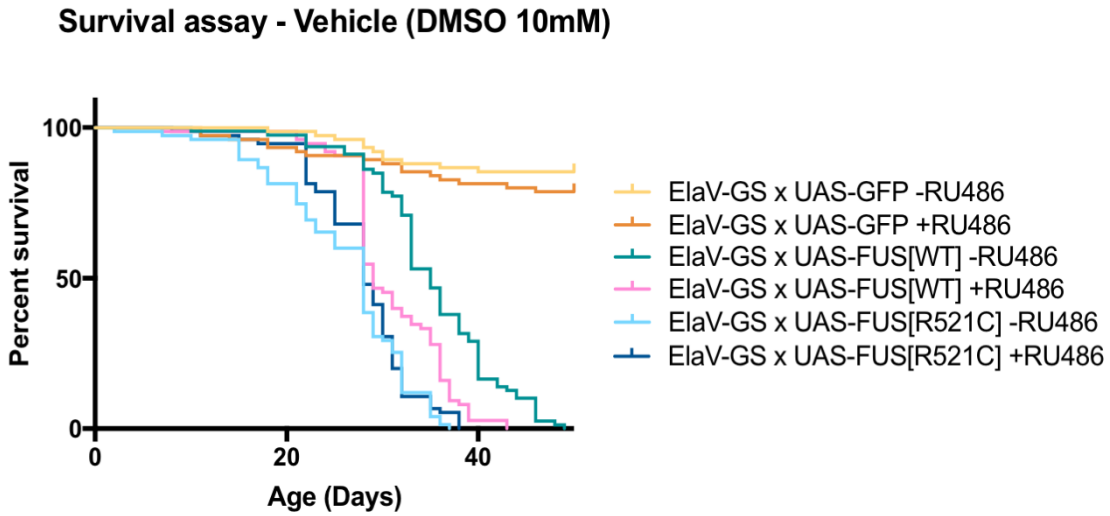

Statistical differences

vs	ElaV-GS x UAS-FUS[WT] - RU486	ElaV-GS x UAS-FUS[WT] + RU486	ElaV-GS x UAS-FUS[R521C] - RU486	ElaV-GS x UAS-FUS[R521C] + RU486
ElaV-GS x UAS-FUS[WT] - RU486	-			
ElaV-GS x UAS-FUS[WT] + RU486	***	-		
ElaV-GS x UAS-FUS[R521C] - RU486	***	***	-	
ElaV-GS x UAS-FUS[R521C] + RU486	***	***	ns	-

Figure 3.3: **Lifespan of female flies expressing FUS alleles under the control of ElaV-GS.** The survival curves show the percentage of flies alive as a function of age. In both flies maintained with (+) or without (-) RU486, the FUS alleles are expressed and the neuronal expression of FUS[R521C] strongly decreases the lifespan, whereas the expression of FUS[WT] has a weaker effect on the reduction of life span. Control flies showed normal life span with many flies living after the end of the experiment. In the FUS alleles, the maximum survival (in days) is indicated for each condition (the mean values indicate the number of days it took for half of the flies to die): FUS[WT] - RU486 49 (mean=33), FUS[WT] + RU486 43 (mean=28), FUS[R521C] - RU486 37 (mean =26), FUS[R521C] + RU486 38 (mean =28). The controls are significantly different from all the other conditions (***) (P<0.001) but they are not significantly different from each other (log-rank, Mantel–Cox test). Statistical significances for FUS alleles are indicated bellow the graph. Statistic significant were considered when $*pvalue \leq 0.05, **pvalue \leq 0.01, ***pvalue \leq 0.001$.

3.2.1 Exposure to DMSO (corresponding to the 2% used in the 10mM of compound C) is not toxic for the flies

To confirm that DMSO was not causing any toxicity in the flies, a survival assay was performed with flies treated only with standard food mixed with RU486. Given that the obtained curves are not significantly different from the ones achieved for DMSO, it seems that DMSO is not toxic for the flies at 2%, its final concentration (Figure 3.4).

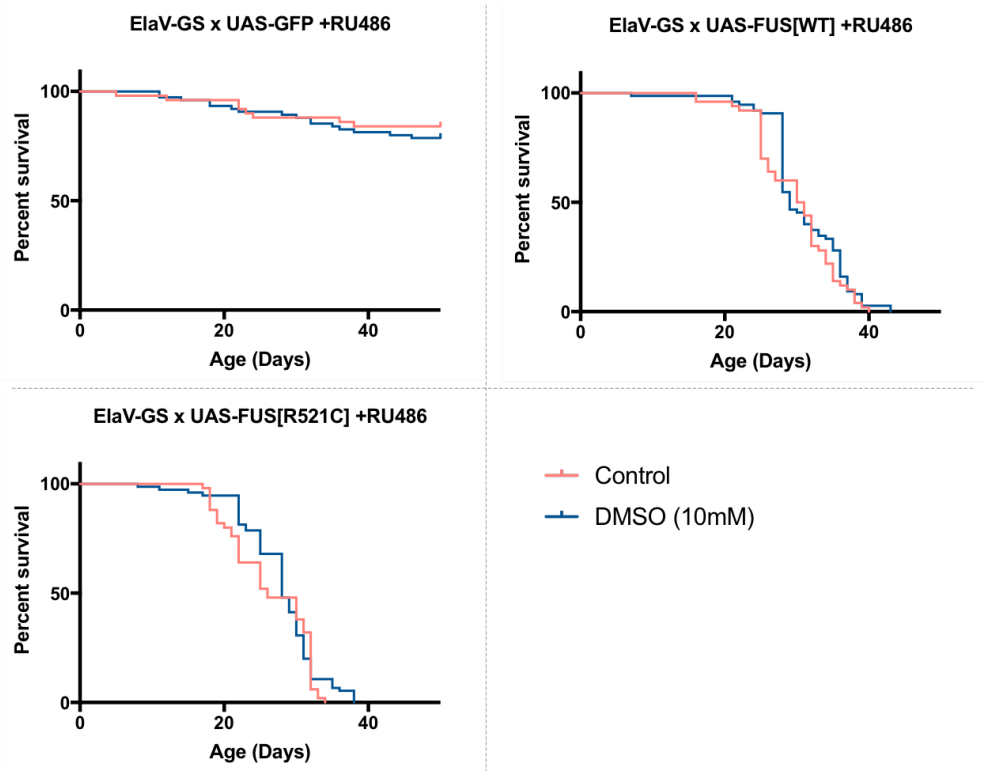

Figure 3.4: **Life span of female flies expressing FUS alleles under the control of ElaV-GS - DMSO toxicity.** The survival curves show the percentage of flies alive as a function of age. The control condition corresponds to the standard feeding. In the three genotypes, the survival of the control condition is not significantly different from the survival of flies fed with DMSO (log-rank, Mantel–Cox test).

3.2.2 The treatment with Compound C extends the life span of FUS[WT] flies

Flies were fed with Compound C during the adult-stage and their lifespan was examined. Comparing to animals fed DMSO, Compound C extended the lifespan of flies expressing FUS[WT] under treatment with RU486 (Figure 3.5). Indeed, 50% of FUS[WT] flies fed with DMSO were dead after 28 days with all of the flies dead in 43 days. On the other hand, in flies expressing FUS[WT] fed with Compound C, approximately 50% of flies were gone after 36 days and there was one fly that survived beyond the end of the study (50 days). These results propose that Compound C ameliorates the decline in the survival rate

caused by the expression of FUS[WT] in the neurons of the fly using RU486. In addition, Compound C did not extend the life span of the flies expressing FUS[521C] possibly because this phenotype is too aggressive or because it kills by a distinct mechanism insensitive to Compound C.

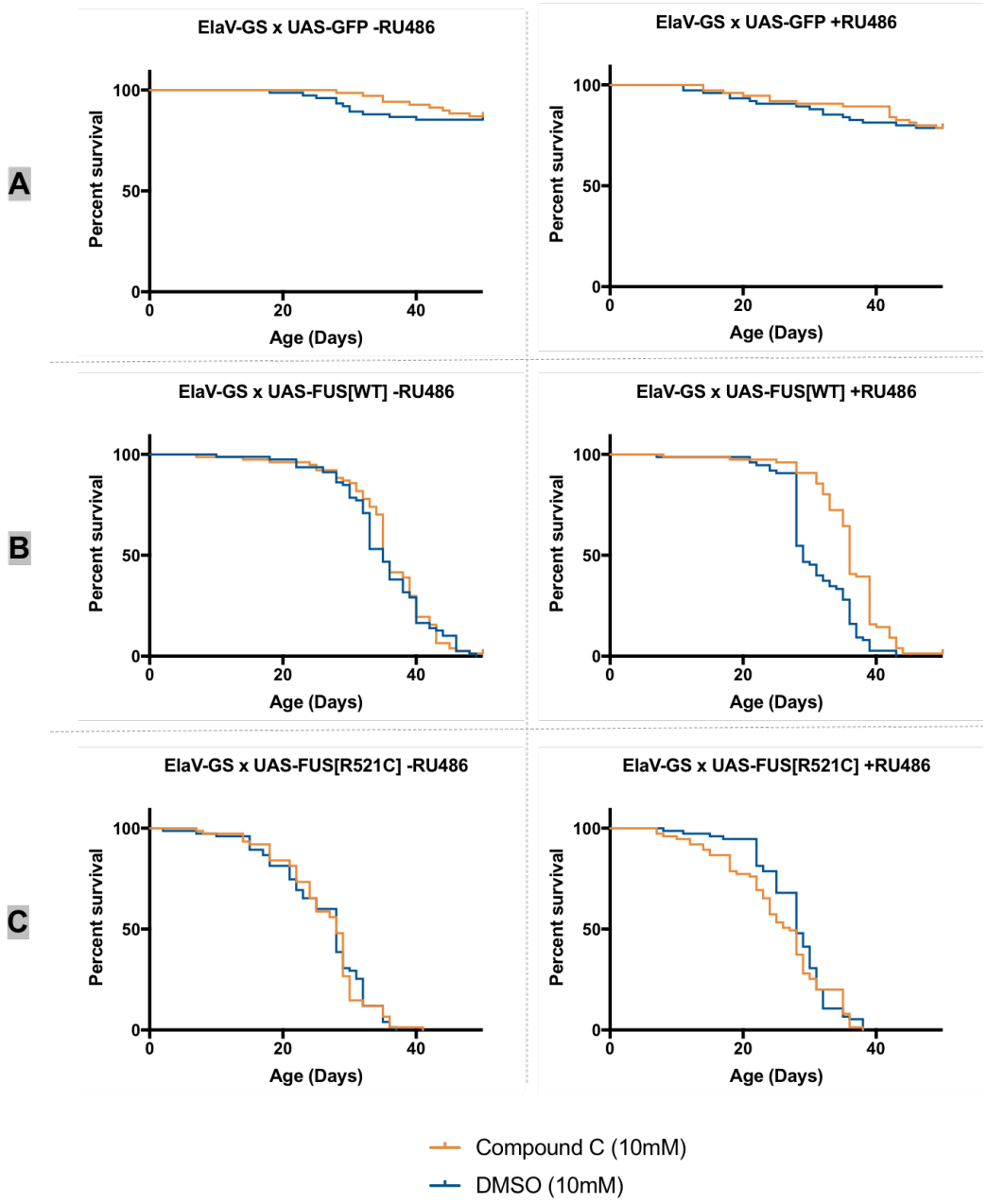

Figure 3.5: **Lifespan of female flies expressing FUS alleles under treatment with Compound C - comparison with vehicle.** The survival curves show the percentage of flies alive as a function of age. Each row corresponds to a different genotype (under treatment with or without RU486): (A) ElaV-GSxUAS-GFP, (B) ElaV-GSxUAS-FUS[WT] and (C) ElaV-GSxUAS-FUS[R521C]. The graphs suggest that Compound C only increases the life span of the flies expressing FUS[WT] in the presence of RU486. In this case, the curves are significantly different from each other (***) ($P<0.001$) (log-rank, Mantel–Cox test).

3.3 FlyWalker analysis

Given that in the survival assay Compound C extended the life span of flies expressing FUS[WT], the FlyWalker analysis was done with two genotypes: the control (ElaV-GS;UAS-GFP) and ElaV-GS;UAS-FUS[WT] under the treatment with RU486. Furthermore, the movies were recorded in time points where motor impairment was visible but not severe, which increased the possibilities to detect any suppression of the degenerative phenotype (Figure 3.6).

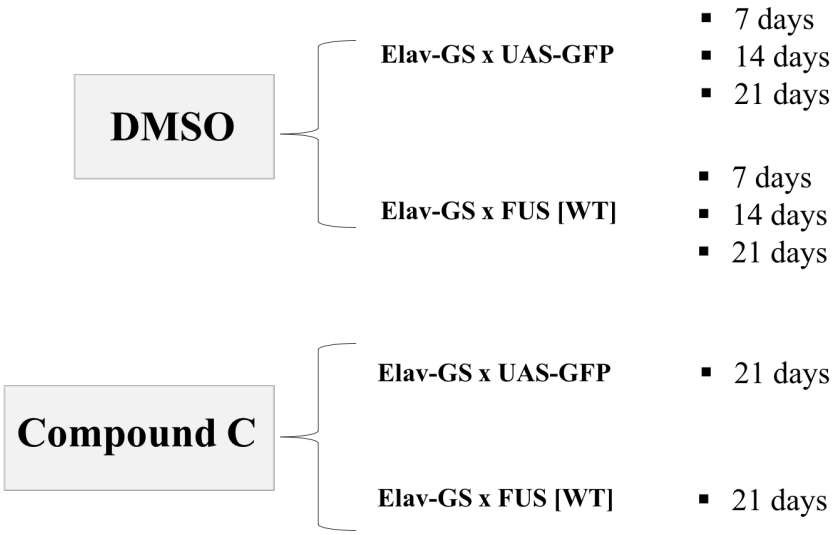

Figure 3.6: Selected time points to do the movies using the FlyWalker system.

3.3.1 A global statistical analysis suggests that the locomotor defect induced by the expression of FUS[WT] is evident at 14 days and the treatment with Compound C partially rescues this motor phenotype

Given that there is a considerable number of motor parameters that characterize the motor behavior of each fly, several Principal Component Analysis with one (Figure 3.7), two or three (Figure 3.8) principal components were performed in order to reduce the complexity of the data and increase interpretability. The principal components were calculated using residual normalized data, expressed as the difference to the control (7 days old ElaV-GS;UAS-GFP flies treated with DMSO).

The PCA allowed comparing the different groups visually. The graphs obtained show that all the flies expressing the driver alone are similar to each other and also to the seven days old FUS[WT] flies supplied with DMSO, in terms of the motor phenotype. Furthermore, 14 and 21 days old FUS[WT] flies treated with DMSO and 21 days old FUS[WT] flies supplied with Compound C are also proximate to each other. However, they are apart from the flies expressing driver alone and from the younger FUS[WT] flies. Therefore, these results suggest that the neurogenerative phenotype of FUS[WT] flies is

evident at 14 days old. In addition, the FUS[WT] flies treated with Compound C are closer to the 14 days old than the 21 days old flies with the same genotype and supplied with DMSO, which is visible in the spatial parameters (Figure 3.7 B) and in statistical tests comparing the three conditions (data not shown). Thus, although the flies treated with Compound C do not reach the motor phenotype of flies expressing driver alone, it seems that they approach the 14 days old flies, which could mean either a reverse on disease development or a delay on disease progression.

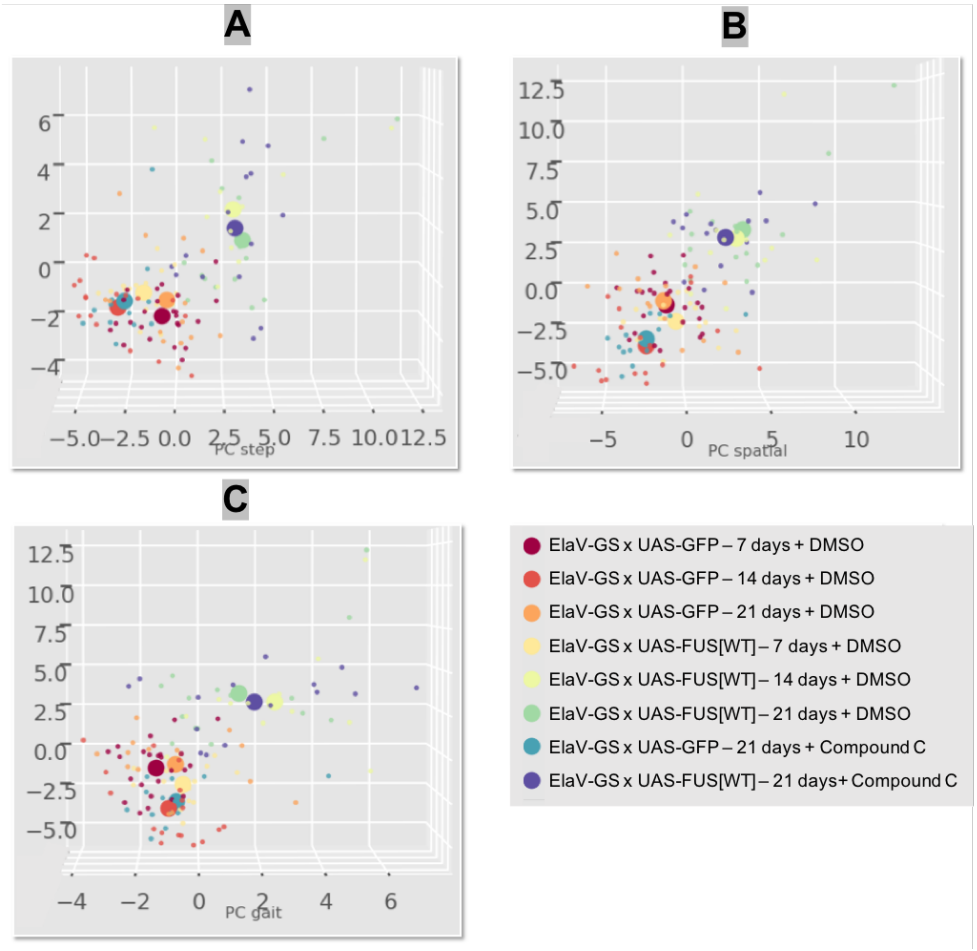

Figure 3.7: **Global PCA: step, spatial and gait motor parameters projection onto one principal component.** The figure represents the projection of (A) step (B) spatial and (C) gait parameters onto one principal component that accounts for the largest possible variance in the data set. "PC"means "Principal Component". In each condition, the centroid correspond to the average position for all points.

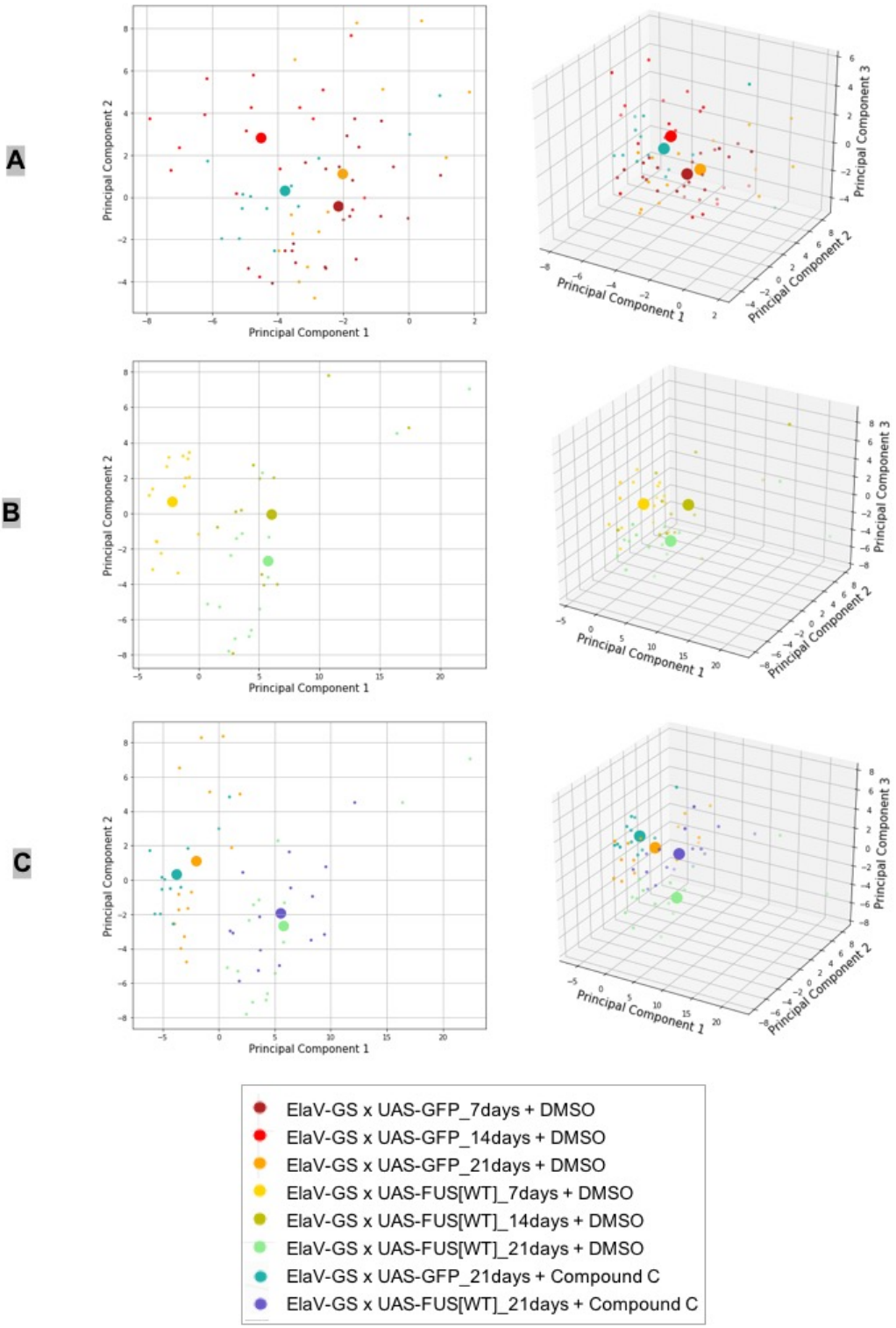

Figure 3.8: **PCA: motor parameters projection onto principal components.** The figures represent the projection of all the motor parameters onto two and three principal components respectively represented in the first and the second column. The rows are linked to (A) the distribution of all the flies expressing driver alone, (B) the evolution of the motor phenotype of flies expressing FUS[WT] over time, and (C) the comparison between the treatment with Compound C and vehicle, at 21 days old.

3.3.2 Deep statistical analysis

As referred above, this work had a two-fold objective. Thus, a deep statistical analysis was done for each one of the goals. Again, the statistical differences were calculated considering the residual values for each parameter.

3.3.2.1 The expression of FUS[WT] affects kinematic parameters of the fly over time

After analyzing the raw data, some kinematic parameters were selected for statistical analysis. Thus, the statistical differences between each condition and the control (seven days old ElaV-GSxUAS-GFP flies treated with DMSO) were plotted in a heat map (Figure 3.9) and the variation of the data of each group was represented in box plots, among various step (Figure 3.10), spatial (Figure 3.11) and gait parameters (Figure 3.12). Moreover, the statistical differences between groups were represented in the box plots.

Consistent with the results obtained for PCA, the heat map and the box plots show that the misexpression of FUS[WT] affects some locomotor parameters of the flies over time. For instance, FUS[WT] expressing flies older than seven days old walk slower and take fewer steps, in each step cycle, than flies expressing driver alone at the same ages (Figure 3.10). Furthermore, the stance traces of 14 and 21 days old FUS[WT] expressing flies are visibly wigglier than the traces of younger flies with the same genotype and the traces of the flies expressing driver alone. Indeed, the quantification of the spatial parameters indicates that the Stance Linearity parameter of the FUS[WT] flies increases and their Stance Straightness decreases over time (Figure 3.11). In addition, visual inspection of the gait maps suggests that FUS[WT] flies older than seven days old walk more using tetrapod gait rather than tripod, when compared to flies expressing driver alone at the same ages. Indeed, the Tripod index of FUS[WT] expressing animals decreases over time and the Tetrapod index becomes higher (Figure 3.12). As a matter of fact, it is well known that as the animals decrease their speed they increasingly use tetrapod and non-canonical combinations [43].

These findings underscore the hypothesis that animals modeling ALS disease become more uncoordinated over time. In addition, it should be noted that seven days old FUS[WT] flies are not statistically different to the control condition in most of the kinematic parameters which confirms that the motor phenotype is evident, at least, at 14 days.

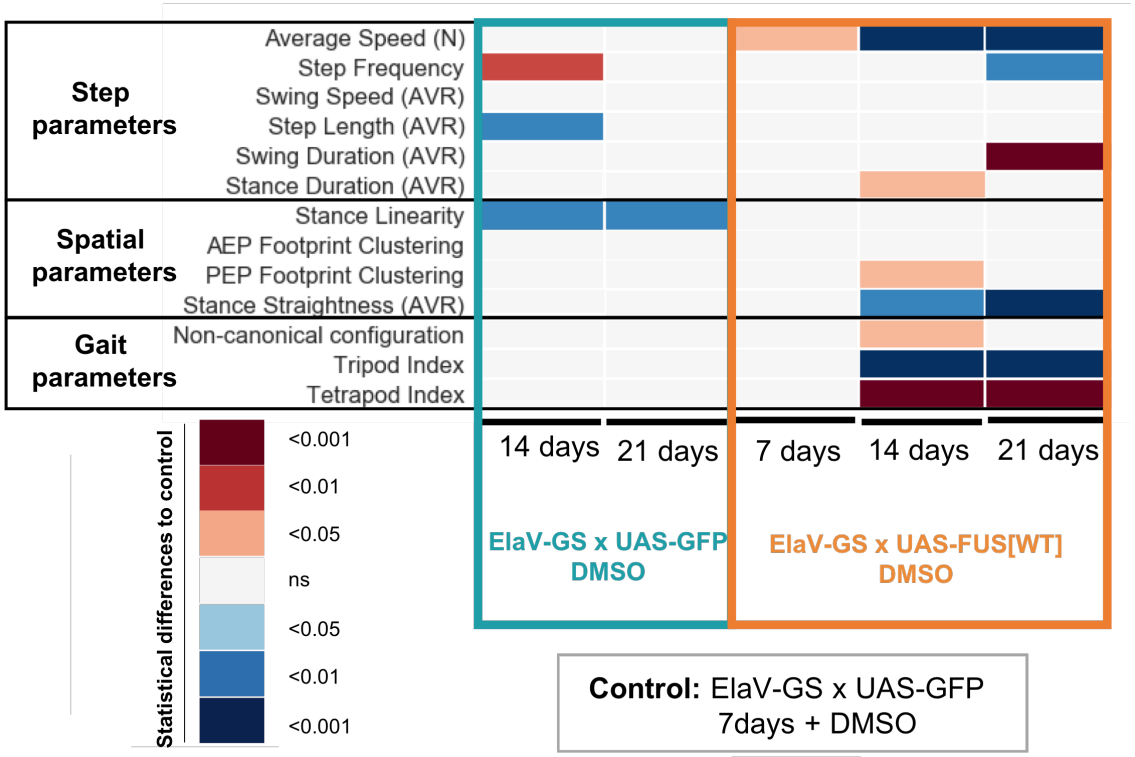

Figure 3.9: **Time dependent degeneration induced by FUS[WT] - statistically significant results.** Rows are related to the 13 kinematic parameters that were analyzed. These are grouped in three major categories: step, spatial and gait parameters. The area framed with the colored lines represents the genotypes: the blue frame indicates the columns that belong to the flies expressing driver alone and the orange frame highlights the columns for FUS[WT] expressing animals. Moreover, each column is linked to one of the time points analyzed (seven, 14 and 21 days) for each genotype. Colored squares represent statistically significant results. White squares represent no significant differences to the control (seven days old ElaV-GSxUAS-GFP flies treated with DMSO). Warm colors are significant results that had higher values than the control. Cold colors are the significant results with lower values than the control. A one-way ANOVA followed by a Tukey post-test was done for normal and homoscedastic data. Otherwise, a Kruskal-Wallis one-way ANOVA with Dunn's multiple comparison test was applied. Statistic significant were considered when $*pvalue \leq 0.05, **pvalue \leq 0.01, ***pvalue \leq 0.001$.

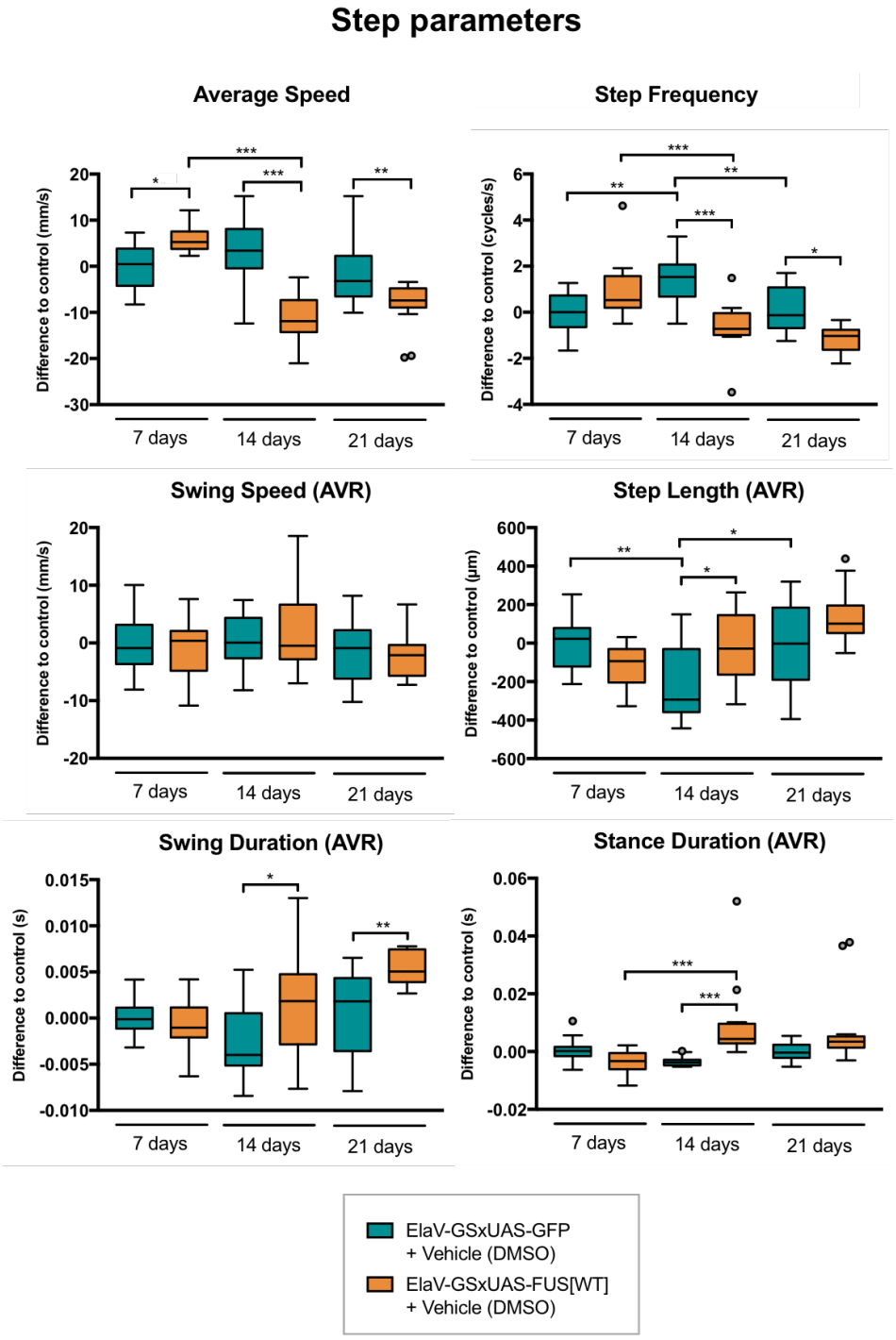

Figure 3.10: **Time dependent degeneration induced by FUS[WT] in step parameters.** The colors are linked to the genotypes: the blue color corresponds to the driver alone and the orange represents the FUS[WT] expressing flies. The median as the middle line, with the lower and upper edges of the boxes representing the 25% and 75% quartiles, respectively; the whiskers represent the range of the full data set, excluding outliers. Circles indicate outliers. Data was residual normalized and expressed as the difference to the control. A one-way ANOVA followed by a Tukey post-test was done for normal and homoscedastic data. Otherwise, a Kruskal-Wallis one-way ANOVA with Dunn's multiple comparison test was applied. Statistic significant were considered when $*pvalue \leq 0.05, ** pvalue \leq 0.01, *** pvalue \leq 0.001$.

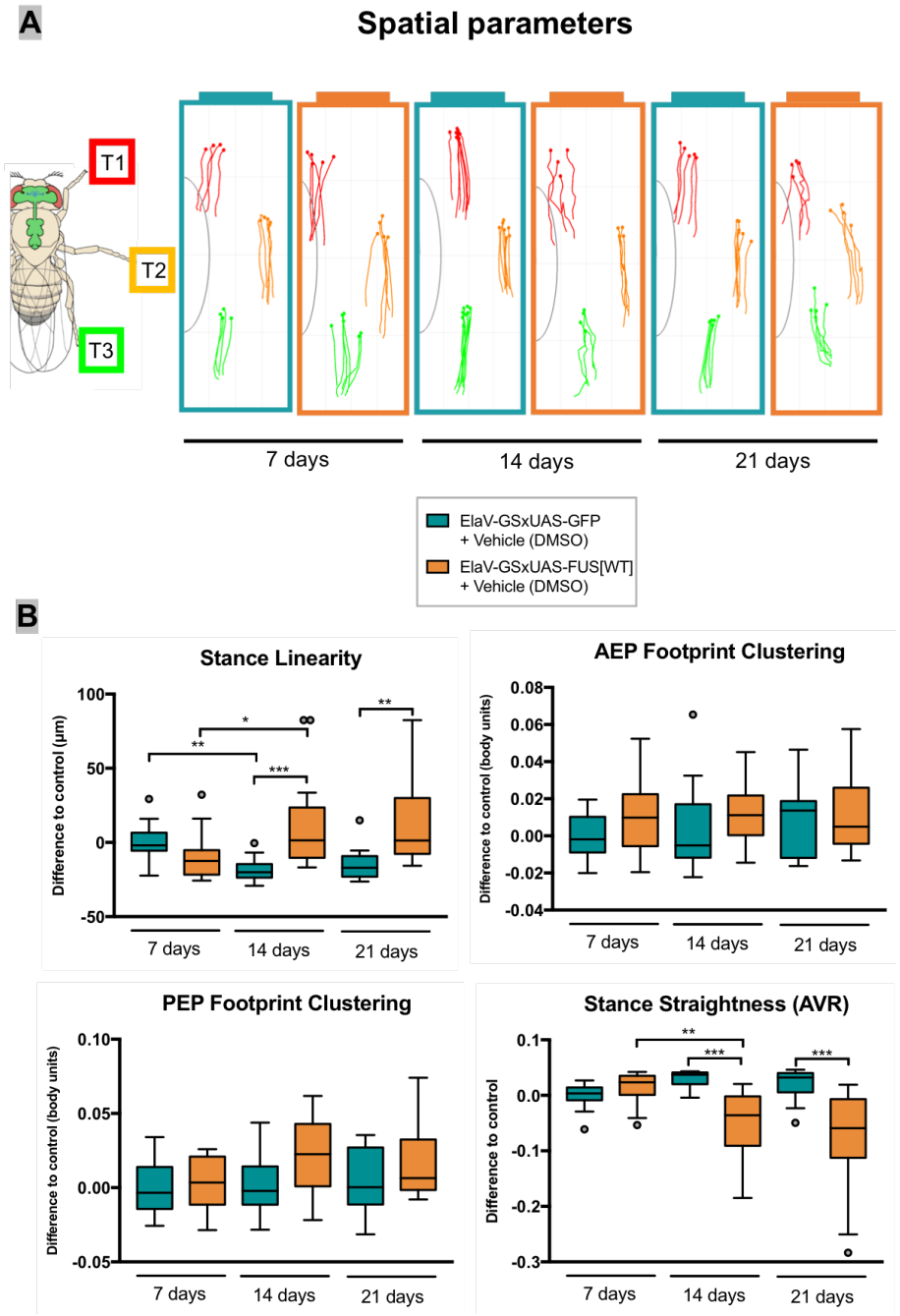

Figure 3.11: **Time dependent degeneration induced by FUS[WT] in spatial parameters.** (A) Stance traces representation of neurodegeneration induced by FUS[WT], in which the Stance Linearity, the AEP/PEP Footprint Clustering and the Stance Straightness can be observed, over the six time points considered. The quantification of these four metrics was made in (B). The colors are linked to the genotypes: the blue color corresponds to the driver alone and the orange represents the FUS[WT] expressing flies. The median as the middle line, with the lower and upper edges of the boxes representing the 25% and 75% quartiles, respectively; the whiskers represent the range of the full data set, excluding outliers. Circles indicate outliers. Data was residual normalized and expressed as the difference to the control. A one-way ANOVA followed by a Tukey post-test was done for normal and homoscedastic data. Otherwise, a Kruskal-Wallis one-way ANOVA with Dunn's multiple comparison test was applied. Statistic significant were considered when $*pvalue \leq 0.05, **pvalue \leq 0.01, ***pvalue \leq 0.001$.

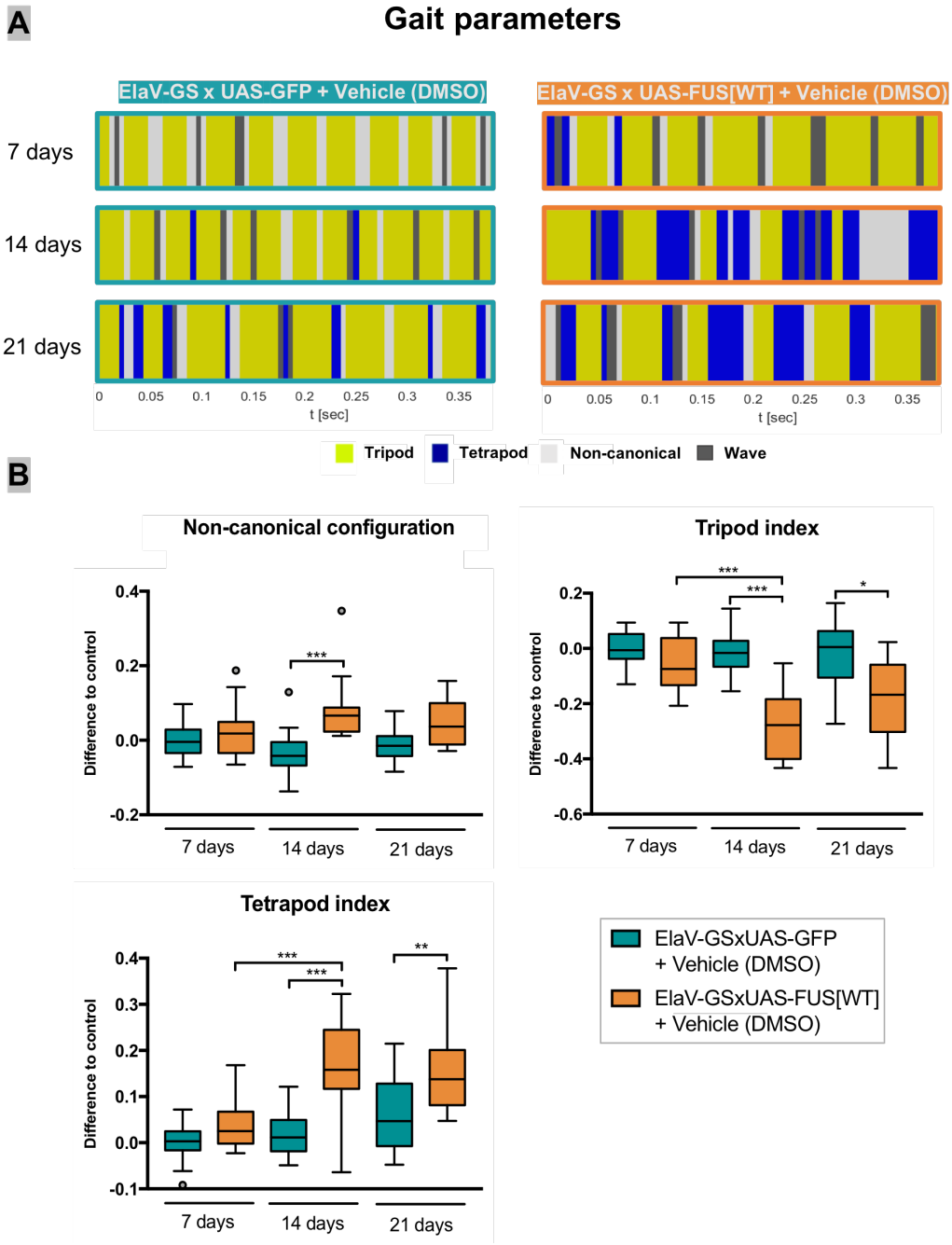

Figure 3.12: **Time dependent degeneration induced by FUS[WT] in gait parameters.** (A) Gait maps representation of neurodegeneration induced by FUS[WT], in which the Non-canonical, Tripod and Tetrapod indexes can be observed, over the six time points considered. The quantification of these three metrics was made in (B). The colors are linked to the genotypes: the blue color corresponds to the driver alone and the orange represents the FUS[WT] expressing flies. The median as the middle line, with the lower and upper edges of the boxes representing the 25% and 75% quartiles, respectively; the whiskers represent the range of the full data set, excluding outliers. Circles indicate outliers. Data was residual normalized and expressed as the difference to the control. A one-way ANOVA followed by a Tukey post-test was done for normal and homoscedastic data. Otherwise, a Kruskal-Wallis one-way ANOVA with Dunn's multiple comparison test was applied. Statistic significant were considered when $*pvalue \leq 0.05, **pvalue \leq 0.01, ***pvalue \leq 0.001$.

3.3.2.2 The treatment with Compound C improves the Swing Speed of FUS[WT] expressing flies

Once profiled the kinematic and the statistical analysis of FUS-induced motor impairment, the putative suppression of the neurodegenerative phenotype (through the treatment with Compound C) was analyzed. Regarding this objective, the residual values were expressed as the difference to the control '21 days old ElaV-GSxUAS-GFP flies treated with DMSO'. The statistical differences between each condition and the control were plotted in the heat map (Figure 3.13). Moreover, the variation of the data of each group was represented in box plots. They were grouped in three categories: step (Figure 3.14), spatial (Figure 3.15) and gait (Figure 3.16) parameters.

The results propose that the treatment with Compound C improves the Swing Speed of FUS[WT] expressing flies. Consequently, the Swing Duration becomes shorter (Figure 3.14). Furthermore, there are no significant changes in the stance traces of FUS[WT] expressing animals treated with Compound C compared to the ones exposed to DMSO, according to the Stance Linearity, AEP/PEP Footprint Clustering and Stance Straightness parameters (Figure 3.15). Similarly, the gait parameters do not reveal differences between these two conditions (Figure 3.16). Thus, although the treatment with Compound C does not improve the most of impaired motor parameters through the FUS[WT] expression, it improves the step parameter Swing Speed.

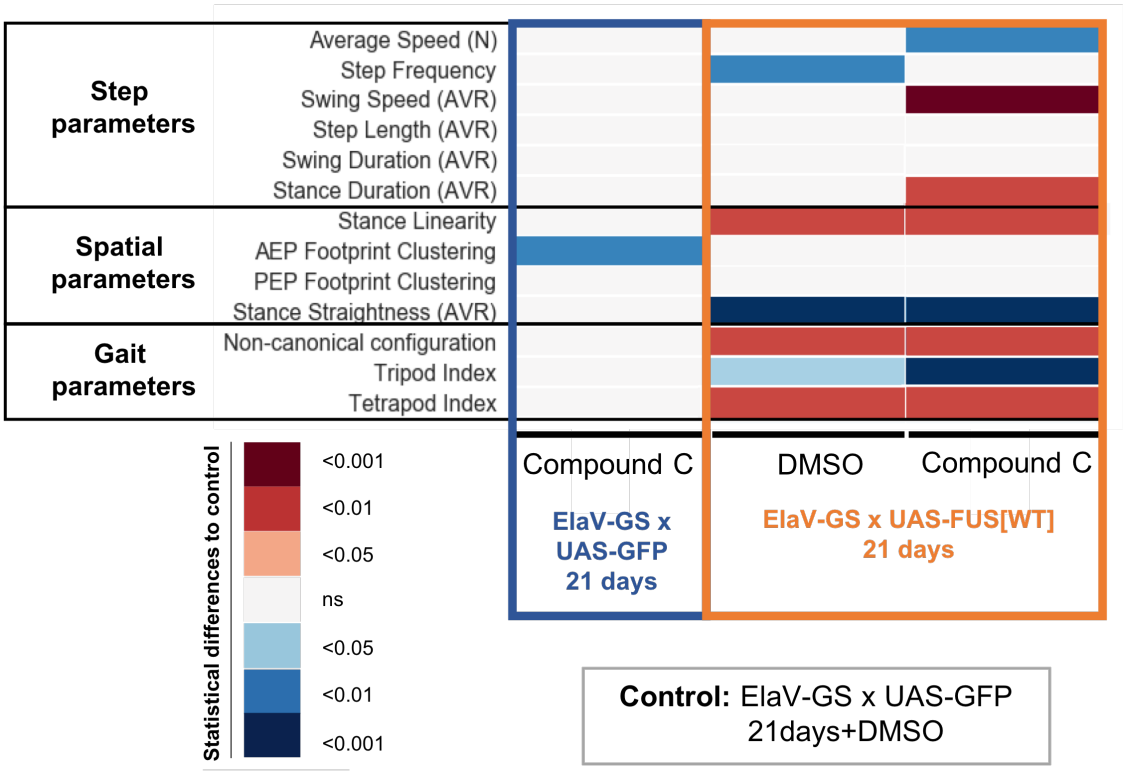

Figure 3.13: **Effect of Compound C on the neurodegeneration of the flies - statistically significant results.** Rows are related to the 13 kinematic parameters that were analyzed. These are grouped in three major categories: step, spatial and gait parameters. The area framed with the colored lines represents the genotypes: the dark blue frame indicates the columns that belong to the flies expressing driver alone and the orange frame highlights the columns for FUS[WT] expressing animals. Moreover, each column is linked to one type of treatment: Compound C or DMSO. Colored squares represent statistically significant results. White squares represent no significant differences to the control (21 days old ElaV-GSxUAS-GFP flies treated with DMSO). Warm colors are significant results that had higher values than the control. Cold colors are the significant results with lower values than the control. A one-way ANOVA followed by a Tukey post-test was done for normal and homoscedastic data. Otherwise, a Kruskal-Wallis one-way ANOVA with Dunn's multiple comparison test was applied. Statistic significant were considered when $*pvalue \leq 0.05, **pvalue \leq 0.01, ***pvalue \leq 0.001$.

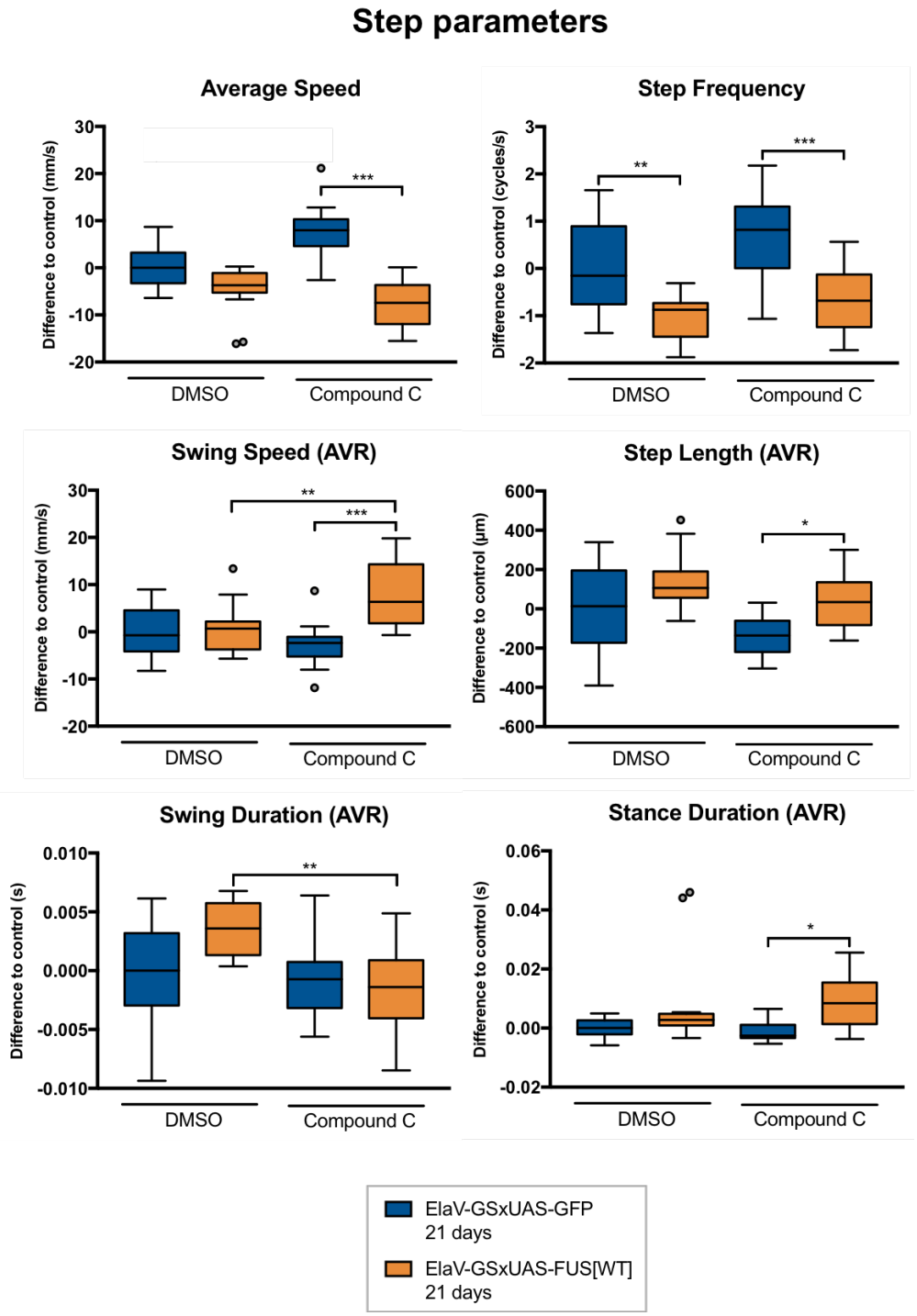

Figure 3.14: **Effect of Compound C on the neurodegeneration of the flies in step parameters.** The colors are linked to the genotypes: the dark blue color corresponds to driver alone and the orange represents the FUS[WT] expressing flies. The median as the middle line, with the lower and upper edges of the boxes representing the 25% and 75% quartiles, respectively; the whiskers represent the range of the full data set, excluding outliers. Circles indicate outliers. Data was residual normalized and expressed as the difference to the control. A one-way ANOVA followed by a Tukey post-test was done for normal and homoscedastic data. Otherwise, a Kruskal-Wallis one-way ANOVA with Dunn's multiple comparison test was applied. Statistic significant were considered when $*pvalue \leq 0.05, **pvalue \leq 0.01, ***pvalue \leq 0.001$.

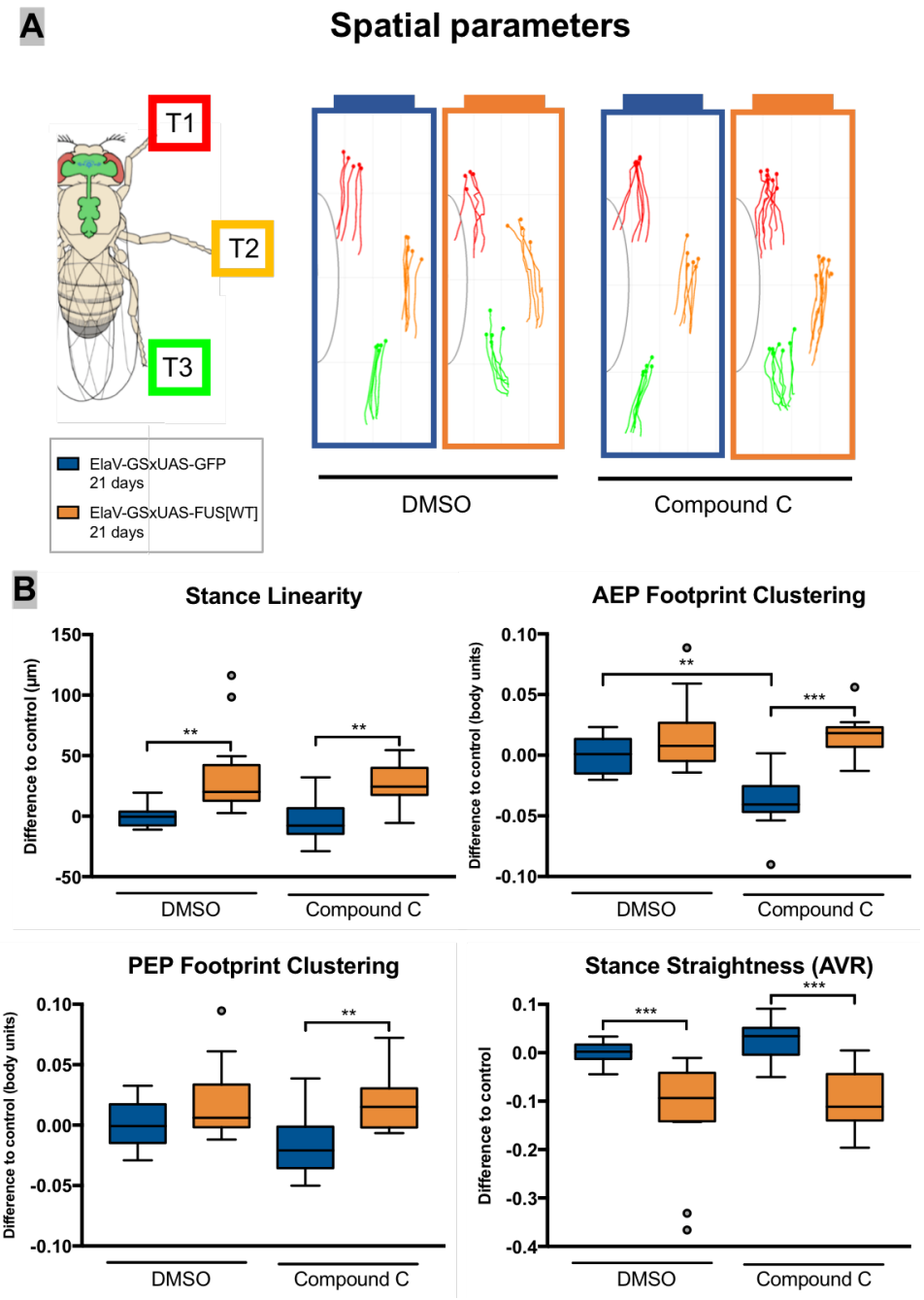

Figure 3.15: **Effect of Compound C on the neurodegeneration of the flies in spatial parameters.** (A) Stance traces representation of effect of Compound C, in which the Stance Linearity, the AEP/PEP Footprint Clustering and the Stance Straightness can be observed, over the four time points considered. The quantification of these four metrics was made in (B). The colors are linked to the genotypes: the blue color corresponds to the driver alone and the orange represents the FUS[WT] expressing flies. The median as the middle line, with the lower and upper edges of the boxes representing the 25% and 75% quartiles, respectively; the whiskers represent the range of the full data set, excluding outliers. Circles indicate outliers. Data was residual normalized and expressed as the difference to the control. A one-way ANOVA followed by a Tukey post-test was done for normal and homoscedastic data. Otherwise, a Kruskal-Wallis one-way ANOVA with Dunn's multiple comparison test was applied. Statistic significant were considered when $*pvalue \leq 0.05, **pvalue \leq 0.01, ***pvalue \leq 0.001$.

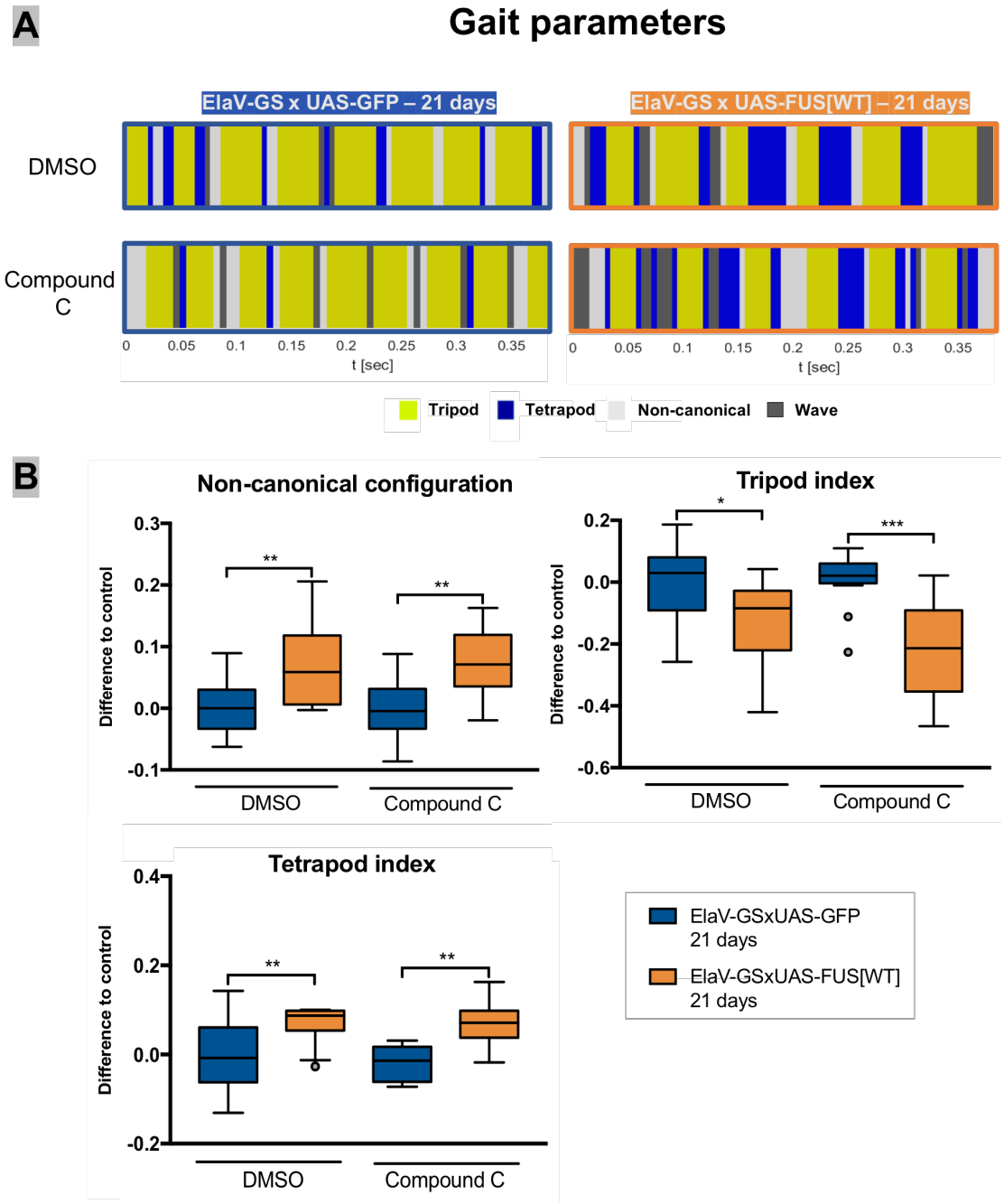

Figure 3.16: **Effect of Compound C on the neurodegeneration of the flies in gait parameters.** (A) Gait maps representation of effect of Compound C, in which the Non-canonical, Tripod and Tetrapod indexes can be observed, over the four time points considered. The quantification of these three metrics was made in (B). The colors are linked to the genotypes: the blue color corresponds to driver alone and the orange represents the FUS[WT] expressing flies. The median as the middle line, with the lower and upper edges of the boxes representing the 25% and 75% quartiles, respectively; the whiskers represent the range of the full data set, excluding outliers. Circles indicate outliers. Data was residual normalized and expressed as the difference to the control. A one-way ANOVA followed by a Tukey post-test was done for normal and homoscedastic data. Otherwise, a Kruskal-Wallis one-way ANOVA with Dunn's multiple comparison test was applied. Statistic significant were considered when $*pvalue \leq 0.05, **pvalue \leq 0.01, ***pvalue \leq 0.001$.

3.4 Expression of FUS alleles in the adult flies causes severe motor dysfunction using the climbing assay

Given that the FlyWalker outputs a set of parameters for each fly and that it was observed a considerable heterogeneity within each FUS genotype during the life span assay (there were healthier flies on the top of the vials), it was done a negative geotaxis assay in order to have a response of a group of animals. Again, two groups were considered: DMSO and Compound C. Moreover, there were considered the same genotypes as in the survival assay, all of them supplemented with RU486 during the adult stage.

To assay the climbing ability of flies fed with DMSO, 10 male flies of each condition were tapped to the bottom of the vial and allowed to climb up the walls. The climbing time was recorded when five flies crossed a 15-cm finish line [54].

The results demonstrate that the climbing ability of the flies expressing the driver alone was not affected. However, the expression of FUS alleles in the neurons of the fly caused severe motor dysfunction over time, compared to controls. Moreover, for each time point, flies expressing FUS[R521C] took more time to reach the finish line than the FUS[WT] which suggests that the mutant flies have a stronger impairment of the motor abilities (Figure 3.17). In addition, after 12 days, the flies expressing FUS alleles were not able to climb; they became weak and fell a lot. Collectively, these findings confirm that the expression of FUS alleles in the neurons leads to time dependent neurodegeneration that progressively affects the climbing ability of the flies.

3.4.1 The treatment with Compound C during seven days does not rescue the climbing ability of flies expressing FUS alleles

After, a comparison between seven days old flies of both groups was performed, considering two finish lines: 8 cm and 15 cm. Given that the difference between the flies treated with DMSO and Compound C is not significant, the results suggest that the treatment with Compound C (during seven days) does not rescue the climbing ability of the flies expressing FUS alleles (Figure 3.18).

After 12 days, it was not possible to perform the climbing assay either with flies exposed to DMSO or Compound C since they were not able to climb, even decreasing the high to 8 cm.

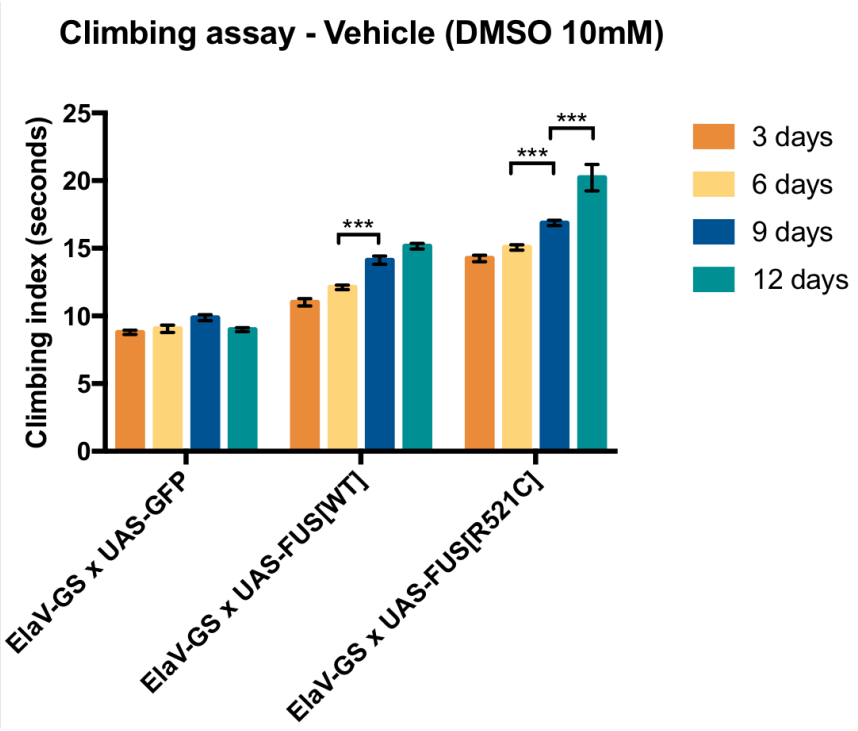

3 days	
ElaV-GS x UAS-GFP vs. ElaV-GS x UAS-FUS[WT]	***
ElaV-GS x UAS-GFP vs. ElaV-GS x UAS-FUS[R521C]	***
ElaV-GS x UAS-FUS[WT] vs. ElaV-GS x UAS-FUS[R521C]	***

6 days	
ElaV-GS x UAS-GFP vs. ElaV-GS x UAS-FUS[WT]	***
ElaV-GS x UAS-GFP vs. ElaV-GS x UAS-FUS[R521C]	***
ElaV-GS x UAS-FUS[WT] vs. ElaV-GS x UAS-FUS[R521C]	***

9 days	
ElaV-GS x UAS-GFP vs. ElaV-GS x UAS-FUS[WT]	***
ElaV-GS x UAS-GFP vs. ElaV-GS x UAS-FUS[R521C]	***
ElaV-GS x UAS-FUS[WT] vs. ElaV-GS x UAS-FUS[R521C]	***

12 days	
ElaV-GS x UAS-GFP vs. ElaV-GS x UAS-FUS[WT]	***
ElaV-GS x UAS-GFP vs. ElaV-GS x UAS-FUS[R521C]	***
ElaV-GS x UAS-FUS[WT] vs. ElaV-GS x UAS-FUS[R521C]	***

Figure 3.17: **Climbing ability of flies expressing FUS alleles under the control of ElaV-GS.** The y-axis represents the time (in seconds), it took for five males to climb 15 cm (mean ± SEM). Statistical significance within groups is represented on the graph and statistical significance between groups is represented in the tables bellow. These differences were calculated by doing two-way ANOVA with Tukey post-test. Statistic significant were considered when $*pvalue \leq 0.05, **pvalue \leq 0.01, ***pvalue \leq 0.001$.

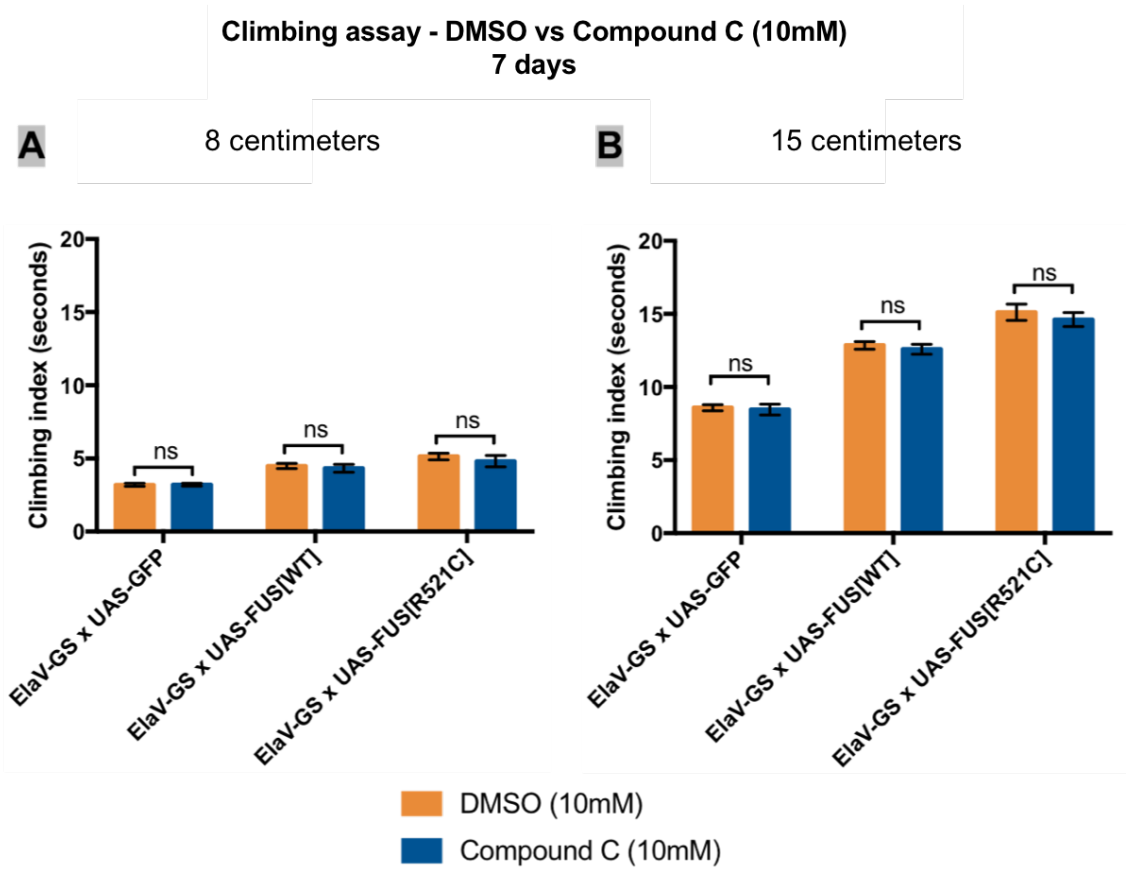

Figure 3.18: **Effect of Compound C on the climbing ability of flies expressing FUS alleles.** The y-axis represents the time (in seconds), it took for five males to climb (A) 8 cm and (B) 15 cm (mean ± SEM). In each genotype, flies treated with or without Compound C are not significantly different. Statistical significance was calculated by doing two-way ANOVA with Tukey post-test. Statistic significant were considered when $*pvalue \leq 0.05, **pvalue \leq 0.01, ***pvalue \leq 0.001$.

3.5 The induction of FUS alleles lead to a decrease in laid eggs and emerged larvae

It is well established that egg production from females or viable offspring from males is a marker of toxicity in *Drosophila* [37]. Besides, the egg laying ability is a neuronal controlled behavior [75]. Thus, after observing that female flies overexpressing FUS alleles (WT and R521C) had a larger abdomen than with the driver alone, it was performed an egg laying assay in order to analyze their reproductive outputs and understand if the larger abdomen was related to an impaired egg laying ability.

It was measured, in different time points, the number of laid eggs during 24 hours and the sequential number of emerged larvae. Regarding the first objective of this work, the characterization of the neuronal degeneration induced by FUS alleles, the flies were exposed to DMSO from day one adult stage on. These flies were used as a control for further comparison with the ones exposed to Compound C.

Female flies exposed to DMSO while overexpressing FUS alleles (under treatment with RU486) exhibited a significant reduction in the number of laid eggs and emerged larvae, compared to control. Moreover, flies expressing FUS[WT] laid, on average, more eggs than the flies expressing mutant FUS. The number of emerged larvae was also higher in FUS[WT] condition at seven days old (Figure 3.19).

Interestingly, these results reveal that the expression of FUS affects the egg laying ability and the larvae emergence, with mutant FUS phenotypes stronger than the wild type form.

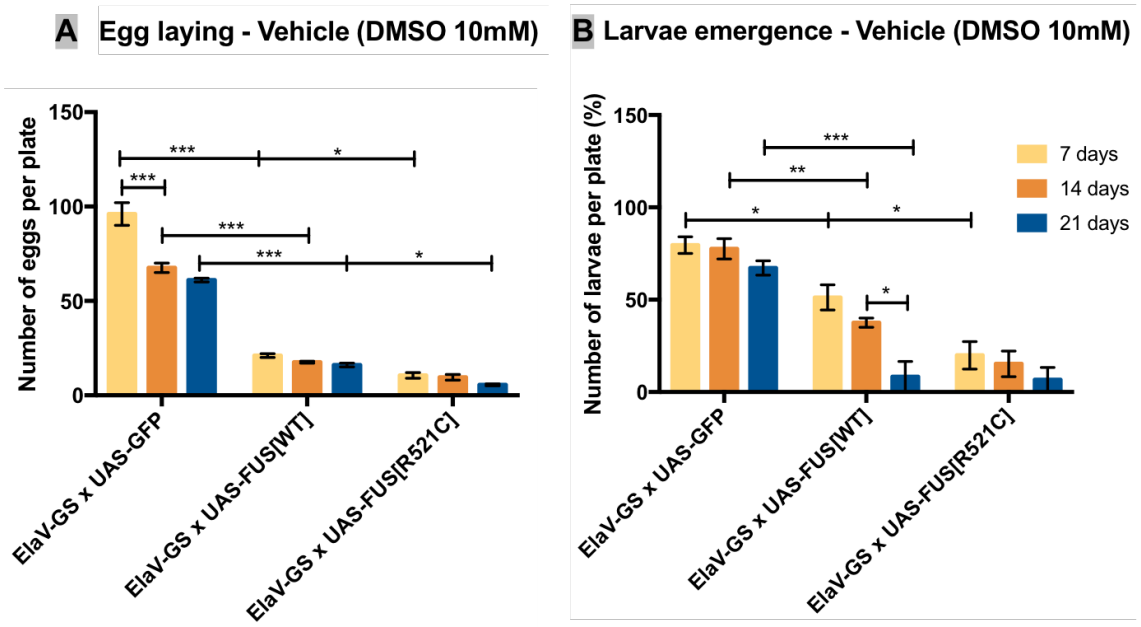

Figure 3.19: **Egg laying and larvae emergence of female flies expressing FUS alleles under the control of ElaV-GS.** The graphs represent (A) the number of laid eggs and (B) the percentage of eggs that turns into larvae (fertilized eggs), per plate and genotype, among various time points. Data are presented as means ± SEM and analyzed by two-way ANOVA with Tukey post-test. Statistic significant were considered when $*pvalue \leq 0.05, **pvalue \leq 0.01, ***pvalue \leq 0.001$.

3.5.1 The treatment with Compound C does not rescue the egg laying ability and larvae emergence in FUS expressing flies

After the treatment with Compound C during 14 days, the number of laid eggs and emerged larvae was quantified. Then, a comparison between the two groups (DMSO and Compound C) was done (Figure 3.20).

FUS expressing animals exposed to Compound C exhibited a significant decrease in reproductive outputs, compared to control, as observed with DMSO. Indeed, the number of eggs laid by females treated with Compound C was not affected by the treatment. Similarly, Compound C does not rescue the larvae emergence.

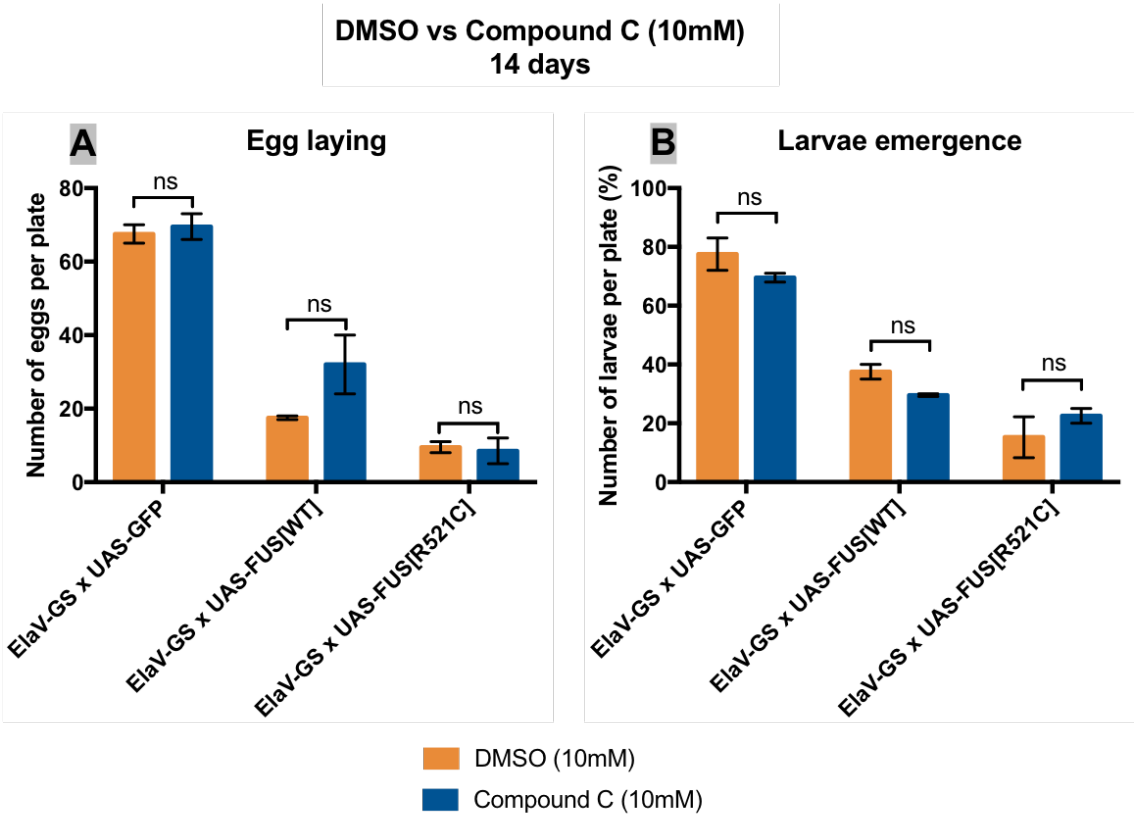

Figure 3.20: **Effect of Compound C on the egg laying ability and larvae emergence of flies expressing FUS alleles.** The graphs represent (A) the number of laid eggs and (B) the percentage of eggs that turns into larvae (fertilized eggs), per plate and genotype, among various time points. Data are presented as means ± SEM and analyzed by two-way ANOVA with Tukey post-test. Statistic significant were considered when $*pvalue \leq 0.05, ** pvalue \leq 0.01, *** pvalue \leq 0.001$.

3.6 Flies expressing FUS alleles do not show changes in the motor neuron projections in the leg NMJ

The *Drosophila* adult leg is organized into segments as the vertebrate limb. Each fly leg has 14 muscles, each one comprising multiple muscle fibers. The cell bodies of the adult leg are located in the T1 (prothoracic), T2 (mesothoracic), and T3 (metathoracic) ganglia on each side of the ventral nerve cord (VNC)[1]. Each ganglia comprises approximately 50 motor neurons that target muscles in four segments of the ipsilateral leg - coxa, trochanter, femur and tibia (Figure 3.21) [27].

[1] VNC is a structure analogous to the vertebrate spinal cord [27].

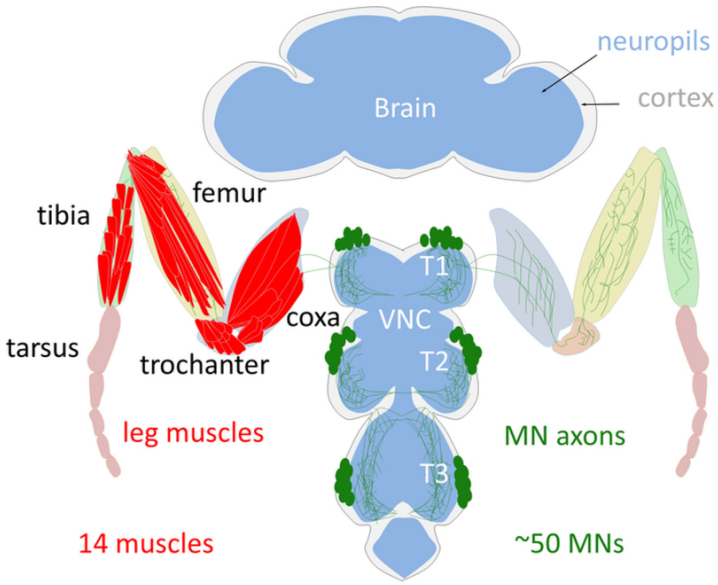

Figure 3.21: **Schematic of the adult *Drosophila* leg motor system.** It is possible to visualize the cell bodies of the adult leg motor neurons (green) which are localized in the cortex (grey) of the thoracic ganglion of the VNC. Motor neurons arborize their dendrites in the leg neuropil (blue) and project their axons into the leg innervating one of the 14 leg muscles (red). It should be noted that only the T1 legs are schematized [Adapted from [27]].

Since ALS targets motor neurons without short-term cell death, an indirect quantification of the number of motor neurons establishing synapses with leg muscles was performed. This was carried out by co-expressing Rab3:YFP, which marks presynaptic regions in motor neurons using the LexA/LexAop system, a binary expression system independent of the GAL4 system. YFP was visualized through the leg cuticle and imaged by confocal microscopy. The flies were fed with DMSO during the adult stage to further compare with Compound C effect.

It was expected a decrease in the Rab3:YFP presence in the legs of FUS expressing flies. However, it was not detected possibly because there are a huge number of motor neurons establishing synapses with leg muscles which makes difficult to perform any quantification (Figure 3.22). Concerning that, the effect of Compound C was not tested.

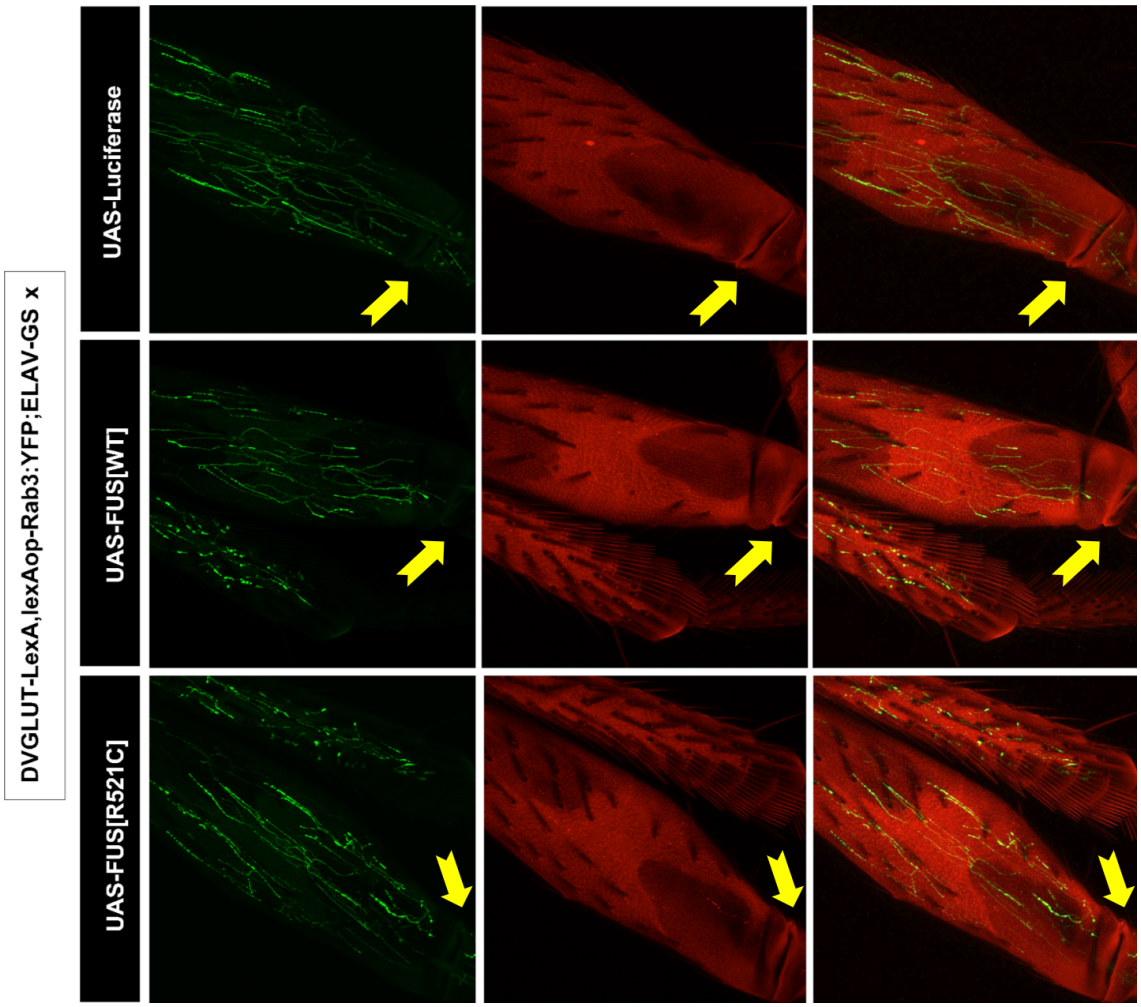

Figure 3.22: **Visualization of neuro-muscular junctions (NMJs) in the adult leg.** Synapses established between motor neurons and muscles in the leg can be visualized using Rab3:YFP (green). Legs are mounted in slides and visualized using confocal microscopy. Leg cuticles can be visualized by acquiring the autofluorescence in the red channel (second column). An overlap of both can be visualized in the third column. These legs belong to seven days old flies. Yellow arrows indicate the trochanter.

Chapter 4

Conclusions

4.1 Summary

Several *Drosophila* models of ALS have emerged in the last decade by mimicking human alleles of the disease. In one of these examples, Lanson *et al.* showed that the overexpression of human FUS alleles in *Drosophila* leads to neurodegeneration in the eyes, reduced longevity and locomotor defects [36]. In this work, we tried to replicate these results and investigate other readouts related to FUS-induced degeneration. Moreover, we tested whether Compound C delays the progression of the neurodegenerative phenotypes.

First, we reported the generation and characterization of transgenic flies expressing wild type and a mutant form of human FUS (R521C). We showed that ectopic expression of ALS-related FUS alleles in *Drosophila* eyes leads to neurodegenerative phenotypes characterized by ommatidial degeneration, partial collapse and loss of eye pigmentation. Moreover, we developed a conditional *Drosophila* model of FUS-related ALS using an inducible neuronal driver (ElaV-GS). The overexpression of mutant human FUS in adult fly neurons drastically increased mortality and led to behavioral abnormalities when compared with FUS[WT] and driver alone. These findings are consistent with previous reports, showing that the overexpression of mutant FUS in neurons can cause reduced lifespan and climbing defects. Interestingly, FUS[WT] expressing flies also presented reduced lifespan and climbing dysfunction. However, their phenotype was less severe than that with mutant FUS, revealing that the expression of FUS[WT] in neurons is also toxic and that neuronal tissues are particularly vulnerable to FUS levels.

Motor decay of freely walking fruit flies was quantified using a method developed previously: the FlyWalker system. This methodology provides not only more information but also higher sensitivity compared to classical motor assays. Here, we analyzed driver

alone and FUS[WT] flies raised in the same conditions as in the survival assay, under treatment with RU486. The results confirmed the FUS[WT]-induced neurodegeneration over time. Indeed, the FUS[WT] expression affected kinematic parameters that characterize the locomotor behavior of the flies. Furthermore, the statistical analysis showed clearly that the motor phenotype is visible after 14 days of FUS[WT] expression.

Since the animals expressing FUS in all the neurons had a larger abdomen than with the driver alone, an interesting phenotype was also investigated: the reproductive output. In fact, FUS expressing flies showed a reduction in the number of laid eggs and emerged larvae compared to control, with a higher decrease in mutant FUS animals, in general. These effects on reproduction could be due to the fact that the egg laying behavior is neuronal controlled [75].

Regarding the Compound C effect, it is undeniable that this small molecule significantly extended the lifespan of FUS wild type expressing animals under treatment with RU486. Moreover, in the FlyWalker analysis, the treatment with Compound C during 21 days increased the Swing Speed of FUS[WT] expressing flies, but the mechanisms underlying the improvement of this kinematic parameter are unknown. Interestingly, the motor phenotype of 21 days old flies treated with Compound C approached to that of 14 days old flies treated with DMSO, instead of 21 days old, which could mean a reverse or a delay on disease progression. Furthermore, the remaining assays suggest that Compound C does not ameliorate the degeneration of the eye and the impaired climbing and egg laying ability, which could be related to the sensitivity of these assays.

Overall, our *Drosophila* model displayed several features strikingly similar to those found in ALS patients. In fact, our results recapitulate specific features of FUS-induced neurodegeneration that are hallmarks of ALS. Furthermore, this project created a set of protocols that allowed, in a relatively short period of time, testing Compound C for its efficacy to prevent or delay the progression of neurodegenerative phenotypes. The aforementioned methodologies can be easily carried out and provide quantifiable metrics regarding the progression of the neurodegenerative phenotype contributing to a result regarding the effect of a candidate compound. Importantly, these experiments could be easily performed on other ALS models (for example SOD1 or TDP-43) in order to understand if the observed effects are exclusive to FUS-mediated toxicity. Besides, the same approach can be expanded to additional neurodegenerative conditions such as Huntington or Parkinson's disease.

4.2 Limitations of this work and proposal of possible solutions

The experiments performed in this work revealed that the FUS[R521C] expressing flies exhibit degenerative phenotypes more aggressive than the FUS wild type flies. However, this assumption can be considered misleading since we do not know the amount of FUS protein that these flies express. One possible solution is to do a western blot. That way we can quantify the FUS expression levels in each genotype and if both of them have the

same level, we can confirm the aggressiveness of FUS[R521C]. In fact, we tried to perform a western blot. However, since there are many limitations in the quality of commercially available antibodies, it was not possible to achieve this quantification.

At advanced stages of the survival assay, there were impaired FUS expressing flies at the bottom of the vials and healthier flies at the top which sets the variability within genotypes as a factor that can mislead the results. To overcome this limitation, we can increase the number of replications of some assays, such as the egg laying assay and the FlyWalker analysis which have a lower number of repetitions compared to other experiments.

Furthermore, it was not possible to visualize a decrease in the Rab3:YFP presence in the legs of seven days old FUS expressing animals, compared to driver alone. One possible solution is to repeat this experiment at another time point, such as 21 days. Other suggestion is to mark the presynaptic regions only with a limited number of motor neurons with Rab3:YFP, which increases the sensitivity of this assay.

To test varying concentrations of Compound C is another improvement that should be considered in order to understand if there is a concentration which effect is more pronounced. Moreover, this bioactive molecule could be tested at more time points. For instance, in the FlyWalker assay, it would be interesting to test the effect of Compound C at 14 days old since its effect on the motor phenotype could be more detectable at earlier stages of the disease. In addition, other assays can be considered to test the protective effect of this small molecule. Finally, it would be pertinent to analyze the mutant human FUS expressing flies with the FlyWalker system at different time points.

Bibliography

[1] S. Ajroud-Driss and T. Siddique. "Sporadic and hereditary amyotrophic lateral sclerosis (ALS)." In: *Biochimica et Biophysica Acta (BBA) - Molecular Basis of Disease* 1852.4 (2015), pp. 679–684. ISSN: 09254439. DOI: 10.1016/j.bbadis.2014.08.010. URL: http://www.ncbi.nlm.nih.gov/pubmed/25193032https://linkinghub.elsevier.com/retrieve/pii/S0925443914002634.

[2] A. Al-Chalabi, A. Jones, C. Troakes, A. King, S. Al-Sarraj, and L. H. van den Berg. "The genetics and neuropathology of amyotrophic lateral sclerosis." In: *Acta Neuropathologica* 124.3 (2012), pp. 339–352. ISSN: 0001-6322. DOI: 10.1007/s00401-012-1022-4. URL: http://www.ncbi.nlm.nih.gov/pubmed/22903397http://link.springer.com/10.1007/s00401-012-1022-4.

[3] S. L. Albarracin, B. Stab, Z. Casas, J. J. Sutachan, I. Samudio, J. Gonzalez, L. Gonzalo, F. Capani, L. Morales, and G. E. Barreto. "Effects of natural antioxidants in neurodegenerative disease." In: *Nutritional Neuroscience* 15.1 (2012), pp. 1–9. ISSN: 1028-415X. DOI: 10.1179/1476830511Y.0000000028. URL: http://www.tandfonline.com/doi/full/10.1179/1476830511Y.0000000028.

[4] M. Allocca, S. Zola, and P. Bellosta. "The Fruit Fly, Drosophila melanogaster: The Making of a Model (Part I)." In: *Drosophila melanogaster - Model for Recent Advances in Genetics and Therapeutics*. InTech, 2018. DOI: 10.5772/intechopen.72832. URL: http://www.intechopen.com/books/drosophila-melanogaster-model-for-recent-advances-in-genetics-and-therapeutics/the-fruit-fly-drosophila-melanogaster-the-making-of-a-model-part-i-.

[5] P. M. Andersen and A. Al-Chalabi. "Clinical genetics of amyotrophic lateral sclerosis: what do we really know?" In: *Nature Reviews Neurology* 7.11 (2011), pp. 603–615. ISSN: 1759-4758. DOI: 10.1038/nrneurol.2011.150. URL: http://www.ncbi.nlm.nih.gov/pubmed/21989245http://www.nature.com/articles/nrneurol.2011.150.

[6] J. M. Aragones, J. Altimiras, P. Roura-Poch, E. Homs, L. Bajo, M. Povedano, E. Cortés-Vicente, I. Illa, A. Al-Chalabi, and R. Rojas-García. "Amyotrophic lateral sclerosis: A higher than expected incidence in people over 80 years of age." In: *Amyotrophic Lateral Sclerosis and Frontotemporal Degeneration* 17.7-8 (2016), pp. 522–527. ISSN: 2167-8421. DOI: 10.1080/21678421.2016.1187175. URL: http:

//www.ncbi.nlm.nih.gov/pubmed/27224687https://www.tandfonline.com/doi/full/10.1080/21678421.2016.1187175.

[7] A. M. Blokhuis, E. J. N. Groen, M. Koppers, L. H. van den Berg, and R. J. Pasterkamp. "Protein aggregation in amyotrophic lateral sclerosis." In: *Acta Neuropathologica* 125.6 (2013), pp. 777–794. ISSN: 0001-6322. DOI: 10.1007/s00401-013-1125-6. URL: http://www.ncbi.nlm.nih.gov/pubmed/23673820http://www.pubmedcentral.nih.gov/articlerender.fcgi?artid=PMC3661910http://link.springer.com/10.1007/s00401-013-1125-6.

[8] R. Bonafede and R. Mariotti. "ALS Pathogenesis and Therapeutic Approaches: The Role of Mesenchymal Stem Cells and Extracellular Vesicles." In: *Frontiers in cellular neuroscience* 11 (2017), p. 80. ISSN: 1662-5102. DOI: 10.3389/fncel.2017.00080. URL: http://www.ncbi.nlm.nih.gov/pubmed/28377696http://www.pubmedcentral.nih.gov/articlerender.fcgi?artid=PMC5359305.

[9] H Brand and N Perrimon. *Targeted gene expression as a means of altering cell fates and generating dominant phenotypes*. Tech. rep. 1993. URL: http://dev.biologists.org/content/develop/118/2/401.full.pdf.

[10] D. Busson and A.-M. Pret. "GAL4/UAS Targeted Gene Expression for Studying Drosophila Hedgehog Signaling." In: Humana Press, 2007, pp. 161–201. DOI: 10.1007/978-1-59745-516-9_13. URL: http://link.springer.com/10.1007/978-1-59745-516-9{_}13.

[11] S. Byrne, C. Walsh, C. Lynch, P. Bede, M. Elamin, K. Kenna, R. McLaughlin, and O. Hardiman. "Rate of familial amyotrophic lateral sclerosis: a systematic review and meta-analysis." In: *Journal of Neurology, Neurosurgery & Psychiatry* 82.6 (2011), pp. 623–627. ISSN: 0022-3050. DOI: 10.1136/jnnp.2010.224501. URL: http://www.ncbi.nlm.nih.gov/pubmed/21047878http://jnnp.bmj.com/cgi/doi/10.1136/jnnp.2010.224501.

[12] R. &. H. Childress, J., Behringer. "G. Learning to Fly: Phenotypic Markers in Drosophila. in Genesis." In: *The Journal of Genetics and Development* (2005).

[13] K. S. Cho, S. M. Bang, and A. Toh. "Lipids and Lipid Signaling in Drosophila Models of Neurodegenerative Diseases." In: *Omega-3 Fatty Acids in Brain and Neurological Health* (2014), pp. 327–336. DOI: 10.1016/B978-0-12-410527-0.00026-0. URL: https://www.sciencedirect.com/science/article/pii/B9780124105270000260.

[14] M. J. Chung and Y.-L. Suh. "Ultrastructural Changes of Mitochondria in the Skeletal Muscle of Patients with Amyotrophic Lateral Sclerosis." In: *Ultrastructural Pathology* 26.1 (2002), pp. 3–7. ISSN: 0191-3123. DOI: 10.1080/01913120252934260. URL: http://www.ncbi.nlm.nih.gov/pubmed/12028652http://www.tandfonline.com/doi/full/10.1080/01913120252934260.

[15] S Cluskey and D. B. Ramsden. "Mechanisms of neurodegeneration in amyotrophic lateral sclerosis." In: *Molecular pathology : MP* 54.6 (2001), pp. 386–92. ISSN: 1366-8714. URL: http://www.ncbi.nlm.nih.gov/pubmed/11724913http://www.pubmedcentral.nih.gov/articlerender.fcgi?artid=PMC1187128.

[16] M. P. Cruz. "Edaravone (Radicava): A Novel Neuroprotective Agent for the Treatment of Amyotrophic Lateral Sclerosis." In: *P & T : a peer-reviewed journal for formulary management* 43.1 (2018), pp. 25–28. ISSN: 1052-1372. URL: http://www.ncbi.nlm.nih.gov/pubmed/29290672http://www.pubmedcentral.nih.gov/articlerender.fcgi?artid=PMC5737249.

[17] K. J. De Vos and M. Hafezparast. "Neurobiology of axonal transport defects in motor neuron diseases: Opportunities for translational research?" In: *Neurobiology of Disease* 105 (2017), pp. 283–299. ISSN: 09699961. DOI: 10.1016/j.nbd.2017.02.004. URL: http://www.ncbi.nlm.nih.gov/pubmed/28235672http://www.pubmedcentral.nih.gov/articlerender.fcgi?artid=PMC5536153https://linkinghub.elsevier.com/retrieve/pii/S0969996117300335.

[18] A. del Valle Rodríguez, D. Didiano, and C. Desplan. "Power tools for gene expression and clonal analysis in Drosophila." In: *Nature methods* 9.1 (2011), pp. 47–55. ISSN: 1548-7105. DOI: 10.1038/nmeth.1800. URL: http://www.ncbi.nlm.nih.gov/pubmed/22205518http://www.pubmedcentral.nih.gov/articlerender.fcgi?artid=PMC3574576.

[19] T. P. A. Devasagayam, J. C. Tilak, K. K. Boloor, K. S. Sane, S. S. Ghaskadbi, and R. D. Lele. "Free radicals and antioxidants in human health: current status and future prospects." In: *The Journal of the Association of Physicians of India* 52 (2004), pp. 794–804. ISSN: 0004-5772. URL: http://www.ncbi.nlm.nih.gov/pubmed/15909857.

[20] T. Dharmadasa and M. C. Kiernan. "Riluzole, disease stage and survival in ALS." In: *The Lancet. Neurology* 17.5 (2018), pp. 385–386. ISSN: 1474-4465. DOI: 10.1016/S1474-4422(18)30091-7. URL: http://www.ncbi.nlm.nih.gov/pubmed/29525493.

[21] M. A. Elhelu. "The role of macrophages in immunology." In: *Journal of the National Medical Association* 75.3 (1983), pp. 314–7. ISSN: 0027-9684. URL: http://www.ncbi.nlm.nih.gov/pubmed/6343621http://www.pubmedcentral.nih.gov/articlerender.fcgi?artid=PMC2561478.

[22] M. Ferrucci, G. Lazzeri, M. Flaibani, F. Biagioni, F. Cantini, M. Madonna, D. Bucci, F. Limanaqi, P. Soldani, and F. Fornai. "In search for a gold-standard procedure to count motor neurons in the spinal cord." In: *Histology and histopathology* 33.10 (2018), pp. 1021–1046. ISSN: 1699-5848. DOI: 10.14670/HH-11-983. URL: http://www.ncbi.nlm.nih.gov/pubmed/29537481.

[23] I. Figueira, G. Garcia, R. C. Pimpão, A. P. Terrasso, I. Costa, A. F. Almeida, L. Tavares, T. F. Pais, P. Pinto, M. R. Ventura, A. Filipe, G. J. McDougall, D. Stewart, K. S. Kim, I. Palmela, D. Brites, M. A. Brito, C. Brito, and C. N. Santos. "Polyphenols journey through blood-brain barrier towards neuronal protection." In: *Scientific Reports* 7.1 (2017), p. 11456. ISSN: 2045-2322. DOI: 10.1038/s41598-017-11512-6. URL: http://www.nature.com/articles/s41598-017-11512-6.

[24] P. H. Gordon, F. Salachas, G. Bruneteau, P.-F. Pradat, L. Lacomblez, J. Gonzalez-Bermejo, C. Morelot-Panzini, T. Similowski, A. Elbaz, and V. Meininger. "Improving survival in a large French ALS center cohort." In: *Journal of neurology* 259.9 (2012), pp. 1788–1792.

[25] D. Graham. "A behavioural analysis of the temporal organisation of walking movements in the 1st instar and adult stick insect (Carausius morosus)." In: *Journal of Comparative Physiology* 81.1 (1972), pp. 23–52. ISSN: 0340-7594. DOI: 10.1007/BF00693548. URL: http://link.springer.com/10.1007/BF00693548.

[26] Greenspan. *R.J. Fly Pushing: The Theory and Practice of Drosophila Genetics*. 2nd. 2004.

[27] W. Guan, L. Venkatasubramanian, M. Baek, R. S. Mann, and J. Enriquez. "Visualize Drosophila Leg Motor Neuron Axons Through the Adult Cuticle." In: *Journal of Visualized Experiments* 140 (2018). ISSN: 1940-087X. DOI: 10.3791/58365. URL: http://www.ncbi.nlm.nih.gov/pubmed/30451217http://www.pubmedcentral.nih.gov/articlerender.fcgi?artid=PMC6544026https://www.jove.com/video/58365/visualize-drosophila-leg-motor-neuron-axons-through-the-adult-cuticle.

[28] K. Hayashi, Y. Mochizuki, R. Takeuchi, T. Shimizu, M. Nagao, K. Watabe, N. Arai, K. Oyanagi, O. Onodera, M. Hayashi, H. Takahashi, A. Kakita, and E. Isozaki. "Clinicopathological characteristics of patients with amyotrophic lateral sclerosis resulting in a totally locked-in state (communication Stage V)." In: *Acta Neuropathologica Communications* 4.1 (2016), p. 107. ISSN: 2051-5960. DOI: 10.1186/s40478-016-0379-3. URL: http://actaneurocomms.biomedcentral.com/articles/10.1186/s40478-016-0379-3.

[29] T. Holmøy. "T cells in amyotrophic lateral sclerosis." In: *European Journal of Neurology* 15.4 (2008), pp. 360–366. ISSN: 1351-5101. DOI: 10.1111/j.1468-1331.2008.02065.x. URL: http://doi.wiley.com/10.1111/j.1468-1331.2008.02065.x.

[30] C. Jardim, M. Ottens, J. Marienhagen, W. Dekker, J. W. Allwood, N. Faria, M. Naesby, R. Menezes, P. Ferreira, J. Oliveira, D. Stewart, C. N. dos Santos, R. Rosado-Ramos, A. R. Silva, D. Méndez Sevillano, N. Kallscheuer, M. D. Henriques da Silva, M. Bott, I. Rocha, M. Sousa, A. Foito, and A. Braga. "Identification and microbial production of the raspberry phenol salidroside that is active against

Huntington's disease." In: *Plant Physiology* (2018), pp.01074.2018. ISSN: 0032-0889. DOI: 10.1104/pp.18.01074.

[31] M. Jaronen, G. Goldsteins, and J. Koistinaho. "ER stress and unfolded protein response in amyotrophic lateral sclerosis-a controversial role of protein disulphide isomerase." In: *Frontiers in cellular neuroscience* 8 (2014), p. 402. ISSN: 1662-5102. DOI: 10.3389/fncel.2014.00402. URL: http://www.ncbi.nlm.nih.gov/pubmed/25520620http://www.pubmedcentral.nih.gov/articlerender.fcgi?artid=PMC4251436.

[32] M. Jimenez-Del-Rio, C. Guzman-Martinez, and C. Velez-Pardo. "The Effects of Polyphenols on Survival and Locomotor Activity in Drosophila melanogaster Exposed to Iron and Paraquat." In: *Neurochemical Research* 35.2 (2010), pp. 227–238. ISSN: 0364-3190. DOI: 10.1007/s11064-009-0046-1. URL: http://www.ncbi.nlm.nih.gov/pubmed/19701790http://link.springer.com/10.1007/s11064-009-0046-1.

[33] I. T. Jolliffe and J. Cadima. "Principal component analysis: a review and recent developments." In: *Philosophical transactions. Series A, Mathematical, physical, and engineering sciences* 374.2065 (2016), p. 20150202. ISSN: 1471-2962. DOI: 10.1098/rsta.2015.0202. URL: http://www.ncbi.nlm.nih.gov/pubmed/26953178http://www.pubmedcentral.nih.gov/articlerender.fcgi?artid=PMC4792409.

[34] M. C. Kiernan, S. Vucic, B. C. Cheah, M. R. Turner, A. Eisen, O. Hardiman, J. R. Burrell, and M. C. Zoing. "Amyotrophic lateral sclerosis." In: *The Lancet* 377.9769 (2011), pp. 942–955. ISSN: 01406736. DOI: 10.1016/S0140-6736(10)61156-7. URL: http://www.ncbi.nlm.nih.gov/pubmed/21296405https://linkinghub.elsevier.com/retrieve/pii/S0140673610611567.

[35] L. Kockel, L. M. Huq, A. Ayyar, E. Herold, E. MacAlpine, M. Logan, C. Savvides, G. E. S. Kim, J. Chen, T. Clark, T. Duong, V. Fazel-Rezai, D. Havey, S. Han, R. Jagadeesan, E. S. J. Kim, D. Lee, K. Lombardo, I. Piyale, H. Shi, L. Stahr, D. Tung, U. Tayvah, F. Wang, J.-H. Wang, S. Xiao, S. M. Topper, S. Park, C. Rotondo, A. E. Rankin, T. W. Chisholm, and S. K. Kim. "A Drosophila LexA Enhancer-Trap Resource for Developmental Biology and Neuroendocrine Research." In: *G3 (Bethesda, Md.)* 6.10 (2016), pp. 3017–3026. ISSN: 2160-1836. DOI: 10.1534/g3.116.031229. URL: http://www.ncbi.nlm.nih.gov/pubmed/27527793http://www.pubmedcentral.nih.gov/articlerender.fcgi?artid=PMC5068927.

[36] N. A. Lanson, A. Maltare, H. King, R. Smith, J. H. Kim, J. P. Taylor, T. E. Lloyd, and U. B. Pandey. "A Drosophila model of FUS-related neurodegeneration reveals genetic interaction between FUS and TDP-43." In: *Human Molecular Genetics* 20.13 (2011), pp. 2510–2523. ISSN: 0964-6906. DOI: 10.1093/hmg/ddr150. URL: http://www.ncbi.nlm.nih.gov/pubmed/21487023http://www.pubmedcentral.nih.

gov/articlerender.fcgi?artid=PMC4288133https://academic.oup.com/hmg/article-lookup/doi/10.1093/hmg/ddr150.

[37] T. E. Lopez, H. M. Pham, J. Barbour, P. Tran, B. Van Nguyen, S. P. Hogan, R. L. Homo, V. Coskun, S. E. Schriner, and M. Jafari. "The impact of green tea polyphenols on development and reproduction in Drosophila melanogaster." In: *Journal of Functional Foods* 20 (2016), pp. 556–566. ISSN: 17564646. DOI: 10.1016/j.jff.2015.11.002. URL: http://www.ncbi.nlm.nih.gov/pubmed/26693252http://www.pubmedcentral.nih.gov/articlerender.fcgi?artid=PMC4683606https://linkinghub.elsevier.com/retrieve/pii/S1756464615005393.

[38] B. Lu and H. Vogel. "Drosophila models of neurodegenerative diseases." In: *Annual review of pathology* 4 (2009), pp. 315–42. ISSN: 1553-4014. DOI: 10.1146/annurev.pathol.3.121806.151529. URL: http://www.ncbi.nlm.nih.gov/pubmed/18842101http://www.pubmedcentral.nih.gov/articlerender.fcgi?artid=PMC3045805.

[39] R. Maccioni, M. D. Setzu, G. Talani, P. Solari, A. Kasture, S. Sucic, S. Porru, P. Muroni, E. Sanna, S. Kasture, E. Acquas, and A. Liscia. "Standardized phytotherapic extracts rescue anomalous locomotion and electrophysiological responses of TDP-43 Drosophila melanogaster model of ALS." In: *Scientific Reports* 8.1 (2018), pp. 1–10. ISSN: 20452322. DOI: 10.1038/s41598-018-34452-1.

[40] D. V. Magalhães, R. F. Bianchi, F. P. Zanella, C. R. Mendonça, M. M. Oliveira, and L. Misoguti. "Frustrated total internal reflection: A simple application and demonstration." In: *American Journal of Physics* 71.5 (2003), pp. 494–496. ISSN: 0002-9505. DOI: 10.1119/1.1523075.

[41] J. Magrané and G. Manfredi. "Mitochondrial function, morphology, and axonal transport in amyotrophic lateral sclerosis." In: *Antioxidants & redox signaling* 11.7 (2009), pp. 1615–26. ISSN: 1557-7716. DOI: 10.1089/ARS.2009.2604. URL: http://www.ncbi.nlm.nih.gov/pubmed/19344253http://www.pubmedcentral.nih.gov/articlerender.fcgi?artid=PMC2789440.

[42] L. McGurk, A. Berson, and N. M. Bonini. "Drosophila as an In Vivo Model for Human Neurodegenerative Disease." In: *Genetics* 201.2 (2015), pp. 377–402. ISSN: 1943-2631. DOI: 10.1534/genetics.115.179457. URL: http://www.ncbi.nlm.nih.gov/pubmed/26447127http://www.pubmedcentral.nih.gov/articlerender.fcgi?artid=PMC4596656.

[43] C. S. Mendes, I. Bartos, T. Akay, S. Márka, and R. S. Mann. "Quantification of gait parameters in freely walking wild type and sensory deprived Drosophila melanogaster." In: *eLife* 2013.2 (2013), pp. 1–24. ISSN: 2050084X. DOI: 10.7554/eLife.00231.

[44] U. Milton Katz, State University of New York. *Introduction to Geometrical Optics*. 2002.

[45] J. C. Mitchell, P. McGoldrick, C. Vance, T. Hortobagyi, J. Sreedharan, B. Rogelj, E. L. Tudor, B. N. Smith, C. Klasen, C. C. J. Miller, J. D. Cooper, L. Greensmith, and C. E. Shaw. "Overexpression of human wild-type FUS causes progressive motor neuron degeneration in an age- and dose-dependent fashion." In: *Acta Neuropathologica* 125.2 (2013), pp. 273–288. ISSN: 0001-6322. DOI: 10.1007/s00401-012-1043-z. URL: http://www.ncbi.nlm.nih.gov/pubmed/22961620http://www.pubmedcentral.nih.gov/articlerender.fcgi?artid=PMC3549237http://link.springer.com/10.1007/s00401-012-1043-z.

[46] A. Musarò. "Understanding ALS: New therapeutic approaches." In: *FEBS Journal* 280.17 (2013), pp. 4315–4322. ISSN: 1742464X. DOI: 10.1111/febs.12087.

[47] D. Of and T. H. E. Disease. "Medical Progress A." In: *English Journal* 344.22 (2001), pp. 1688–1700.

[48] M. Orsini, A. B. Oliveira, O. J. M. Nascimento, C. H. M. Reis, M. A. A. Leite, J. A. de Souza, C. Pupe, O. G. de Souza, V. H. Bastos, M. R. G. de Freitas, S. Teixeira, C. Bruno, E. Davidovich, and B. Smidt. "Amyotrophic Lateral Sclerosis: New Perpectives and Update." In: *Neurology international* 7.2 (2015), p. 5885. ISSN: 2035-8385. DOI: 10.4081/ni.2015.5885. URL: http://www.ncbi.nlm.nih.gov/pubmed/26487927http://www.pubmedcentral.nih.gov/articlerender.fcgi?artid=PMC4591493.

[49] C. Peng, H. Y. E. Chan, Y. Huang, H. Yu, and Z.-Y. Chen. "Apple Polyphenols Extend the Mean Lifespan of Drosophila melanogaster." In: *Journal of Agricultural and Food Chemistry* 59.5 (2011), pp. 2097–2106. ISSN: 0021-8561. DOI: 10.1021/jf1046267. URL: http://www.ncbi.nlm.nih.gov/pubmed/21319854http://pubs.acs.org/doi/abs/10.1021/jf1046267.

[50] O. M. Peters, M. Ghasemi, and R. H. Brown. "Emerging mechanisms of molecular pathology in ALS." In: *Journal of Clinical Investigation* 125.5 (2015), pp. 1767–1779. ISSN: 0021-9738. DOI: 10.1172/JCI71601. URL: http://www.ncbi.nlm.nih.gov/pubmed/25932674http://www.pubmedcentral.nih.gov/articlerender.fcgi?artid=PMC4463186http://www.jci.org/articles/view/71601.

[51] D. Petrov, C. Mansfield, A. Moussy, and O. Hermine. "ALS Clinical Trials Review: 20 Years of Failure. Are We Any Closer to Registering a New Treatment?" In: *Frontiers in aging neuroscience* 9 (2017), p. 68. ISSN: 1663-4365. DOI: 10.3389/fnagi.2017.00068. URL: http://www.ncbi.nlm.nih.gov/pubmed/28382000http://www.pubmedcentral.nih.gov/articlerender.fcgi?artid=PMC5360725.

[52] T. Philips and W. Robberecht. "Neuroinflammation in amyotrophic lateral sclerosis: role of glial activation in motor neuron disease." In: *The Lancet Neurology* 10.3 (2011), pp. 253–263. ISSN: 14744422. DOI: 10.1016/S1474-4422(11)70015-1. URL: http://www.ncbi.nlm.nih.gov/pubmed/21349440https://linkinghub.elsevier.com/retrieve/pii/S1474442211700151.

[53] V. Picher-Martel, P. N. Valdmanis, P. V. Gould, J. P. Julien, and N. Dupré. "From animal models to human disease: A genetic approach for personalized medicine in ALS." In: *Acta Neuropathologica Communications* 4.1 (2016), pp. 1–29. ISSN: 20515960. DOI: 10.1186/s40478-016-0340-5.

[54] G. M. Poças, J. Branco-Santos, F. Herrera, T. F. Outeiro, and P. M. Domingos. "α-Synuclein modifies mutant huntingtin aggregation and neurotoxicity in Drosophila." In: *Human molecular genetics* 24.7 (2015), pp. 1898–907. ISSN: 1460-2083. DOI: 10.1093/hmg/ddu606. URL: http://www.ncbi.nlm.nih.gov/pubmed/25452431http://www.pubmedcentral.nih.gov/articlerender.fcgi?artid=PMC4355023.

[55] L. Poirier, A. Shane, J. Zheng, and L. Seroude. "Characterization of the Drosophila Gene-Switch system in aging studies: A cautionary tale." In: *Aging Cell* 7.5 (2008), pp. 758–770. ISSN: 14749718. DOI: 10.1111/j.1474-9726.2008.00421.x.

[56] R. Rademakers, H. Stewart, M. Dejesus-Hernandez, C. Krieger, N. Graff-Radford, M. Fabros, H. Briemberg, N. Cashman, A. Eisen, and I. R. A. Mackenzie. "Fus gene mutations in familial and sporadic amyotrophic lateral sclerosis." In: *Muscle & nerve* 42.2 (2010), pp. 170–6. ISSN: 1097-4598. DOI: 10.1002/mus.21665. URL: http://www.ncbi.nlm.nih.gov/pubmed/20544928http://www.pubmedcentral.nih.gov/articlerender.fcgi?artid=PMC2969843.

[57] J. Ravits, S. Appel, R. H. Baloh, R. Barohn, B. Rix Brooks, L. Elman, M. K. Floeter, C. Henderson, C. Lomen-Hoerth, J. D. Macklis, L. McCluskey, H. Mitsumoto, S. Przedborski, J. Rothstein, J. Q. Trojanowski, L. H. van den Berg, and S. Ringel. "Deciphering amyotrophic lateral sclerosis: What phenotype, neuropathology and genetics are telling us about pathogenesis." In: *Amyotrophic Lateral Sclerosis and Frontotemporal Degeneration* 14.sup1 (2013), pp. 5–18. ISSN: 2167-8421. DOI: 10.3109/21678421.2013.778548. URL: http://www.ncbi.nlm.nih.gov/pubmed/23678876http://www.pubmedcentral.nih.gov/articlerender.fcgi?artid=PMC3779649http://www.tandfonline.com/doi/full/10.3109/21678421.2013.778548.

[58] A. E. Renton, A. Chiò, and B. J. Traynor. "State of play in amyotrophic lateral sclerosis genetics." In: *Nature Neuroscience* 17.1 (2014), pp. 17–23. ISSN: 1097-6256. DOI: 10.1038/nn.3584. URL: http://www.ncbi.nlm.nih.gov/pubmed/24369373http://www.pubmedcentral.nih.gov/articlerender.fcgi?artid=PMC4544832http://www.nature.com/articles/nn.3584.

[59] H. D. Ryoo, P. M. Domingos, M.-J. Kang, and H. Steller. "Unfolded protein response in a Drosophila model for retinal degeneration." In: *The EMBO journal* 26.1 (2007), pp. 242–52. ISSN: 0261-4189. DOI: 10.1038/sj.emboj.7601477. URL: http://www.ncbi.nlm.nih.gov/pubmed/17170705http://www.pubmedcentral.nih.gov/articlerender.fcgi?artid=PMC1782370.

[60] J. Scekic-Zahirovic, O. Sendscheid, H. El Oussini, M. Jambeau, Y. Sun, S. Mersmann, M. Wagner, S. Dieterlé, J. Sinniger, S. Dirrig-Grosch, K. Drenner, M.-C. Birling, J. Qiu, Y. Zhou, H. Li, X.-D. Fu, C. Rouaux, T. Shelkovnikova, A. Witting, A. C. Ludolph, F. Kiefer, E. Storkebaum, C. Lagier-Tourenne, and L. Dupuis. "Toxic gain of function from mutant FUS protein is crucial to trigger cell autonomous motor neuron loss." In: *The EMBO journal* 35.10 (2016), pp. 1077–97. ISSN: 1460-2075. DOI: 10.15252/embj.201592559. URL: http://www.ncbi.nlm.nih.gov/pubmed/26951610http://www.pubmedcentral.nih.gov/articlerender.fcgi?artid=PMC4868956.

[61] F. Scialo, A. Sriram, R. Stefanatos, and A. Sanz. "Practical Recommendations for the Use of the GeneSwitch Gal4 System to Knock-Down Genes in Drosophila melanogaster." In: *PLOS ONE* 11.8 (2016). Ed. by C. Antoniewski, e0161817. ISSN: 1932-6203. DOI: 10.1371/journal.pone.0161817. URL: http://dx.plos.org/10.1371/journal.pone.0161817.

[62] Y. Shang and E. J. Huang. "Mechanisms of FUS mutations in familial amyotrophic lateral sclerosis." In: *Brain research* 1647 (2016), pp. 65–78. ISSN: 1872-6240. DOI: 10.1016/j.brainres.2016.03.036. URL: http://www.ncbi.nlm.nih.gov/pubmed/27033831http://www.pubmedcentral.nih.gov/articlerender.fcgi?artid=PMC5003642.

[63] P. J. Shaw and P. G. Ince. "Glutamate, excitotoxicity and amyotrophic lateral sclerosis." In: *Journal of Neurology* 244.S2 (2009), S3–S14. ISSN: 0340-5354. DOI: 10.1007/bf03160574.

[64] D. Szwajgier, K. Borowiec, and K. Pustelniak. "The Neuroprotective Effects of Phenolic Acids: Molecular Mechanism of Action." In: *Nutrients* 9.5 (2017). ISSN: 2072-6643. DOI: 10.3390/nu9050477. URL: http://www.ncbi.nlm.nih.gov/pubmed/28489058http://www.pubmedcentral.nih.gov/articlerender.fcgi?artid=PMC5452207.

[65] E. Talbott, A. Malek, and D. Lacomis. "The epidemiology of amyotrophic lateral sclerosis." In: *Handbook of clinical neurology*. Vol. 138. 2016, pp. 225–238. DOI: 10.1016/B978-0-12-802973-2.00013-6. URL: http://www.ncbi.nlm.nih.gov/pubmed/27637961https://linkinghub.elsevier.com/retrieve/pii/B9780128029732000136.

[66] J. P. Taylor, R. H. Brown, and D. W. Cleveland. "Decoding ALS: from genes to mechanism." In: *Nature* 539.7628 (2016), pp. 197–206. ISSN: 0028-0836. DOI: 10.1038/nature20413. URL: http://www.ncbi.nlm.nih.gov/pubmed/27830784http://www.pubmedcentral.nih.gov/articlerender.fcgi?artid=PMC5585017http://www.nature.com/doifinder/10.1038/nature20413.

[67] The Tauber Lab. "The Fly Manual: A guide to working with Drosophila." In: (), pp. 3–13. URL: www.tinyurl.com/livegene.

[68] U. Tracy Hussell, Manchester University. *Helper and Cytotoxic T Cells | British Society for Immunology*. URL: https://www.immunology.org/public-information/bitesized-immunology/cells/helper-and-cytotoxic-t-cells (visited on 02/21/2019).

[69] P. N. Valdmanis and G. A. Rouleau. "Genetics of familial amyotrophic lateral sclerosis." In: *Neurology* 70.2 (2008), pp. 144–152. ISSN: 0028-3878. DOI: 10.1212/01.wnl.0000296811.19811.db. URL: http://www.ncbi.nlm.nih.gov/pubmed/18180444http://www.neurology.org/cgi/doi/10.1212/01.wnl.0000296811.19811.db.

[70] J. J. Valletta, C. Torney, M. Kings, A. Thornton, and J. Madden. "Applications of machine learning in animal behaviour studies." In: *Animal Behaviour* 124 (2017), pp. 203–220. ISSN: 0003-3472. DOI: 10.1016/J.ANBEHAV.2016.12.005. URL: https://www.sciencedirect.com/science/article/pii/S0003347216303360.

[71] L. Van Den Bosch, P. Van Damme, E. Bogaert, and W. Robberecht. "The role of excitotoxicity in the pathogenesis of amyotrophic lateral sclerosis." In: *Biochimica et Biophysica Acta (BBA) - Molecular Basis of Disease* 1762.11-12 (2006), pp. 1068–1082. ISSN: 09254439. DOI: 10.1016/j.bbadis.2006.05.002. URL: http://www.ncbi.nlm.nih.gov/pubmed/16806844https://linkinghub.elsevier.com/retrieve/pii/S0925443906000822.

[72] J.-W. Wang, J. R. Brent, A. Tomlinson, N. A. Shneider, and B. D. McCabe. "The ALS-associated proteins FUS and TDP-43 function together to affect Drosophila locomotion and life span." In: *Journal of Clinical Investigation* 121.10 (2011), pp. 4118–4126. ISSN: 0021-9738. DOI: 10.1172/JCI57883. URL: http://www.ncbi.nlm.nih.gov/pubmed/21881207http://www.pubmedcentral.nih.gov/articlerender.fcgi?artid=PMC3195475http://www.jci.org/articles/view/57883.

[73] L. C. Wijesekera and P. N. Leigh. "Amyotrophic lateral sclerosis." In: *Orphanet Journal of Rare Diseases* 4.1 (2009), p. 3. ISSN: 1750-1172. DOI: 10.1186/1750-1172-4-3. URL: http://www.ncbi.nlm.nih.gov/pubmed/19192301http://www.pubmedcentral.nih.gov/articlerender.fcgi?artid=PMC2656493http://ojrd.biomedcentral.com/articles/10.1186/1750-1172-4-3.

[74] D. M. Wilson. "Insect Walking." In: *Annual Review of Entomology* 11.1 (1966), pp. 103–122. ISSN: 0066-4170. DOI: 10.1146/annurev.en.11.010166.000535. URL: http://www.annualreviews.org/doi/10.1146/annurev.en.11.010166.000535.

[75] C.-L. Wu, T.-F. Fu, Y.-Y. Chou, and S.-R. Yeh. "A single pair of neurons modulates egg-laying decisions in Drosophila." In: *PloS one* 10.3 (2015), e0121335. ISSN: 1932-6203. DOI: 10.1371/journal.pone.0121335. URL: http://www.ncbi.nlm.nih.gov/pubmed/25781933http://www.pubmedcentral.nih.gov/articlerender.fcgi?artid=PMC4363143.

[76] S. Zarei, K. Carr, L. Reiley, K. Diaz, O. Guerra, P. F. Altamirano, W. Pagani, D. Lodin, G. Orozco, and A. Chinea. "A comprehensive review of amyotrophic lateral sclerosis." In: *Surgical neurology international* 6 (2015), p. 171. ISSN: 2229-5097. DOI: 10.4103/2152-7806.169561. URL: http://www.ncbi.nlm.nih.gov/pubmed/26629397http://www.pubmedcentral.nih.gov/articlerender.fcgi?artid=PMC4653353.

[77] A. Şahin, A. Held, K. Bredvik, P. Major, T.-M. Achilli, A. G. Kerson, K. Wharton, G. Stilwell, and R. Reenan. "Human SOD1 ALS Mutations in a *Drosophila* Knock-In Model Cause Severe Phenotypes and Reveal Dosage-Sensitive Gain- and Loss-of-Function Components." In: *Genetics* 205.2 (2017), pp. 707–723. ISSN: 0016-6731. DOI: 10.1534/genetics.116.190850. URL: http://www.ncbi.nlm.nih.gov/pubmed/27974499http://www.pubmedcentral.nih.gov/articlerender.fcgi?artid=PMC5289846http://www.genetics.org/lookup/doi/10.1534/genetics.116.190850.

ANNEX I

FLY BASIS

I.1 *Drosophila melanogaster* features

Drosophila melanogaster, known as the fruit fly, is found worldwide in rotting fruit where adult flies lay its eggs. In the last years, fruit flies have been cultured in the laboratory, in bottles or shell vials, by using a solid food. The life cycle of fly has different phases including egg, larvae, pupa and adult (Figure I.1). Raised at 25ºC in rich culture medium in the laboratory, these insects have a very short generation time, approximately 10 days, and each female can lay several hundred eggs. Since the length of the life cycle is dependent on temperature, researchers can increase the life span of flies by raising them at 18ºC [67].

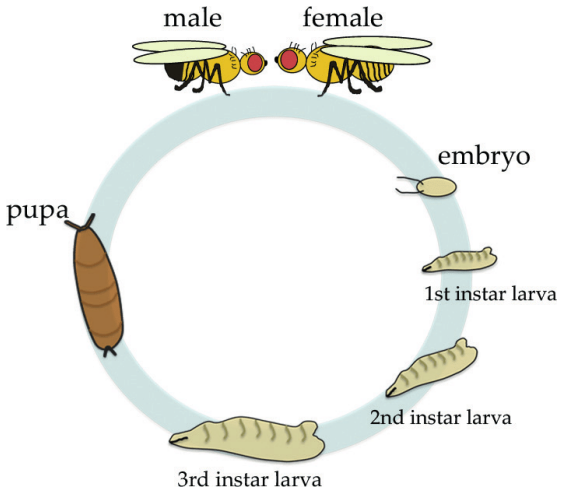

Figure I.1: **The life cycle of *Drosophila melanogaster*.** The larvae hatches approximately one day after the egg is fertilized and in the next four or five days the larvae progress from the first instar through the second instar to third instar stages. During pupation, most of the larval tissues are destroyed and replaced by adult tissues [Adapted from [4]].

The sequencing of the entire genome of the fly was one of the most important breakthroughs for the scientific community, particularly for the *Drosophila* research community. The annotated genome sequence of *Drosophila melanogaster*, which has four pairs of chromosomes, 180 million bases and 13.600 genes, indicated that more than 90% of the fly genes are similar to the human and mouse genes. However, the *Drosophila* genome offers a much simpler than mammalian models. The fly chromosomes are designated as 2, 3, 4 and X/Y. The Y chromosome contains only a few genes that are essential for spermatogenesis.

One advantage of *Drosophila* is that, for each chromosome, there were created balancer chromosomes. These are special modified chromosomes designed by multiple, nested chromosomal inversions. The balancer chromosomes are genetic tools used to prevent crossing over between homologous during meiosis. If, for some reason, the crossing over involving balancer chromosomes occurs, it results in chromatids which lacks some genes or have duplicated genes and consequently leads to a non-viable progeny.

Importantly, a balancer chromosome also contain dominant mutations that are visible phenotypic markers and thus enabling researchers to follow the balancer and genetic insertions through crosses. Moreover, balancer chromosomes allows the maintenance of lethal mutations in heterozygous stable stocks. Balancers are usually termed based on the chromosome that they serve to stabilize (F for first, which is the X chromossome; S for second; and T for third), with an M which means "multiply inverted". M is followed by a number and sometimes a lowercase letter to distinguish balancers of the same chromosome. Additionally, the genetic symbol for the principal markers carried by that balancer is listed after the name. Some markers usually used in several studies are represented below (Figure I.2)[26, 67].

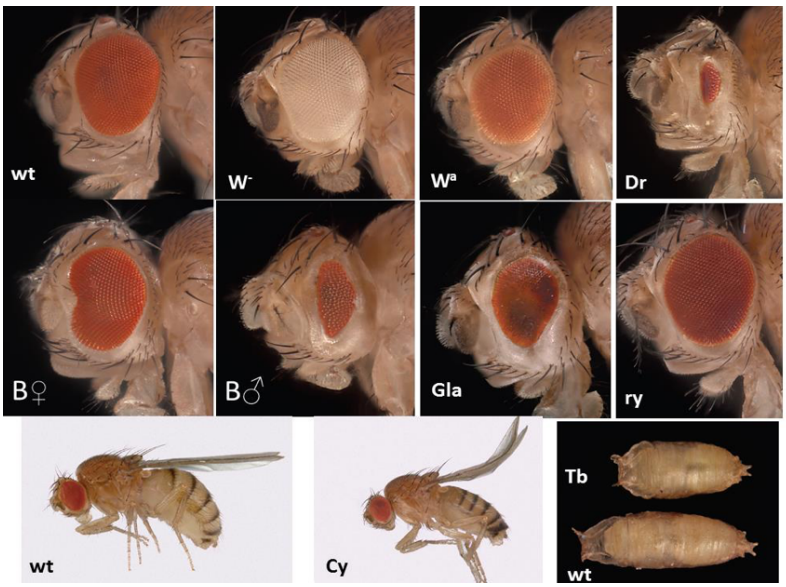

Figure I.2: **Examples of *Drosophila* phenotypic markers.** These markers aids on tracing the inheritance of alleles. Wild-type (WT) refers to a Drosophila stock in which flies are similar to those found in natural populations [Adapted from[12]].

I.2 Expression systems in *Drosophila*

I.2.0.1 GAL4/UAS

In the last 30 years, there has been a huge expansion in the genetic toolbox of model organisms, particularly in the fruit fly. One example of tool development was the creation of the GAL4/UAS system for targeted gene expression in *Drosophila* which constitutes one of the most powerful tools for studying gene function [3, 10].

This system is based on the properties of the GAL4 transcription factor, derived from the yeast *Saccharomyces cerevisiae*, which activates transcription of its target genes by binding to upstream activation sequence (UAS). The UAS is a specific enhancer to the GAL4 protein. The two components, GAL4 and UAS, are carried in different lines allowing for several combinatorial possibilities. When flies of these two lines undergo crossing, the GAL4 protein binds to the UAS activating the gene at the tissue that the promoter is specific for (Figure I.3) [9, 13].

One of the advantages of this system is that the expression of toxic genes will only be enabled when bound to the GAL4 transcription factor; thus, flies can carry the inactivated form of a toxic gene and survive normally. Moreover, this system allows the study of the effects of numerous genes through their over-expression or misexpression at several sites in the body using the large collection of tissue-specific promoters available [13].

I.2.0.2 GeneSwitch/UAS

Gene Switch (GS) system is an inducible system that allows temporal and tissue-specific control of gene expression in *Drosophila*. GS uses a modified GAL4 protein fused to a

progesterone steroid receptor enabling the regulation of its GAL4 activity by the presence or absence of the synthetic progesterone analogue mifespristone (RU486). In the presence of RU486, the GAL4 is activated leading to increased gene expression. Conversely, in the absence of RU486, GAL4 activity is maintained at a minimum (Figure I.3) [55, 61].

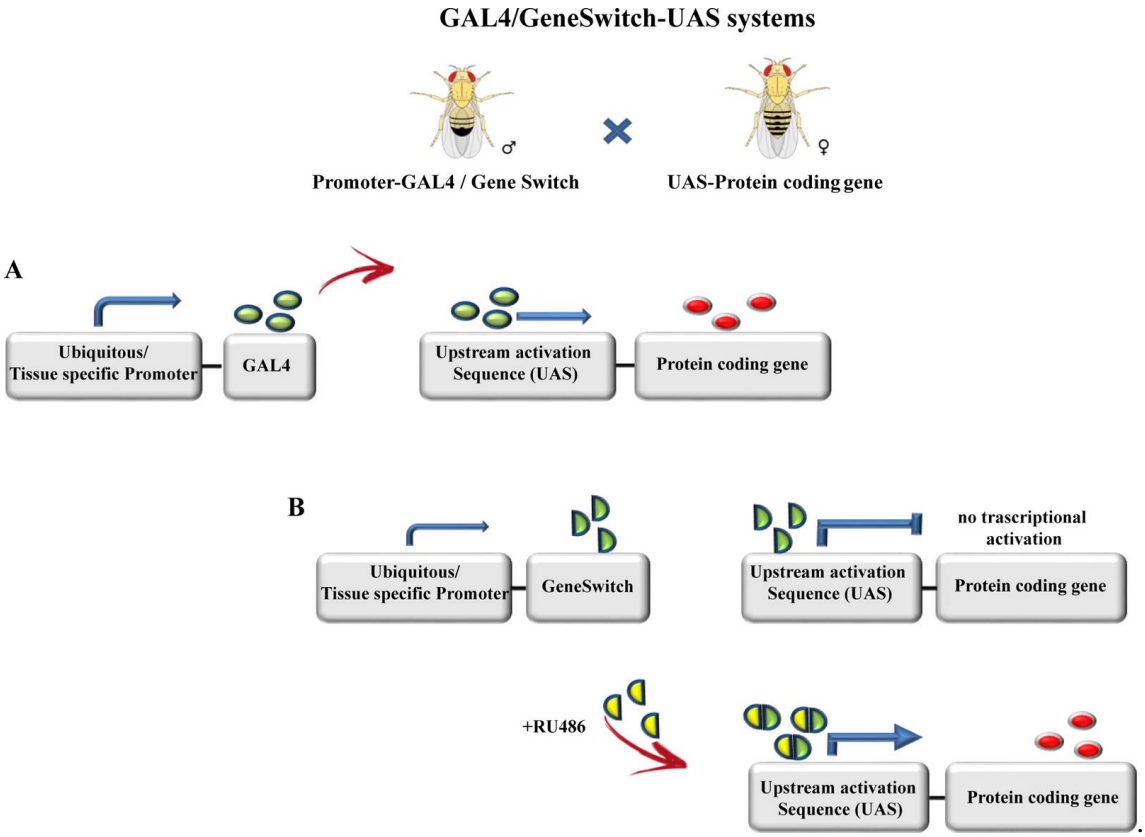

Figure I.3: **Gal4/UAS and GeneSwitch/UAS systems.** (A) The GAL4/UAS system enables spatial control of gene expression. (B) The GS system allows temporal control of gene expression due to a modified GAL4 protein that is active only when RU486 binds to the fused progesterone steroid receptor [Adapted from[61]].

I.2.0.3 LexA/LexAop

A different binary system is based on the LexA transcription factor, derived from *Escherichia coli*, that regulates expression of transgenes fused to a LexA operator-promoter (LexAop) [35]. Basically, the GAL4 system is the default expression system for most studies owing to the abundance of characterized lines. The LexA/LexAop system is frequently used in combination with GAL4 since it allows *Drosophila* researchers to simultaneously perform two manipulations of gene expression [18, 35].